SEQUENCE STRATIGRAPHIC ASSESSMENT OF THE MULEY CANYON SANDSTONE & MASUK FORMATION, HENRY MOUNTAINS SYNCLINE: IMPLICATIONS FOR UNDERSTANDING THE MULEY CANYON COAL ZONE

BY LAUREN P. BIRGENHEIER, CHRISTOPHER R. FIELDING, MATTHEW J. CORBETT, AND CHRISTOPHER KESLER

Open-File Report 557
Utah Geological Survey
a division of
Utah Department of Natural Resources
2009

Utah Geological Survey
60 years
1949 2009
Excellence, Integrity, and Objectivity

SEQUENCE STRATIGRAPHIC ASSESSMENT OF THE MULEY CANYON SANDSTONE AND MASUK FORMATION, HENRY MOUNTAINS SYNCLINE: IMPLICATIONS FOR UNDERSTANDING THE MULEY CANYON COAL ZONE

by Lauren P. Birgenheier[1], Christopher R. Fielding[2], Matthew J. Corbett[2], and Christopher Kesler[1]

[1]Energy and Geoscience Institute
University of Utah
423 Wakara Way, Suite 300
Salt Lake City, UT 84108

[2]Department of Geosciences
University of Nebraska-Lincoln
214 Bessey Hall
Lincoln, NE 68588-0340

OPEN-FILE REPORT 557
UTAH GEOLOGICAL SURVEY
a division of
UTAH DEPARTMENT OF NATURAL RESOURCES
2009

STATE OF UTAH
Gary R. Herbert, Governor

DEPARTMENT OF NATURAL RESOURCES
Michael Styler, Executive Director

UTAH GEOLOGICAL SURVEY
Richard G. Allis, Director

PUBLICATIONS
contact
Natural Resources Map & Bookstore
1594 W. North Temple
Salt Lake City, UT 84114
telephone: 801-537-3320
toll-free: 1-888-UTAH MAP
Web site: mapstore.utah.gov
email: geostore@utah.gov

UTAH GEOLOGICAL SURVEY
contact
1594 W. North Temple, Suite 3110
Salt Lake City, UT 84114
telephone: 801-537-3300
Web site: geology.utah.gov

Contents

Figures

Tables

Plates

SEQUENCE STRATIGRAPHIC ASSESSMENT OF THE MULEY CANYON SANDSTONE AND MASUK FORMATION, HENRY MOUNTAINS SYNCLINE: IMPLICATIONS FOR UNDERSTANDING THE MULEY CANYON COAL ZONE

by Lauren P. Birgenheier, Christopher R. Fielding, Matthew J. Corbett, and Christopher Kesler

ABSTRACT

World-class, extensive exposures of the Upper Cretaceous (Campanian) Muley Canyon Sandstone and Masuk Formation in the Henry Mountains Syncline, southeastern Utah, have not been previously evaluated in a sequence stratigraphic context, despite their proximity to time-equivalent terrigenous clastic strata in the Book Cliffs region from which seminal sequence stratigraphic models were developed. Furthermore, the coal-bearing Masuk Formation contains a key economic resource, but sequence stratigraphic models that may help predict subsurface coal location and thickness are lacking. Herein, we provide a detailed facies and sequence stratigraphic analysis of the Muley Canyon Sandstone and Masuk Formation based on outcrop (~100 km^2, 40 mi^2, total coverage), with particular emphasis on the Muley Canyon Coal Zone at the base of the Masuk Formation. Stratigraphic patterns recognized in outcrops of the coal-bearing interval at the base of the Masuk Formation are then correlated to subsurface wireline log and well log data, which have been compiled and georeferenced into an ArcGIS® (version 9.2) database. The basal sandstone unit of the Muley Canyon Sandstone is interpreted as a deltaic mouthbar deposit (unit 1) and is overlain by two cycles of alternating offshore transition-shoreface (units 2 and 4) and fluvial-estuarine deposits (units 3 and 5). Based on the recognition of unit-bounding key surfaces of regional extent, we interpret the Muley Canyon Sandstone to contain four high-frequency sequences that are arranged into two lower-frequency sequence sets. The lower two high-frequency sequences constitute a lower-frequency falling stage sequence set and the upper two a transgressive sequence set. The Masuk Formation comprises a stack of fluvial to estuarine channel and floodbasin deposits, arranged in repetitive, erosionally-based vertical cycles, interpreted as high-frequency sequences that comprise a lower-frequency highstand sequence set (topped by a lower-frequency sequence boundary located on the contact with the overlying Tarantula Mesa Sandstone). Surface-subsurface correlations demonstrate that packages of coal beds are continuous over 10's of km, suggesting a regional allogenic control on coal zone deposition. Bound by the transgressive sequence set of the upper Muley Canyon Sandstone below and the highstand sequence set of the Masuk Formation above, the coal-bearing interval at the base of the Masuk Formation is interpreted to represent a period of maximum accommodation and flooding. Coals are found in the late transgressive systems tract and early highstand systems tract. This work has resulted in an improved sequence stratigraphic understanding of the region that can be 1) used to predict coal bed location and thickness in areas that lack subsurface data, and 2) compared with sequence stratigraphic models of time-equivalent strata in surrounding regions in order to test the regional extent of relative sea level changes.

INTRODUCTION

Sequence stratigraphic models are useful for their predictive capabilities. Continuous exposures of the Upper Cretaceous (Campanian) Muley Canyon Sandstone and the overlying Masuk Formation, deposited as a terrigenous clastic succession on the western edge of the Cretaceous Western Interior Seaway, extend over 95 km (60 mi) from north to south in the Henry Mountains Syncline, southeastern Utah. Previous investigations of Upper Cretaceous strata in the Henry Mountains Syncline have focused mainly on geologic mapping, resolving stratigraphic nomenclature and age, providing a generalized lithologic and paleoenvironmental analysis, and evaluating coal thickness and quality (Hunt and others, 1953; Peterson and Ryder, 1975; Law, 1980; Peterson and others, 1980; Smith, 1983; Morton, 1984; Whitlock, 1984; Eaton, 1990; Tabet, 1999, 2000; Smith, 2003). A detailed sedimentologic and stratigraphic analysis of the Muley Canyon Sandstone and Masuk Formation using modern sedimentary methods (i.e., facies, architectural, and sequence stratigraphic analysis) and criteria has not previously been attempted. Because the base of the Masuk Formation is coal-bearing (termed the Muley Canyon Coal Zone) and is perceived to have economic potential as a minable resource (Tabet, 1999,

2000), an improved understanding of the lateral continuity of coal beds and the development of sequence stratigraphic models from outcrop will improve predictions about where thick coal zones are present, particularly in areas where subsurface data are lacking. Such models will result in reduced future economic investment risk for companies and improved land management decisions by mineral management agencies.

Despite the proximity to the Book Cliffs region, some 100 km to the north where early seminal research focused on developing sequence stratigraphic models of the same age strata, a sequence stratigraphic analysis of the Muley Canyon Sandstone and Masuk Formation has, to date, been lacking. Such analysis is necessary in order to test whether sequence stratigraphic patterns recognized in the Book Cliffs extend further afield and, therefore, whether such patterns are likely to be controlled by regionally variable tectonic drivers or inter-regional sea level fluctuations.

In this study, we conduct a detailed facies, architectural, and sequence stratigraphic analysis of the Muley Canyon Sandstone and the Masuk Formation based on outcrop in a well-exposed area (~100 km^2, 40 mi^2) at and around Blind Trail in the Henry Mountains Syncline, with particular emphasis on correlation of the Muley Canyon Coal Zone in order to: 1) provide a predictive model of the geometry of component units in the subsurface, with emphasis on the coal zone for resource assessment purposes, and 2) develop a sequence stratigraphic model than can test the regional extent of models of time equivalent strata in nearby regions.

GEOLOGIC BACKGROUND

The Henry Mountains Syncline lies to the east of the Waterpocket Fold Monocline and to the west of the Henry Mountains in southeastern Utah (Fig. 1). The former is a N-S-trending Laramide fold structure contained within Capitol Reef National Park, and the Henry Mountains Syncline is an eastern extension of this fold structure, exposing Cretaceous strata at the surface in a series of continuous cliffs, mesas, and badlands. The onset of tectonism associated with the formation of the Henry Mountains Syncline likely predates or is penecontemporaneous with the deposition of the Upper Cretaceous Muley Canyon Sandstone and the Masuk Formation, as evidenced by local changes in coal thickness that mirror the trend of the syncline (Law, 1980). The Henry Mountains are composed of a number of a laccoliths formed in the Oligocene, sharing a common geologic history with the nearby La Sal and Abajo Mountains (Friedmann and Huffman, 1998). Their formation resulted in deformation of strata, forming the eastern limb of the syncline.

The succession of Cretaceous strata exposed in the Henry Mountains syncline totals approximately 1300 m (4300 ft) in thickness (Peterson and Ryder, 1975). The terrigenous succession, sourced from the Sevier Orogenic Belt to the west, was deposited on the western margin of the Cretaceous Interior Seaway in a variety of environments ranging from fluvial, through paralic (deltaic-estuarine-coastal plain) to fully marine. Gross stratigraphic variations reflect changes in relative sea level driven by changes in the balance between sediment supply and accommodation related to tectonism and eustasy. In stratigraphic order, Cretaceous units include the Dakota Sandstone, Tununk Shale, Ferron Sandstone, Blue Gate Shale, Muley Canyon Sandstone, Masuk Formation, Tarantula Mesa Sandstone, and "beds on Tarantula Mesa" (Fig. 2).

The Muley Canyon Sandstone and the Masuk Formation are thought to be early Campanian in age, based on age-diagnostic fossils found in the underlying Blue Gate Shale (marine invertebrates) and from within the Masuk itself (invertebrates, vertebrates, and palynomorphs) (Peterson and Ryder, 1975; Eaton, 1990). Figure 2 displays the age-relationships between Cretaceous strata in the Henry Mountains Syncline and neighboring regions in central and southern Utah. Peterson and others (1980) tentatively correlate the Muley Canyon Sandstone to the Star Point Sandstone in the Wasatch Plateau and Book Cliffs regions to the north and west. The Masuk Formation shares common palynomorph taxa with the Blackhawk Formation to the north (Wasatch Plateau and Book Cliffs) and a common mammalian fauna with the Wahweap Formation to the southwest (Kaiparowits Plateau), suggesting these formations are at least partially correlative (Eaton, 1990).

The evolution of stratigraphic nomenclature of the Muley Canyon Sandstone and the Masuk Formation in the Henry Mountains Syncline, as plotted in Figure 3, has been complex. Tabet (1999, 2000) provides a thorough review of stratigraphic nomenclature evolution. Herein, we adopt the stratigraphic scheme for the Muley Canyon Sandstone and Masuk Formation as proposed by Eaton (1990) because it is the most recent available and was developed based on investigations near Blind Trail, which is central to this study's area of investigation. In Eaton's (1990) scheme, the base of the Muley Canyon Sandstone is placed at the base of the lowest laterally persistent sandstone above the mudrock-dominated to heterolithic succession of Blue Gate Member of the Mancos Shale. The boundary between the Muley Canyon Sandstone and the Masuk Formation is placed at the base of the first coal or carbonaceous mudrock unit above the cliff-forming sandstone at the top of the Muley Canyon Sandstone. The Muley Canyon Sandstone and Masuk Formation are approximately 90 m (300 ft) and 200 m (650 ft) thick, respectively, at Blind Trail (reference and type section locality, respectively) (Eaton, 1990). The contact between the Masuk Formation and the overlying Tarantula Mesa Sandstone is marked by a sharp transition (erosionally-based) to coarse orange or pinkish trough cross-bedded sandstone. The Masuk Formation is divided into three informal members, the lower, middle, and upper. The "Muley Canyon Coal Zone" is found at the base of the lower member of the Masuk Formation, as earlier stratigraphic schemes placed the coal-bearing interval in the Muley Canyon Sandstone. The top of the lower member (~44 - 60 m thick, Eaton, 1990) is at the top of a broad sandstone bench below the more mudrock-dominated, slope-forming middle member (~120 m thick, Eaton, 1990). The base of the

Figure 1. Map of Henry Mountains Syncline, SE Utah, highlighting geologic units, and the area of investigation. Mancos includes Tununk, Ferron, Blue Gate, Muley Canyon, and Masuk.

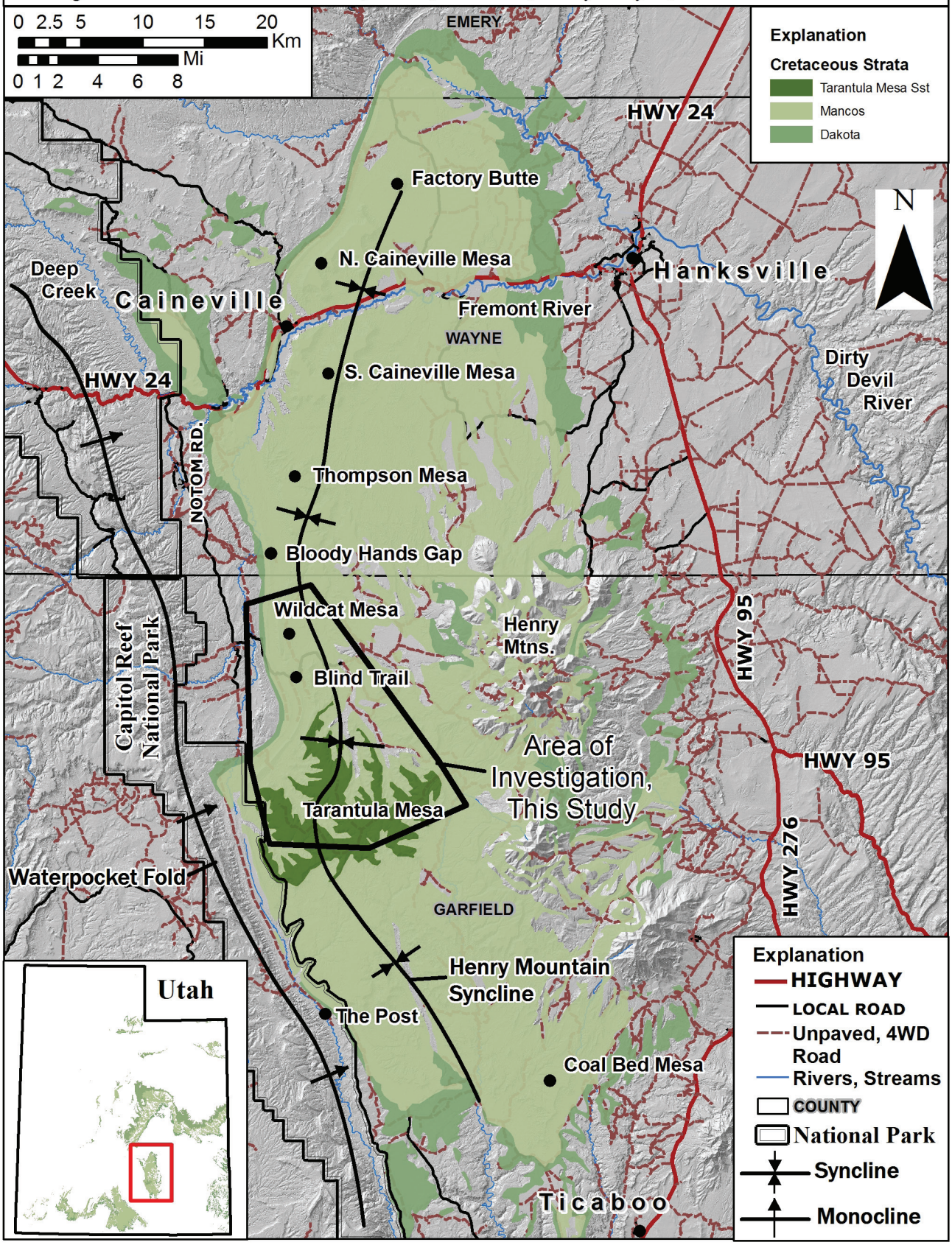

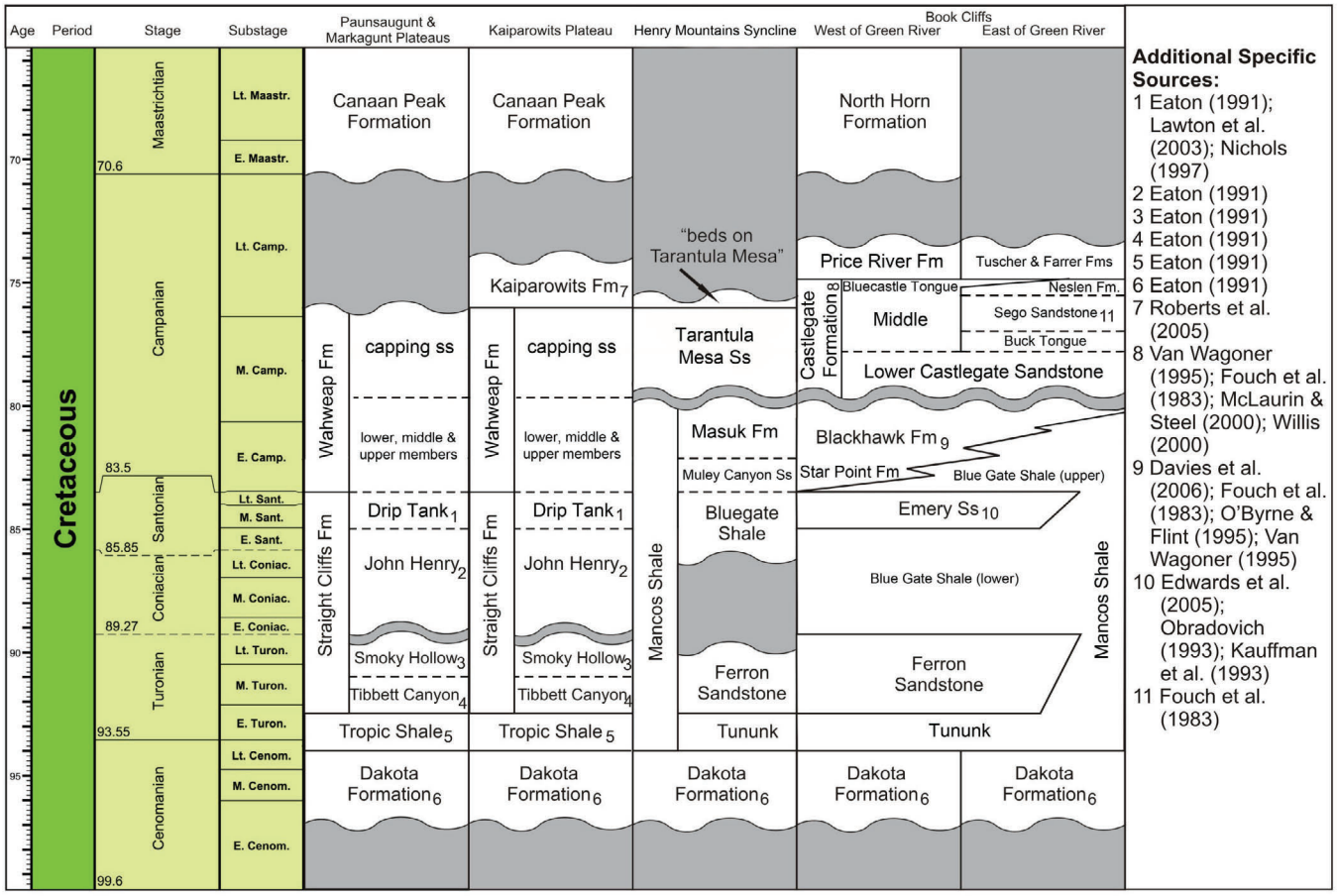

Figure 2. Time-space correlation of Upper Cretaceous stratigraphic units in Utah. Timescale created using T-S creator (Ogg, J. and Lugowski, A., 2007) utilizing the timescale of Gradstein et al. (2004). Main sources: Eaton (1990, 1991); Fouch et al. (1983); Roberts et al. (2005).

upper member (~38 m thick, Eaton, 1990) is placed at the base of the first thick sandstone above the mudrock-dominated middle member. Unfortunately, detailed geologic maps of the region predate Eaton's (1990) stratigraphic revision (Fig. 1), but Hunt and others' (1953) older, detailed geologic map is useful, when subsequent nomenclature revisions are considered (Fig. 4).

Existing paleoenvironmental interpretations of the Muley Canyon Sandstone and Masuk Formation have been both somewhat general in nature and varying. Earlier authors interpreted the Muley Canyon Sandstone as the record of a wave-dominated delta (Smith, 1983; Whitlock, 1984), a wave-dominated coastline (Eaton, 1990), or a coastal barrier environment (Peterson and others, 1980). Paleoenvironmental interpretations of the Masuk Formation have ranged widely from marine (Hunt and others, 1953) to dominantly nonmarine (Peterson and Ryder, 1975). Law (1980) and Eaton (1990) interpret the coal-bearing interval of the Masuk Formation to have been deposited as a series of tidally-influenced channels on a poorly drained coastal floodplain. The degree of marine influence in the middle and upper members of the Masuk Formation is debated, with interpretations ranging from a purely fluvial to estuarine channel and floodplain environment (Smith, 1983; Whitlock, 1984; Eaton, 1990; Corbett, 2009).

The Muley Canyon Coal Zone contains several individual coal beds that reach a total thickness of at least 1.5 m (5 ft) in most of the Henry Mountains Syncline region and reach a maximum aggregate thickness of 11.5 m (27.5 ft) (Tabet, 2000). Overall, the coal zone thins from west to east (Tabet, 2000), likely reflecting the shoreward to basinward paleogeographic transition from paralic coal to marine deposition, respectively. The coal zone is at shallow depths (< 30 m, < 100 ft) and is of sufficient thickness for surface mining operations under Wildcat Mesa, Cave Flat, and Swap Mesa (Tabet, 1999, 2000) (Fig. 1). However, the region is visible from the Capitol Reef National Park, so environmental constraints would likely hinder open-pit mining development (Tabet, 1999, 2000). Tabet (2000) proposed underground coal mining beneath Tarantula Mesa as a viable alternative, as the coal is thickest in this location, is covered by approximately 300 m (1000 ft) of overburden, and is accessible on the flanks of the mesa (Fig. 1).

METHODS

A full sedimentologic and stratigraphic analysis of the Muley Canyon Sandstone and Masuk Formation was performed using outcrop exposed mostly on the western and axial portions of the syncline, with one locality on the eastern limb of the syncline (Fig. 5). Separately, publicly available subsurface data from the Henry Mountains Syncline were compiled into a single ArcGIS® document. Because most wells were drilled as a part of earlier coal mining

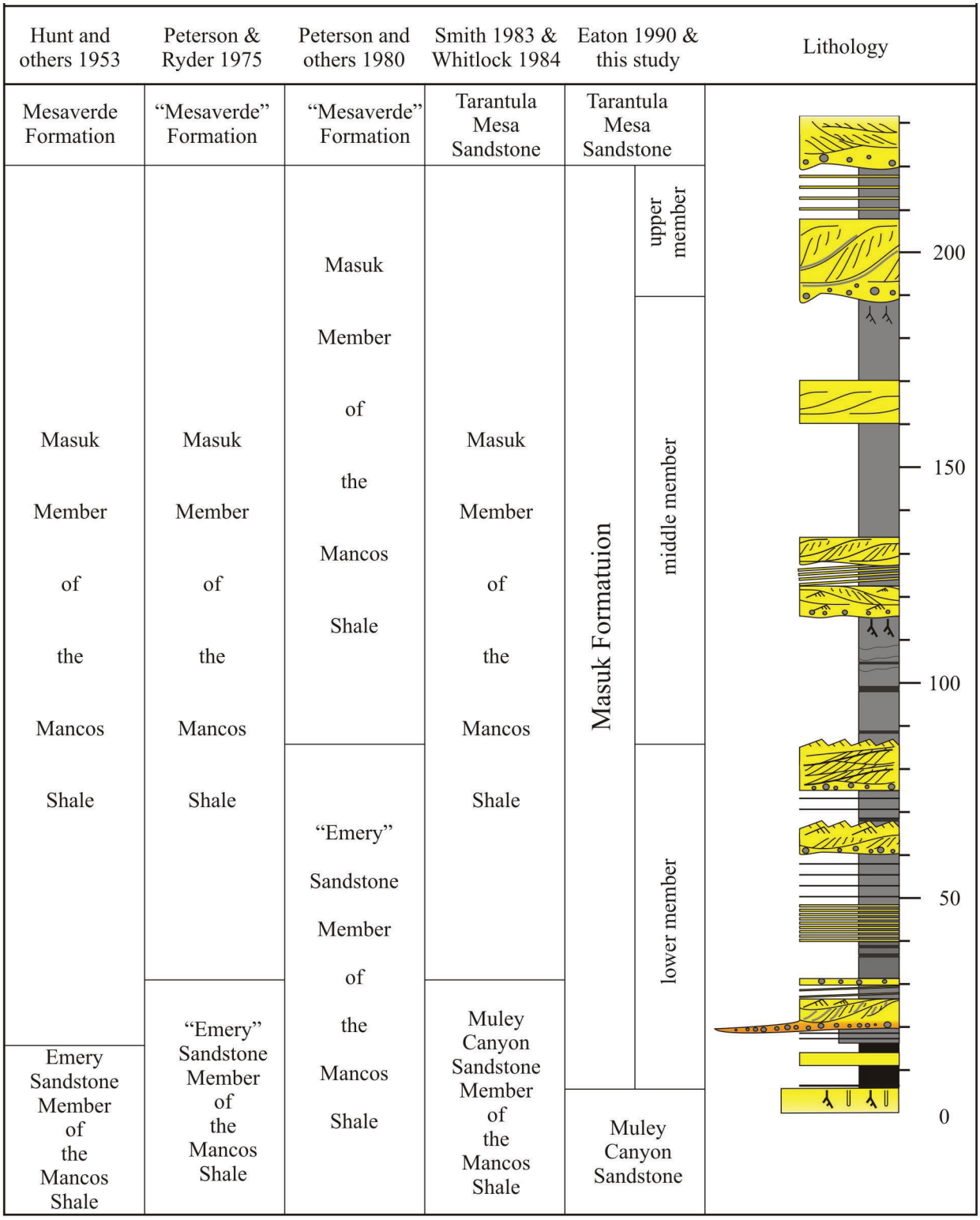

Figure 3. A summary table incorporating previous and up-to-date terminology for the upper reaches of the succession in the Henry Mountains Syncline. A stratigraphic column of the Masuk Formation type section (Section 1, this study; Appendix A) is shown alongside the nomenclature developed by Eaton (1990), which is used in this study. Numbers beside column indicate height from the base of the section in meters. Table modified from Eaton (1990).

Figure 4. Map of Henry Mountains Syncline with geology from Hunt and others (1953). Cretaceous units, as defined and mapped at the time include Kmv (Mesaverde Fmn.), Kmm (Masuk Mbr.), Kme (Emery Sst. Mbr.), Kmbg (Blue Gate Shale Mbr.), Kmf (Ferron Sst. Mbr.), Kmt (Tununk Shale Mbr.), Kd (Dakota Sst.).

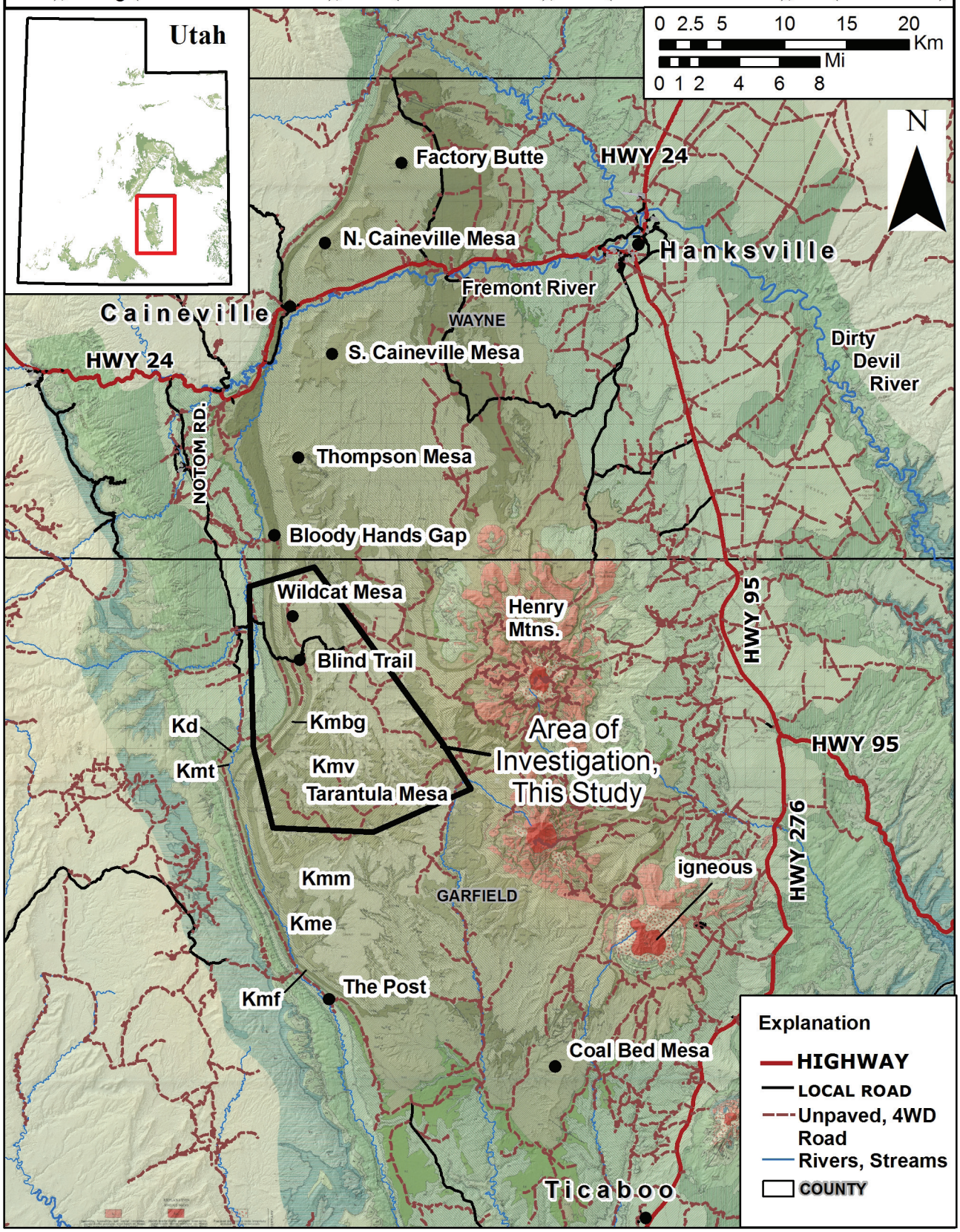

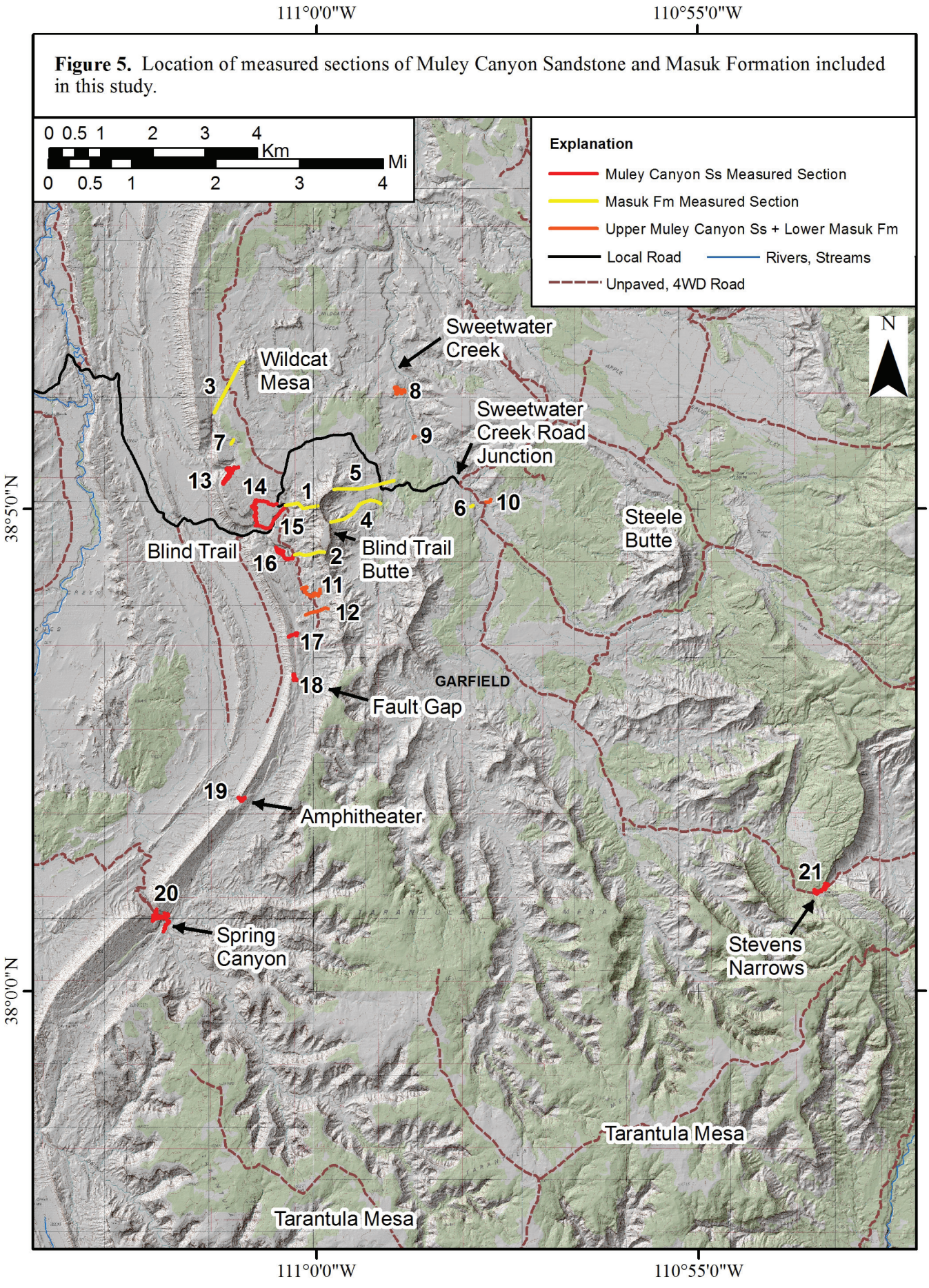

Figure 5. Location of measured sections of Muley Canyon Sandstone and Masuk Formation included in this study.

exploration efforts, the subsurface data available focus heavily on the stratigraphic window containing the Muley Canyon Coal Zone. Subsequently, measured sections and interpretations made from the outcrop surface analysis of the coal zone were tied into the subsurface in a series of correlation panels.

Outcrop Analysis

A total of 21 sections were measured for this study (Fig. 5). Sections #1-7 document the Masuk Formation, #13-21 the Muley Canyon Sandstone, and #8-12 the upper portion of the Muley Canyon Sandstone and the lower member of the Masuk Formation (Fig. 5). Locations of Muley Canyon Sandstone measured sections cover an area of ~84 km^2 (32 mi^2), and extend ~11 km (7 mi) along the prominent N-S-trending cliffs on the western limb of the syncline and ~14 km (9 mi) in the E-W direction (Fig. 5). Sections were measured where access could be gained up the steep cliff exposures of the Muley Canyon Sandstone on the west side of the syncline. Accessible exposure in the axial and eastern portions of the syncline is limited to a few quality exposures, several along Sweetwater Creek, at and to the north of the road crossing (axial, sections 8, 9, 10), and a second at Stevens Narrows (eastern limb, section 21; Fig. 5). These sections were examined in order to document any significant directional depositional trends. At each locality, conventional facies analysis was performed. Paleocurrent indicators were measured where available, and then compiled and plotted as rose diagrams in EZ-ROSE (Baas, 2000). The bioturbation index (BI) and trace fossil assemblage were noted throughout the succession using outcrop-based techniques as defined by Bann and others (2004), with BI ranging from 0 (bioturbation absent) to 6 (complete bioturbation, total biogenic homogenization of sediment). Continuous photomosaics of the cliff exposures on the west side of the syncline were taken, totalling a distance of 13 km from north to south. Facies architecture, key stratigraphic packages, and key surfaces were followed along the cliffs between measured section localities and marked on photomosaics (Fig. 6).

A hand-held Exploranium portable gamma ray spectrometer (model GR-256 with model GPS-21 detector) was used to obtain gamma ray readings from outcrop of the Muley Canyon Sandstone at Blind Trail (section 15; Fig. 5; Appendix A), using a ~1 m spacing between measurements and a 30 second count time. Total gamma ray (K + U + Th) was measured in parts per million (ppm) and then converted to and plotted in American Petroleum Institute (API) units, using a scale in which 0 - 20 ppm equals 0 - 150 API units. Because subsurface spectral gamma ray logs are not available in the region, spectral gamma ray measurements were not recorded.

Sections of the Masuk Formation, which include the Muley Canyon Coal Zone, cover an area of 22 km^2 (8.5 mi^2) at and around Blind Trail, ~ 6 km (3.7 mi) along a NNW-SSE trend and ~4 km (2.5 mi) along a WSW-ESE trend. Similarly, conventional facies analysis at each locality was combined with facies architectural analysis in the cliff, mesa, and badland exposures between sections (Fig. 6). Lithologic units forming the coal zone were carefully followed and walked out to the south of Blind Trail, over a distance of ~2.5 km (1.5 mi). Measured sections of the coal zone were correlated over a ~12 km^2 (5 mi^2) area (Fig. 6). Hand-held gamma ray spectrometer readings were obtained from outcrop of the Muley Canyon Coal Zone at the North Sweetwater Creek locality (section 8; Fig. 5; Appendix A), as the coal zone is best-exposed here. Measurements were obtained using the same instrumentation, techniques, and parameters as described for the Muley Canyon Sandstone.

Compilation of Subsurface Data: ArcGIS® Document

In this study, we provide a compilation of previous surface and subsurface data and our data from the Henry Mountains Syncline, placing all the datasets into a common spatial framework using ArcGIS® (Appendix B; Supplementary File 1). This allows for surface to subsurface correlation performed in this study and builds a database foundation onto which future work can add. Available well data and drilling reports were scanned and georeferenced into a common ArcGIS® document, composing a spatially-linked database of subsurface data. Appendix B describes the contents of this ArcGIS® document and contains instructions for its use. Publicly available well locations and scanned images of well data from the Henry Mountains Syncline, including wireline logs, lithologic logs, and well reports, were provided by the Utah Geological Survey. The region contains 151 wells drilled during the period of 1968-1977, by a number of parties interested in developing coal mining operations (AMAX Coal Company, Cayman Corporation, Consolidation Coal Company, Gulf Mineral Resources, and U.S. Geological Survey [USGS]) (Fig. 7; Appendix C). Wireline logs and/or lithologic data from 118 of the 151 wells are available and hyperlinked to their respective locations in the ArcMap® document (Supplementary File 1; Appendix C). The suite of wireline logs available from each well varies, but includes gamma ray, bulk density, gamma density, caliper, and resistivity logs. In some wells, written or graphical lithologic logs are available in lieu of wireline logs. The mappable extent of subsurface coal greater than 4 ft in thickness, as determined by Tabet (2000), is plotted in the ArcMap® document (Appendix B; Supplementary File 1). None of the oil and gas wells drilled in the region capture data from the Muley Canyon Sandstone or Masuk Formation (Appendix B; Supplementary File 1).

Two key datasets from past surface investigations of the Henry Mountains Syncline were georeferenced and included in the ArcGIS® document: 1) 321 surface measured sections of the Muley Canyon Coal Zone throughout the syncline (Law, 1979a, b), and 2) a detailed early geologic map of the region (Hunt and others, 1953). Useful reference layers, such as a UGS generalized geologic map, a 5-m (16.4-ft) resolution digital elevation model (DEM), and topographic maps of the region are also displayed (Appendix B; Supplementary File 1).

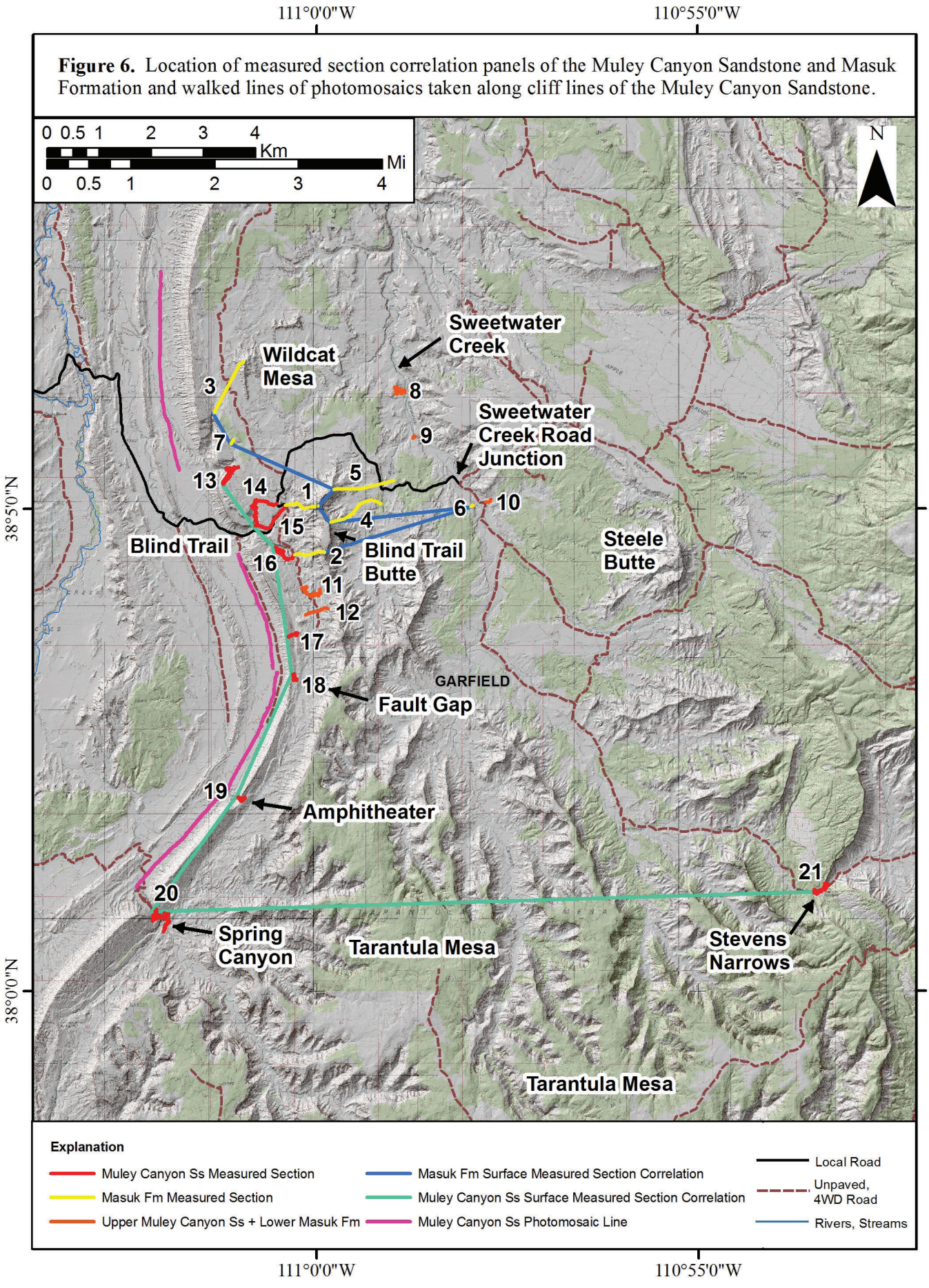

Figure 6. Location of measured section correlation panels of the Muley Canyon Sandstone and Masuk Formation and walked lines of photomosaics taken along cliff lines of the Muley Canyon Sandstone.

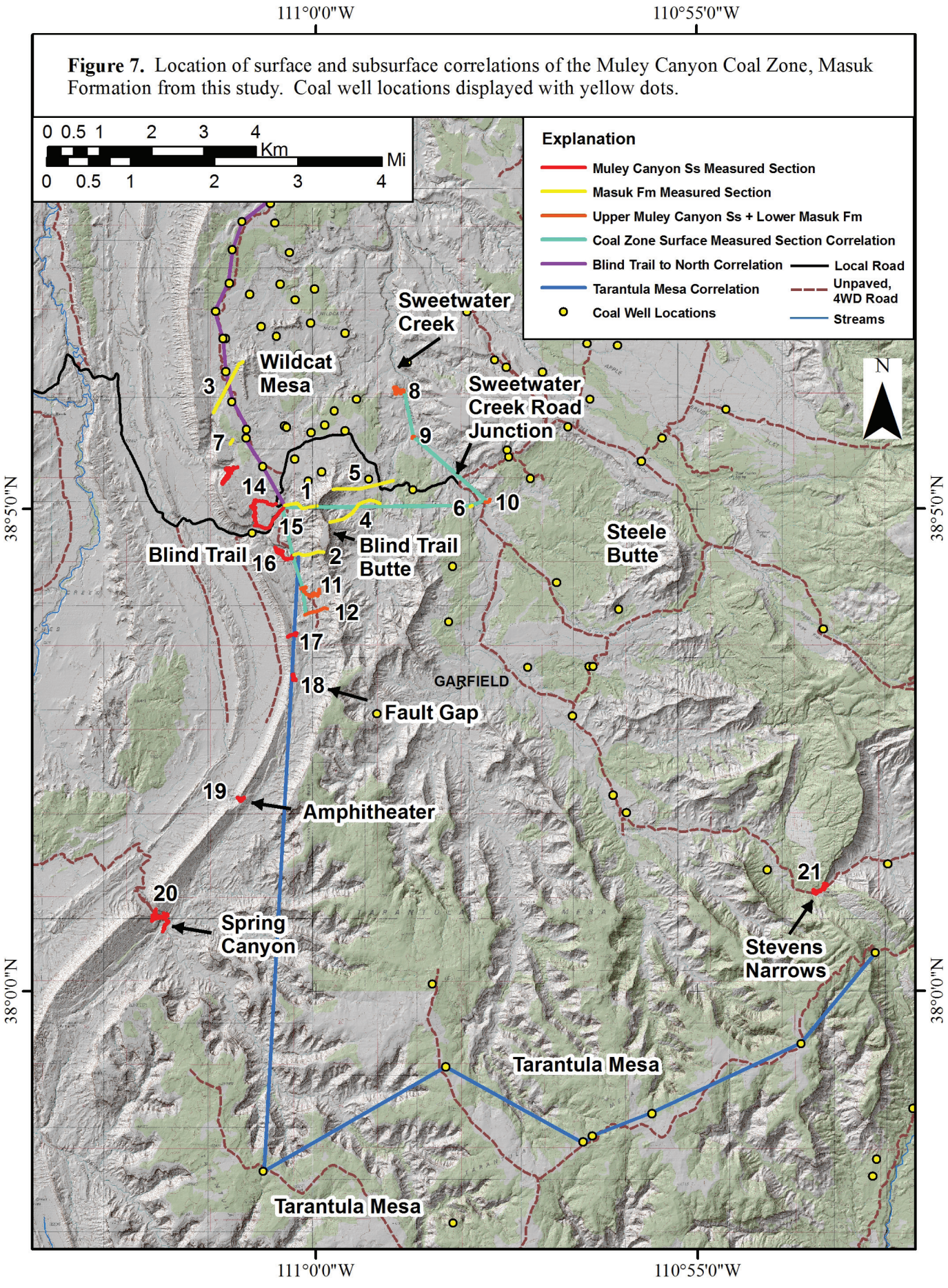

Figure 7. Location of surface and subsurface correlations of the Muley Canyon Coal Zone, Masuk Formation from this study. Coal well locations displayed with yellow dots.

Correlation of Coal Zone

This study integrates new outcrop based data and interpretations with the subsurface coal zone data that is available. Three correlation lines were chosen that utilize surface and/or subsurface datasets: 1) a N-S transect of measured sections of the coal zone, between which units were followed to assess lateral continuity and architectural geometric relationships (sections 1, 2, 6, 8-12), 2) a 14 km (8.7 mi) W-E transect across Tarantula Mesa using seven USGS and Gulf Mineral Resource wells and accompanying wireline log suites that is tied to a surface measured section 11.9 km to the north, and 3) a 6.5 km (4.0 mi) S-N transect extending north from Blind Trail and including three measured surface sections (#1, 3, 15), one subsurface lithologic log from a USGS well, and ten wireline logs from AMAX wells (Fig. 7). Correlated horizons include formation boundaries, laterally persistent units within the coal zone, and key sequence stratigraphic surfaces, as designated by outcrop analysis.

MULEY CANYON SANDSTONE

Paleoshoreline Orientation

Paleocurrent analysis of the Muley Canyon Sandstone indicates a dominant offshore direction to the E-SE. This direction is based on 1) dip direction measurement of a clinoform set in the top of Blue Gate Member (142°, n = 3), and 2) a total of 463 paleocurrent measurements throughout the Muley Canyon Sandstone on unidirectional features including trough cross-bed sets, ripple cross lamination, convolute bedding, and low-angle dipping surfaces and bidirectional features including wave ripples. Rose diagrams are plotted in measured sections (Appendix A, Plates 1, 2, 4, and 5). Paleocurrent measurements throughout the Muley Canyon Sandstone vary between localities and stratigraphic units, as might be expected, particularly in bimodal systems, but indicate an overall E-SE-directed sediment transport pattern. Therefore, the paleoshoreline was likely oriented in the NNE-SSW direction. Modern-day cliff exposures of the Muley Canyon Sandstone investigated here are oriented roughly N-S and, hence, represent a view strike parallel to slightly oblique (Fig. 5). The locality at Stevens Narrows, the most E-SE locality, provides the most basinward or depositional down-dip view of the Muley Canyon Sandstone (Fig. 5).

Lithofacies Analysis

The Muley Canyon Sandstone contains seven major lithofacies (1-7), that can best be grouped into six depositional environments, representing various shallow marine to continental environments of deposition, including deltaic mouthbar, offshore transition, shoreface, fluvial to tidally-influenced channels, estuarine channels, and estuarine mouth deposits (Table 1; Figs. 8 - 9). Measured sections 8, 9, 11, 12, and 16-21 detail the Muley Canyon Sandstone and are found in Appendix A.

Facies 1: Deltaic Mouthbar Deposits

The basal fine-medium grained sandstone unit of the Muley Canyon Sandstone, informally designated as unit A herein, displays characteristic unidirectional low-angle dipping surfaces (facies 1; Table 1; Figs. 8 - 9). The base of the unit is erosional, whereas the top is bioturbated with *Ophiomorpha*, *Conichnus*, *Thalassinoides*, *Diplocraterion habichi*, and *D. parallelum*, with a bioturbation index (BI) ranging from 0 at the base up to 2 at the top of the bed. This unit is thickest at Blind Trail, South Gully (section 16) and expresses an overall thinning in the depositional down-dip direction toward the SE (Plates 1 - 2). Laterally to the S the unit becomes indistinguishable from the underlying and overlying strata grading into interbedded sandstone and siltstone. The underlying Blue Gate Member of the Mancos Shale at Blind Trail is interpreted to have been deposited in a prodelta to middle delta front environment, and it contains several hallmark indicators of deltaic influence including suppressed bioturbation, synaeresis cracks, common soft sediment deformation in the form of profoundly deformed horizons, convolute bedding and load casts, and one heterolithic clinoform set indicating a SE regional dip slope direction (142°, n = 3). In association with the underlying Blue Gate Member, unit A is interpreted as the record of deltaic mouthbar deposition (Figs. 8 - 9). Paleocurrent directions from this unit vary with locality, ranging from N to SE, but average to an eastward (097°, n = 14) sediment dispersal direction overall. Variations between localities are not surprising considering many modern and ancient deltaic systems illustrate an overall radial pattern of sediment dispersal through an amalgamation of lobes through time (Olariu and Bhattacharya, 2006). To the south (roughly strike parallel), the unit grades into facies 2.

Facies 2: Offshore Transition Deposits

Heterolith, specifically interbedded and interlaminated sandstone and siltstone with plane-parallel laminated to hummocky cross-stratified or rippled sandstone beds, characterizes facies 2 (Figs. 8 - 9). In general, this facies is poorly exposed, but where well-exposed, the base and top of sandstone beds display long wavelength undulating bedding surfaces, some amalgamated sandstone beds, and bioturbation. BI reaches 2-3 locally in well-exposed intervals. At Blind Trail, bivalve shells are present. Due to the presence of bioturbation, shell material, hummocky cross-stratification, and significant mudrock content, this facies is interpreted to have been deposited above storm wave base but below fair weather wave base, representing deposition in the offshore transition realm of the shallow marine system (Figs. 8 – 9). Offshore transition deposits are found within informal Muley Canyon Sandstone units B and D (Plates 1 – 2).

Facies 3: Shoreface Deposits

Facies 3 contains fine- to coarse-grained amalgamated, tabular, yellow to brown sandstone beds dominated by hummocky cross-stratification, and low angle and plane-parallel lamination

Table 1. - *Lithofacies of the Muley Canyon Sandstone*

Facies	Facies Description	Depositional Environment	Informal unit designation (in stratigraphic order)
1	Fine to medium sandstone containing unidirectional low angle dipping surfaces; erosionally-based; top of beds bioturbated with *Ophiomorpha, Conichnus, Thlassinoides, Diplocraterion Habichi, D. parallelum* ; bioturbation index ranging from 0 at base of bed up to 2 at top of bed.	Deltaic mouthbar	Unit A, basal unit of Muley Canyon Sandstone
2	Interbedded sandstone and siltstone; plane-parallel lamination, hummocky cross-stratification; current, wave, or wave-modified current ripples present; base and top of sandstone beds display long wavelegth undulating bedding surfaces; sandstone beds amalgamated in places; bioturbation index of 2-3 in well-exposed intervals	Offshore transition	Unit B & D, overlies Unit A and Unit 3
3	Amalgamated, tabular sandstone; fine to coarse-grained with medium-grained sandstone dominant; dominated by hummocky cross-stratification with secondary plane-parallel lamination and low angle lamination; siltstone and heterolithic partings present locally; deep vertical to sub-vertical trending burrows at the top of sandstone beds; bioturbation index ranging from 0 to 2, with 1-2 at the tops of sandstone beds; traces include *Ophiomorpha, Cylindrichnus, Diplocraterion habichi, D. parallelum, Planolites, and Fugichnia*	Shoreface	Unit B & D, Unit D overlies Unit C
4	Heterolithic channel fill containing trough-cross bedded sandstone, carbonaceous partings, mud drapes, current ripples, and wave-modified current ripples; bimodal paleocurrent trends present; interlaminated and interbedded sandstone and siltstone beds exhibit channel forms, accretionary surfaces, and inclined heterolithic strata in places; complex, multi-storey channel fills evident; siltstone and heterolithic rip-up clasts, carbonaceous foreset laminae, plant debris, and petrified wood common; largely unbioturbated with minor bioturbation in siltstone parting at one locality	Fluvial to tidally-influenced channels	Unit C, overlies Unit B
5	Large-scale trough cross-bedded (50cm to several meter sets), medium sandstone; overall sheet architecture with internal channel forms evident; no bioturbation evident	Fluvial to tidally-influenced channels	Unit C, overlies Unit B
6	Smaller-scale (10cm to 1 m) trough cross-bedded fine to medium sandstone; herringbone cross-stratification and bimodal paleocurrent trends present; internal channel forms evident with multistorey architecture; siltstone and heterolithic partings evident locally; rhythmically interlaminated sandstone and carbonaceous siltstone present locally; bioturbation absent excepting some localities that display sub-tending burrows at the top of the channel complex	Estuarine channels	Unit E, overlies Unit D
7	Plane-parallel laminated to low angle laminated fine to medium sandstone; bioturbation commonly present at the top of the unit (sub-tending burrows common); locally heterolithic.	Estuarine mouth	Unit E, overlies Unit D; directly overlies estuarine channels

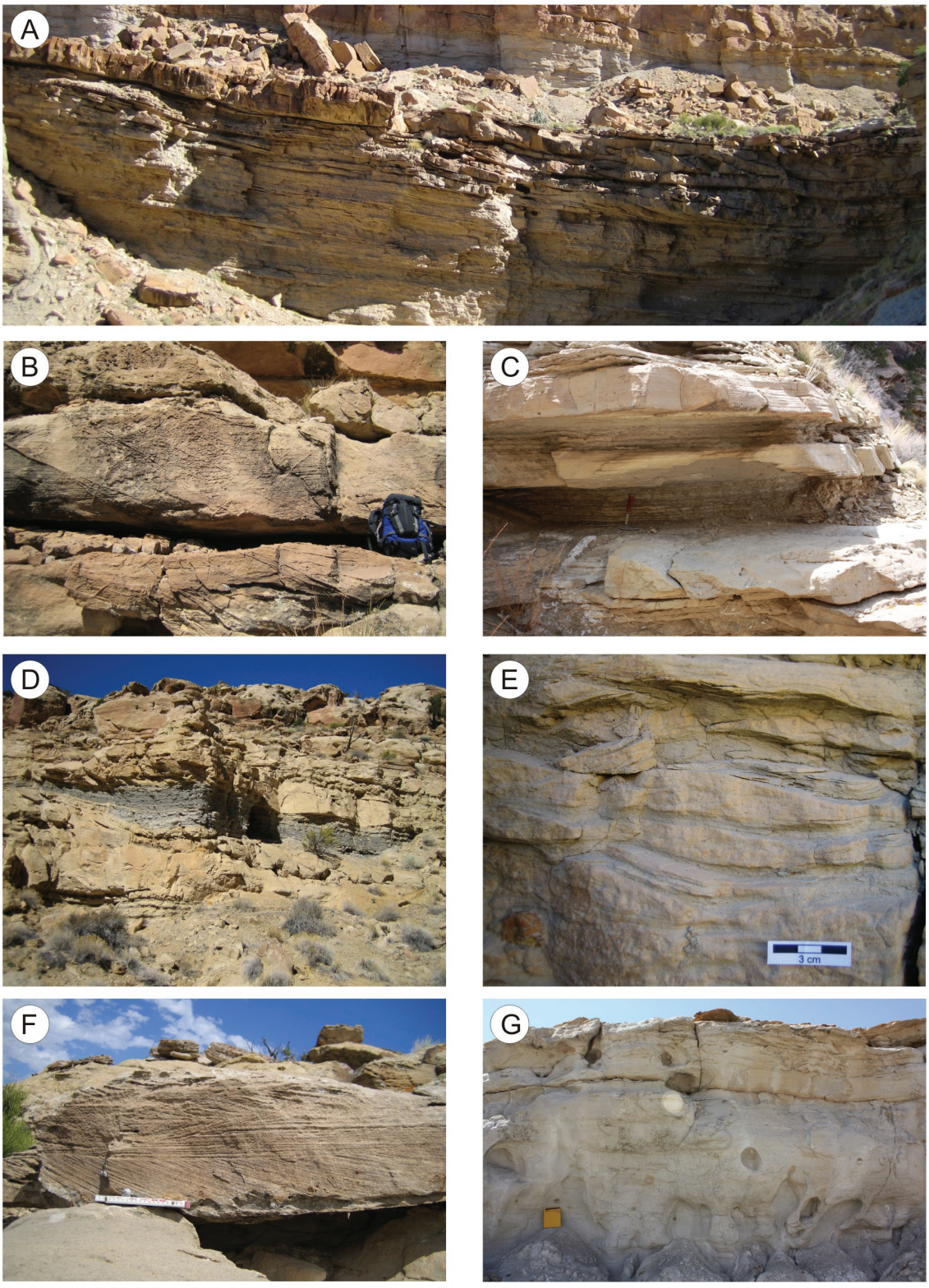

Figure 8. Facies of the Muley Canyon Sandstone. A) Facies 1, deltaic mouthbar deposit, illustrating erosional base and low angle unidirectional dipping surfaces. B) Facies 3, shoreface deposit, displaying low-angle to hummocky cross-stratification within amalgamated, tabular sandstone displaying local siltstone partings. Backpack for scale. C) Facies 2, offshore transition deposits, comprised of heterolith, specifically interbedded and interlaminated sandstone and siltstone. Bioturbation evident. Hammer for scale. D) Facies 4, fluvial to mixed energy channel deposits, illustrating characteristic features of heterolithic channel fill, including multi-storey architecture with internal channel forms. E) Evidence for tidal influence in the form of current-modified wave ripples and mud drapes within facies 4. 3 cm scale. F) smaller-scale (10 cm to 1 m) trough cross-bedded white sandstone characteristic of facies 6, estuarine channel deposits. G) Facies 7, estuarine mouth deposits, dominated by plane-parallel lamination. Field book for scale.

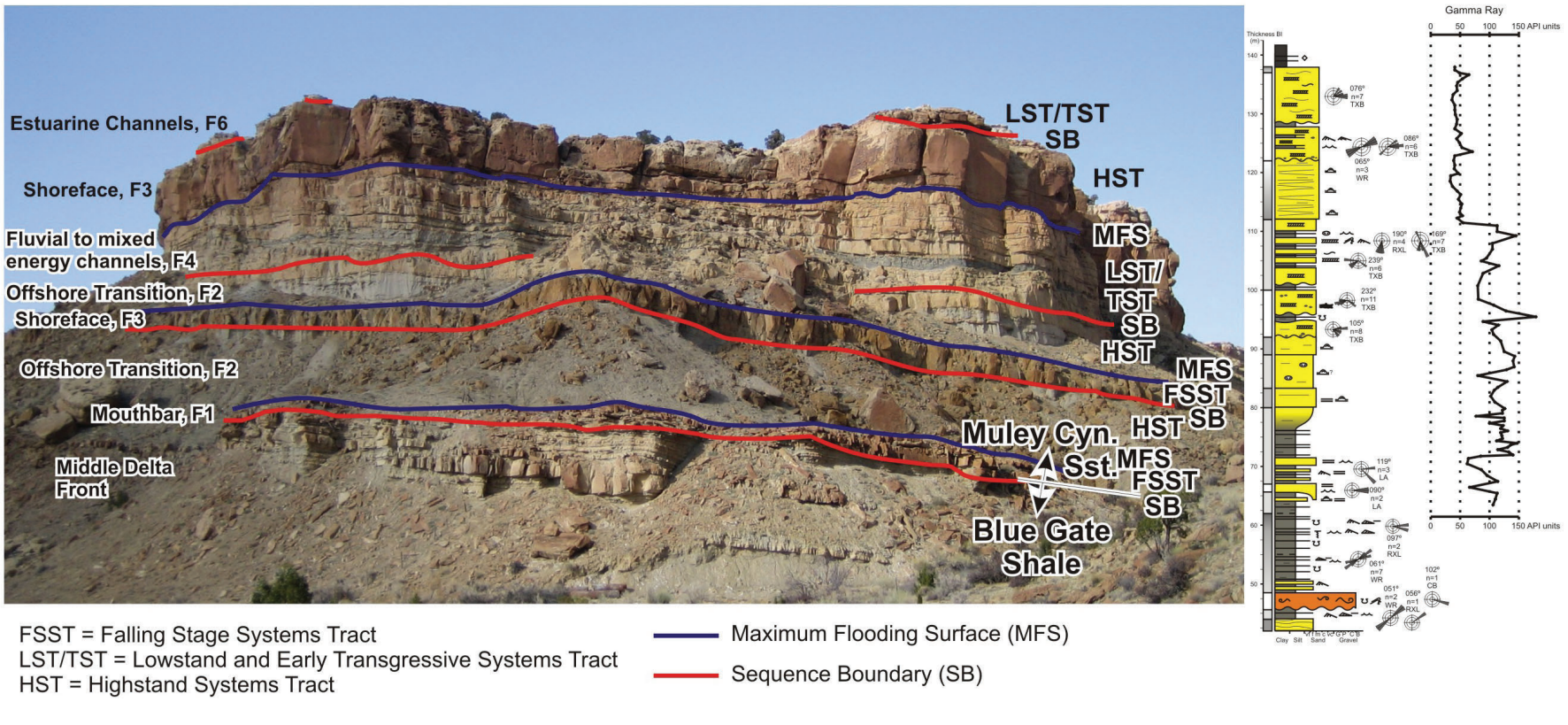

Figure 9. Illustration of measured section, outcrop gamma ray, facies character and architecture, and sequence stratigraphic interpretations from the Muley Canyon Sandstone at Blind Trail (Reference Section). F1 = Facies 1, F2 = Facies 2, etc., Exposed Muley Canyon Sandstone in photo is approximately 65 m thick.

(Figs. 8 - 9). Local siltstone partings are present. Such features are typical of deposition above fair weather wave base, in the shoreface environment (Figs. 8 - 9). Deep vertical traces are present at the top of sandstone beds, including *Ophiomorpha*, *Cylindrichnus*, *Diplocraterion habichi*, *D. parallelum*, *Planolites*, and *fugichnia*. BI ranges from 0 - 2, with a significant increase at the top of sandstone beds, indicating relative depositional quiescence in the shoreface realm. Shoreface deposits occur in units B and D and are laterally and vertically transitional with offshore transition deposits. For instance, along a N-S transect oblique to depositional dip, unit D transitions from cliff-forming shoreface deposits at Blind Trail (sections 13 – 16) to offshore transition deposits to the south (sections 17 – 18) and back to shoreface deposits even farther south at the Amphitheater, Spring Canyon, and Stevens Narrows (sections 19 – 21) (Plate 1).

Facies 4 and 5: Fluvial to Tidally-influenced Channel Deposits

Erosionally-based, heterolithic channel-fill deposits (Facies 4) contain trough cross-bedded and rippled fine- to medium-grained sandstone with carbonaceous siltstone interbeds and interlaminations (Figs. 8 – 9). Tidal indicators, such as rhythmically laminated sandstone and siltstone, mud drapes, wave-modified current ripples, and bimodal paleocurrent measurements, are common but not universal (Fig. 8). Paleocurrent measurements on trough cross-bed and ripple cross-lamination sets from within this unit indicate bimodality at all localities, though the directions vary between localities. In general though, measurements indicate a primary eastward to southward (offshore-directed) sediment dispersal direction, with a secondary southwest to northwest (onshore-directed) sediment dispersal direction (Appendix A; Plates 1, 2, 4, and 5). Downdip, at Stevens Narrows (section 21), predominantly southwesterly paleocurrent measurements indicate onshore-directed currents are dominant in a more basinward location.

Facies 4 displays multi-storey, amalgamated, channel-fill geometry with accretionary surfaces and inclined heterolithic strata. The bases of channel bodies contain siltstone and heterolithic rip-up clasts ranging from several cm to 2 m (6.5 ft) in size, forming intraclast breccias, in some cases.

Carbonaceous foreset laminae and plant debris are also common in Facies 4. Broad leaf plant fossils are observed at the Blind Trail, South Gully locality. Petrified wood is common at the base of these deposits. This facies is largely unbioturbated, with the exception of minor bioturbation in a siltstone parting within the unit at one locality (1st Gully North of Blind Trail, section 13) and bioturbation at the top of the unit at two other localities (Dripping Rock Seep, section 9; Stevens Narrows, section 21).

Facies 4 is laterally transitional with Facies 5, which comprises large-scale (50 cm to several m, 20 in to 10 – 13 ft sets) trough cross-bedded medium sandstone with uncommon local siltstone partings. Internal channel forms are evident in Facies 5 among an overall sheet architecture (Fig. 9).

Facies 4 and 5 are defined informally as unit C, herein. Unit C is sharply bounded at the base and top, is regionally extensive over the ~100 km^2 (40 mi^2) area of investigation, and is always found in the same stratigraphic position overlying unit B. The thickness of unit C varies, documenting incision at its base. Due to the regional extent of erosion recorded by the basal surface and significant tidal influence within the channel fill deposits, we interpret Facies 4 and 5 (unit C) to record a fluvial to tidally-influenced channel environment within a fluvial-estuarine facies model context (sensu Dalrymple and others, 1992; Plink-Bjorklund, 2005; Boyd and others, 2006). Facies 4 and 5's (unit C's) extent contrasts with deltaic distributary channels which are typically more areally restricted in their extent. Furthermore, sedimentologic evidence of deltaic influence is lacking above the basal sandstone unit (deltaic mouthbar, unit A) of the Muley Canyon Sandstone.

Facies 6: Estuarine Channel Deposits

Facies 6 typically comprises fine- to medium-grained, white, trough cross-bedded sandstone (Fig. 8). Cross-set thickness is typically less than that of Facies 4 (0.1 – 1.0 m, 0.3 – 3.3 ft sets). Internal channel forms are evident within a multi-storey architecture that forms a sheet sandstone. Siltstone and heterolithic partings are locally evident. Current ripples, wave-modified current ripples, and wave ripples are present, with current ripples and wave-modified current ripples more common at the base of the unit and wave ripples near the top, illustrating transgression. The white color, also known as "white caps", is attributed to chemical alteration from the overlying coal zone. Tidal indicators, such as herringbone cross-stratification and bimodal paleocurrent trends are common, and rhythmically interlaminated sandstone and carbonaceous siltstone and mud drapes are present locally. Bioturbation within this facies is absent with the exception of two localities that display bioturbation at the top of the channel complex. Similar to Facies 4, Facies 6 exhibits bimodal paleocurrent trends at all localities, though directions vary between localities. In contrast to Facies 4, Facies 6 exhibits a stronger bimodality with more onshore-directed measurements. Onshore-directed measurements from Facies 6 range from SW to NE and balance or outweigh offshore-directed measurements (roughly NE to SW). Because Facies 6 is more sandstone-prone overall than Facies 4 and because the abundance of onshore-directed paleocurrent measurements indicate more seaward or basinward depositional position relative to Facies 4, Facies 6 is interpreted as estuarine channel deposits (Fig. 8), within a fluvial-estuarine facies model context (*sensu* Dalrymple and others, 1992; Plink-Bjorklund, 2005; Boyd and others, 2006). Specifically, this facies likely records seaward tidal bar forms such as those documented in Eocene tide-dominated estuarine deposits of the Central Basin, Spitsbergen (Plink-Bjorklund, 2005). Facies 6 makes up the basal portion of unit E.

Facies 7: Estuarine Mouth Deposits

Plane-parallel laminated to low-angle laminated, fine- to medium-grained, white sandstone and local heterolith typify Facies 7 (Fig. 8). Bioturbation is commonly found at the top of the sandstone unit. Siltstone is commonly carbonaceous, and carbonaceous material

is found within sandstone units. This facies where present, always overlies Facies 6 and underlies the coal zone in the overlying Masuk Formation. Hence, it comprises the upper portion of unit E. Because Facies 7 is associated with Facies 6, contains evidence of transgression at the top of the unit in the form of bioturbation, and is dominated by plane-parallel to low-angle lamination, this facies is interpreted as an estuarine mouth deposit. It shares similar characteristics to basinward, upper flow-regime, tidal flat deposits documented by Plink-Bjorklund (2005).

Stratigraphic Architecture

Over the ~100km^2 (40 mi^2) areal extent of the eleven Muley Canyon Sandstone localities examined, units A – E are consistent in their stacking pattern and thickness, and their defining basal and upper boundaries can be correlated along cliff exposures (Fig. 9; Plates 1, 3). For instance, fluvial to tidally-influenced channel deposits (Facies 4 and 5, unit C) consistently underlie shoreface deposits (Facies 3, unit D) which, in turn, are directly overlain by estuarine channel deposits (Facies 6, unit E) (Fig. 9). The thickness of fluvial to tidally-influenced channel and estuarine channel and mouth deposits (units C and E) varies between localities, likely reflecting the depth of incision into the underlying shallow marine units (Plate 1). Some lateral and downdip changes are documented, including mouthbar deposits grading into offshore transition deposits to the south, oblique to the down-dip direction (unit A; Plate 1). Additionally, cliff-forming shoreface deposits (Facies 3, unit D) at Blind Trail pass southward into mudrock-bearing offshore transition deposits (Facies 2, unit D) and back again to cliff-forming shoreface deposits (Facies 3, unit D) further south at the Amphitheater and Stevens Narrows (Plate 1). Finally, an erosionally-based shoreface deposit (Facies 3) within unit B at Blind Trail grades laterally into offshore transition deposits (Facies 2) to the south (Plate 1).

Examination of the Muley Canyon Sandstone at its farthest down-dip depositional location, Stevens Narrows, reveals several key patterns: 1) the major cliff-forming shoreface deposit (Facies 3, unit D), is considerably thicker there than other localities (at least 7 m, 23 ft), 2) fluvial to tidally-influenced and estuarine channel deposits (Facies 4 and 6, units C and E) indicate dominantly onshore-directed paleocurrent directions (SW), 3) estuarine mouth deposits (Facies 7) are thicker and estuarine channel deposits (Facies 6) are thinner than other localities, 4) the deltaic mouthbar deposit (Facies 1, unit A) is thinner (Plate 1). All of these down-dip changes are consistent with a more basinward position in the depositional system.

Sequence Stratigraphic Interpretation

Key erosion and flooding surfaces are regional in extent (Plates 2 - 3). This observation is based on: 1) documentation at each of the eleven localities examined (Plate 2), and 2) tracing of key surfaces along well-exposed cliff lines (Plate 3). Four sequence boundaries and maximum flooding surfaces and, hence, four sequences within the Muley Canyon Sandstone are identified (Plate 2). These four sequences are arranged into two higher-order sequence sets (Plate 2). Each of the high-frequency sequences, in stratigraphic order, are described below, followed by a description of the lower-frequency sequence sets.

High-frequency Sequences

The first sequence boundary (SB) is at the base of the Muley Canyon Sandstone (base of unit A, facies 1, deltaic mouthbar deposit) (Plate 2). This erosion surface extends to the north of Blind Trail and down depositional dip to Stevens Narrows but becomes a correlative conformity within the upper Blue Gate Shale at Sections 19 and 20 to the south, oblique to dip direction. The top of this mouthbar deposit is sharp and bioturbated, and, hence, interpreted as a maximum flooding surface (MFS). The mouthbar unit 1) truncates a shallowing-upward deltaic succession in the Blue Gate Member below, expressing a foreshortened stratigraphy, 2) is sharp-based, and 3) lacks coeval coastal plain strata. The presence of these key diagnostic characteristics suggests the unit records forced regression and comprises the falling stage systems tract (FSST) (Posamentier and Allen, 1999; Plint and Nummedal, 2000; Posamentier and Morris, 2000; Howell and Flint, 2003). This, in turn, is overlain by offshore transition deposits (Facies 2), which are interpreted as the highstand systems tract (HST). In this case, the lowstand and transgressive systems tracts are likely missing.

The second SB is placed at the sharp base of the shoreface deposit (Facies 3) within unit B (Plate 2). The shoreface unit is erosionally-based at Blind Trail. This surface can be followed to the north of Blind Trail and to the south, where it becomes a correlative conformity. The top of the unit is interpreted as a MFS because it is sharp, bioturbated, and traceable over several km. Similar to the underlying sequence, the shoreface unit truncates a shallowing-upward succession abruptly, expresses a foreshortened stratigraphy, is sharp-based, and lacks coeval coastal plain strata suggesting it records forced regression and the FSST (Posamentier and Allen, 1999; Plint and Nummedal, 2000; Posamentier and Morris, 2000; Howell and Flint, 2003). Again, offshore transition deposits (Facies 2), interpreted as the HST, overlie the sharp-based shoreface deposit (Facies 3).

The third sequence is bound by a prominent SB at the base of the fluvial to tidally-influenced channel deposits (Facies 4 and 5, unit C; Plate 2). This surface is expressed as either a sandstone-on-sandstone or carbonaceous siltstone-on-sandstone contact. Picking the SB in the cliffs from a distance can be difficult, as the sandstone on sandstone contact is cryptic and the siltstone on sandstone contact is often obscured by colluvial debris. However, heterolithic expressions of the fluvial to tidally-influenced deposits (facies 4) are easily recognizable in well-exposed cliffs. The SB marks relative sea level fall and regional fluvial incision. The authors were unable to document the edge of the incised system in the ~100 km^2 (40 mi^2) study area. Judging from the low-relief, low-gradient nature of the SB, incision was shallow and covered a wide area. Based on a regional SE dip direction and the location of measured sections, we deduce that the incised system was at least

10 km (6 mi) wide. The thickness of channel fill preserved suggests incision of no more than 20 m (66 ft), but typically 10 – 15 m (33 – 50 ft). The multi-storey fluvial to tidally-influenced channel fill deposits (Facies 4 and 5, unit C) are topped by a regionally extensive MFS. We interpret the fluvial to tidally-influenced channel deposits (Facies 4 and 5, unit C) to comprise the lowstand systems tract (LST) and/or early trangressive systems tract (TST). The authors were unable to identify a transgressive surface (TS) in the succession. The MFS is overlain by a tabular shoreface deposit (Facies 3, unit D), which is interpreted as the HST.

The base of the fourth sequence is defined by a SB at the base of the estuarine channels (Facies 6, unit E) (Plate 2). This surface also marks shallow regional incision. Again, the margins of the incisional area were not found within the study area. Estuarine channel and estuarine mouth deposit thicknesses suggest incision up to 20 m (66 ft), but typically 10 – 15 m (33 – 50 ft). The estuarine channel deposits are interpreted to represent the LST and/or early TST. The vertical transition from dominantly trough cross-bedded sandstone in the estuarine channel deposits to dominantly plane-parallel to low-angle laminated sandstone in the estuarine mouth deposits is interpreted to mark the TS. Bioturbation at the top of unit 5 is further evidence of transgression. Therefore, the estuarine mouth deposits are interpreted to comprise the TST. Again, delineation of the LST and TST within this package is debatable. However, evidence of transgression is documented, suggesting both the systems tracts are likely represented. The overlying MFS is found within the coal zone in the Masuk Formation and is documented in the "Muley Canyon Coal Zone" section of this report. The SB bounding the top of the fourth sequence is found in the lower member of the Masuk Formation at the base of the first major laterally extensive sandstone channel belt and is documented in the "Masuk Formation" section of this report.

Lower-frequency Sequence Sets

The basal two sequences are interpreted to comprise the falling stage sequence set as they uniquely contain a FSST. The second sequence is interpreted to be a more distal equivalent of the first because the FSST in the second sequence is composed of a shoreface deposit, whereas the FSST in the first sequence contains a more shoreward mouthbar deposit. Both of the bounding surfaces at the base of these sequences become correlative conformities basinward and the units become an undifferentiated succession of offshore transition deposits.

The upper two sequences are thought to represent the transgressive sequence set. Both of these sequences feature the LST/ TST prominently, in contrast to the two sequences below. Furthermore, estuarine channel deposits that comprise the LST/ TST of the fourth sequence were deposited basinward relative to the fluvial to tidally-influenced deposits comprising the LST/ TST of the third sequence. This implies the two sequences are arranged in a retrogradationl stacking pattern typical of a TSS.

MASUK FORMATION

Lithofacies Analysis

In this study six facies are recognized from seven sections through the Masuk Formation in its type area around Blind Trail, southern Utah. A summary of these facies is found in Table 2.

Facies 1: Coal and Carbonaceous Mudrock

Facies 1 consists of carbonaceous mudrock and shales that grade vertically and laterally into ~0.5 – 2 m (1.5 – 6.5 ft) thick coal beds with subordinate thin siltstones and fine-grained sandstones. The mudrock in Facies 1 is black or very dark grey and rich in organic matter (i.e., carbonaceous). Abundant plant and woody coal debris can be found in carbonaceous beds throughout the formation. Facies 1 is only found in abundance at the basal contact of the Masuk Formation, where 2-3 coal beds are found within the first ~10 – 22 m (33 – 72 ft) of section. These coal beds are often separated by ~2 – 4 m (6.5 – 13 ft) thick sandstone bodies of Facies 4-5. Thin beds of carbonaceous mudrock are present higher in the unit, and are typically found along with Facies 2 within the lower member and bottom half of the middle member.

Intervals containing Facies 1 formed as a series of coastal mires situated along the edge of the inland sea. The presence of moderately thick coal beds (~0.5 – 2 m, 1.5 – 6.5 ft) indicates that a high water table and relatively low sediment input must have been maintained for a suitable length of time for the thick accumulation of plant biomass. Sandstone bodies within the coaly interval of the Masuk Formation indicate a network of channels incised into mire deposits.

Facies 2: Grey-grey/green Mudrock

Facies 2 consists primarily of mudrocks interbedded with minor carbonaceous shales, siltstones, and fine-grained ripple cross-laminated sandstones. The mudrock is greygrey/green in color and there is often wavy bedding and fine plant debris visible from fresh exposures. In extensive exposures there is evidence for large scale architectural elements (e.g., low-angle bedding, erosional surfaces) within these mudrock sections. However, as a result of weathering, most intervals dominated by Facies 2 form slopes covered in debris and highly weathered mudrock. Facies 2 is recognized through the whole of the Masuk Formation, but is most abundant in the middle member.

Facies 2 represents a coastal floodplain depositional setting. The few areas exhibiting large scale architectural features also display mud-filled channels or lacustrine deposits, but limited physical access to these outcrops hindered the ability to diagnose the proportion of these deposits that display channel architecture. Carbonaceous mudrocks correspond to thin mire deposits on the floodplain. Some intervals within Facies 2 are characterized by intensely fractured mudrock and pale, mottled coloring. This

Table 2. - *Lithofacies of the Masuk Formation*

Lithofacies	Lithology	Sedimentary Structures and Small-scale Features	Geometry and Architectural Elements	Depositional Environment
1	Coal and carbonaceous mudrock with few thin beds of fine sandstone	Thin sulfur residue common on exposed surfaces and cleats	Seams may pinch out or are washed out by overlying erosionally based sandstones	Coastal plain swamps and floodplains
2	Grey to grey/green mudrock with minor siltstones and sandstones; thin carbonaceous mudrock beds common	Where well exposed there are portions that are wavy bedded with thin ripple cross laminated sandstones; has intervals that are slickensided and contain rhizoliths and small plant/coaly debris up to *in situ* logs	Evidence of some low angle bedding and erosional surfaces in well exposed large cliff faces	Floodplains and mud filled channels or lacustrine deposits Poorly drained paleosols - gleysol
3	Thinly interlaminated siltstone and sandstone	Pinstripe to wavy bedded with common ripple cross-lamination and paired mud drapes; one interval has a trace fossi assemblage composed primarily of *Teichichnus, Thalassinoides* and *Planolites*	Usually sheetlike; in some instances appears to form erosionally based lense shaped bodies	Tidal lagoon/central estuary and marine with elements of the *Cruziana* and *Skolithos* Ichnofacies
4	Thickly interbedded sandstone and mudrock	Fine sandstone beds are largely small-scale trough cross-bedded or ripple cross-laminated while interbedded mudstones are usually plane laminated or deformed; *Lockeia* resting traces common on underside of sandstones	Inclined heterolithic strata (IHS) forming lateral and downstream accretionary elements	Fluvio-estuarine meandering channels
5	Trough cross-bedded sandstone; Fine sandstones, some fining upward from medium sand and intraformational conglomerates at the base; minor mudstone and carbonaceous shale partings; abundant iron concretions	Small to large scale trough cross-bedded, sometimes fining upward into ripple cross-laminated beds; often contain clay rip-up clasts at the base Fine organic and paired mud drapes were observed in trough cross-bedding of some intervals and are more closely associated with facies H_s There are also many thin and discontinuous beds, often containing climbing ripples and small scale troughs	Internal architecture varies from aggradational trough cross-bedded fills to large scale lateral accretionary structures; overall geometry varies from extensive and sheet-like to large incised lense shaped bodies which can be amalgamated, stacked, or single units	Single and multi-storey meandering and tidally influenced channels Small single storey channels and overbank splays
6	Intraformational conglomerates; matrix of siltstone to coarse sandstone with pebble to boulder sized mudstone clasts	Outsized clasts are composed of laminated clay rip-up	Form discontinuos beds at the base or within facies 5	Basal channel lag and bank collapse deposits

is accompanied by an abundance of rhizoliths and occasional upright stumps. These intervals are interpreted as paleosols and, since they tend to be generally drab or grey, contain carbonaceous beds, and have no evidence of horizon development, they may signify poorly drained gleysols, which are similar to modern day inceptisols (Retallack, 1990).

Facies 3: Thinly Interlaminated Siltstone and Sandstone

Facies 3 comprises thinly interlaminated beds of siltstone and fine-grained sandstone. Facies 3 is found in the lower member of the Masuk Formation and at the top of the Muley Canyon Sandstone in some sections. Laminations are linsen (pinstripe) to lenticular/wavy bedded and ripple cross-lamination appears to be both unimodal and bimodal in orientation. Paired mud drapes are also visible within fine sandstone ripple cross-lamination sets. Major architectural features are absent from the sections measured in this study and most exposures of Facies 3 appear as sheetlike bodies, although there is evidence these deposits may fill small heterolithic channels along Sweetwater Creek NNW of Section 6. These channels incise into underlying coals near the base of the lower member and are locally dominated more by sandstone or carbonaceous shale in transition with Facies 1 and 4.

Some exposures of Facies 3 are bioturbated by a relatively low diversity trace fossil assemblage (Fig. 10). Overall the bioturbation is uncommon with a bioturbation index range of 1-2 in most cases, having a low trace density and high preservation of bedding (Bann and others, 2004). *Teichichnus*, *Thalassinoides*, and *Planolites* are the dominant traces, although moderate numbers of *Ophiomorpha irregulare*, and fugichnia escape traces can be found as well. Navichnia sediment swimming traces associated with *Teichichnus* burrows are also moderately abundant (Fig. 10a). A few *Cylindrichnus*, *Palaeophycus*, and Rhizocorallium burrows were identified.

The trace fossils in Facies 3 record burrowing behaviors from a combination of elements of the *Cruziana* and *Skolithos* Ichnofacies assemblages. From the relatively depauperate nature

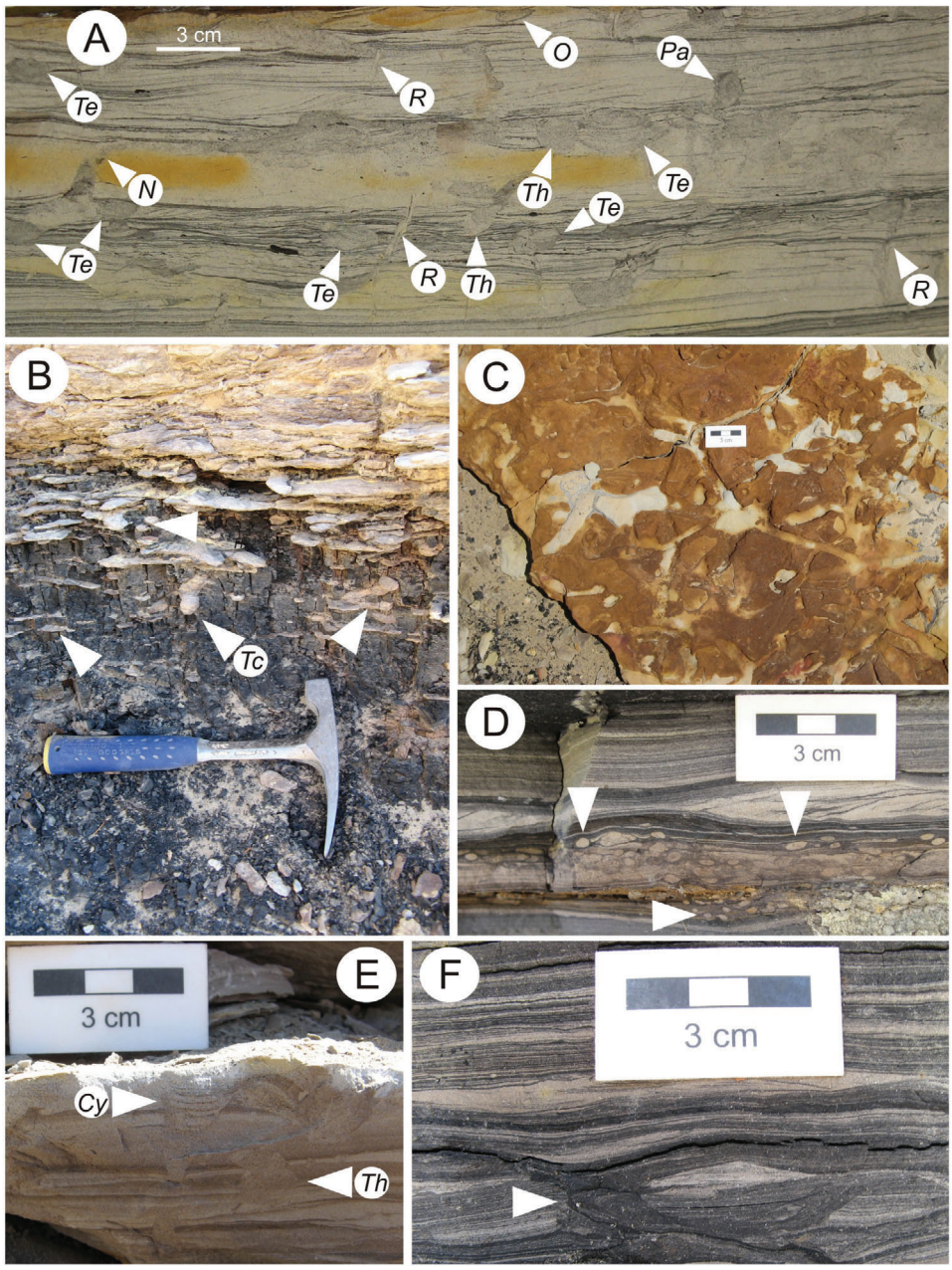

Figure 10. A restricted ichnofossil assemblage combining elements of *Cruziana* and *Skolithos* Ichnofacies within Facies 3 estuarine/lagoonal or marine sandstones and laminated mudstones from a bed at the MFS in the lower member of the Masuk Formation. A) Typical expression of the complete assemblage in interval ~ 0.5 m from the base of Section 6. B) Estuarine Facies 3 deposit overlying coal bed at the base of Section 5. A *Thalassinoides*-dominated (indicated by arrows) *Teredolites* assemblage is found at the top of the coal. C) Plan view of Thalassinoides burrows in top of the same interval. D) *Planolites* near base of Section 6. Uncommon traces include E) Possible *Cylindrichnus* (near base of Section 7) and F) Probable *Rhizocorallium* (near base of Section 6). Abbreviations for trace fossil markers: (Cy) *Cylindrichnus*, (N) navichnia, (O) *Ophiomorpha irregulare*, (Pa) *Palaeophycus*, (R) rhizoliths from overlying coal bed, (Tc) *Teredolites clavatus*, (Te) *Teichichnus*, (Th) *Thalassinoides*.

of the assemblage, it is likely the trace makers were influenced by some tidal and/or stressed brackish-water conditions (MacEachern and others, 2005; MacEachern and others, 2007a; MacEachern and others, 2007b). The bedding characteristics and trace fossil assemblage also imply a tidal and/or estuarine depositional setting. It has been argued that wavy or lenticular bedding and bimodal cross-laminations are most common in tidal settings dominated by reversing currents, while paired mud drapes found along the downstream side of dunes or ripples record semi-diurnal deposition during slack water conditions, likely in an estuarine environment (Shanley and others, 1992; MacEachern and others, 2005). Synaeresis (subaqueous shrinkage) cracks found in some of these deposits can also point to a tidal setting, as they are thought to form in sediment experiencing fluctuations in fluid salinity (Plummer and Gostin, 1981). Figure 11 illustrates all sedimentary structures found

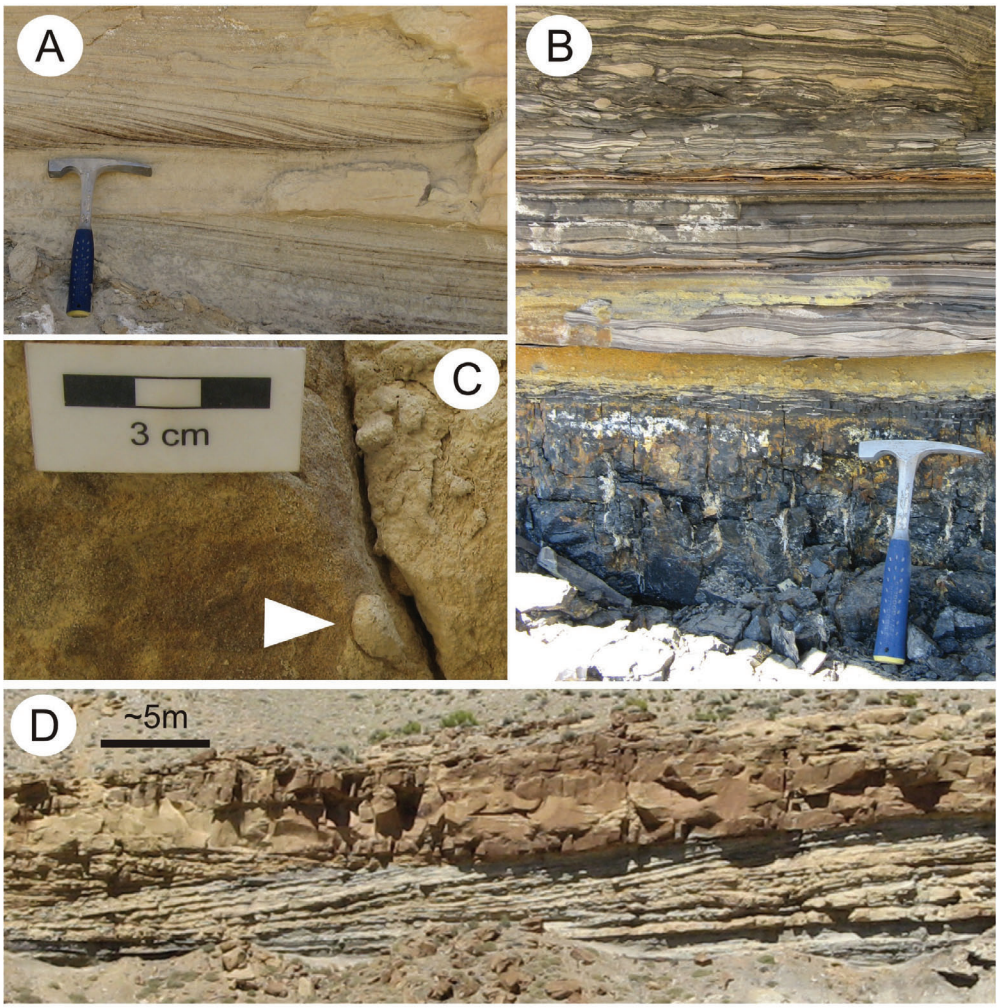

Figure 11. Sedimentary features interpreted as evidence of tidal influences in the Masuk Formation. **A)** Paired mud drapes within a trough cross-bedded sandstone. Hammer for scale. **B)** Wavy and lenticular bedding in a thinly interlaminated claystone and sandstone (Facies 3). This interval overlies the lowest coal seam in the Masuk and contains the trace fossil assemblage shown in Figure 10. Hammer for scale. **C)** *Lockeia* bivalve resting trace (white arrow) on the underside of a fluvial sandstone bed. **D)** Inclined heterolithic stratification (IHS) forming laterally accreting point bar deposits within a tidally-influenced channel (Facies 4). 5-m (16.4-ft) scale bar.

in the Masuk Formation that are suggestive of tidal processes. Facies 3 is interpreted as tidal lagoon, marginal marine central estuary bay, or shallow marine deposits.

Facies 4: Thickly Interbedded Sandstone and Mudrock

Facies 4 is composed of thickly interbedded (~5 – 40 cm, 2 – 16 in) fine-grained sandstone and siltstone or claystone. Small scale trough cross-bedding and ripple cross-lamination are common in the sandstone intervals. Planar lamination in the interbedded silt/claystones is in many places homogenized by soft-sediment deformation. Tool marks and *Lockeia* bivalve resting traces (Fig. 11c) are found along the underside of many of the sandstone beds.

This facies is found throughout the Masuk Formation and is closely associated with thick sandstones of Facies 5. It is most widespread within the lower member where it occurs as stacked, widely correlated units. This facies is generally erosionally based, suggesting fluvial incision. Individual bodies are not laterally extensive and most form accretionary sets of beds ~5 – 10 m (16 – 33 ft) thick that dip at a shallow angle as part of a larger macroscale fluvial unit (Figs. 11d, 12). Often these units form an amalgamated basal storey of extensive multi-lateral channel bodies throughout the Masuk Formation, especially in the lower member (Figs. 11d, 12). Referred to as inclined heterolithic stratification (IHS), these accretionary fluvial channel bodies consisting of alternating sand and mud are thought to result from deposition during slackwater and tidal fluctuations when accompanied by other features indicative of tidal settings (Thomas and others, 1987). Therefore Facies 4 represents heterolithic channel fills within widespread fluvio-estuarine deposits.

Facies 5: Trough Cross-bedded Sandstone

Facies 5 is composed of fine-grained sandstones that contain predominantly 0.07-1 m (0.2-3.3 ft) thick trough cross-bedding, with minor mudrock partings. In some cases the units fine

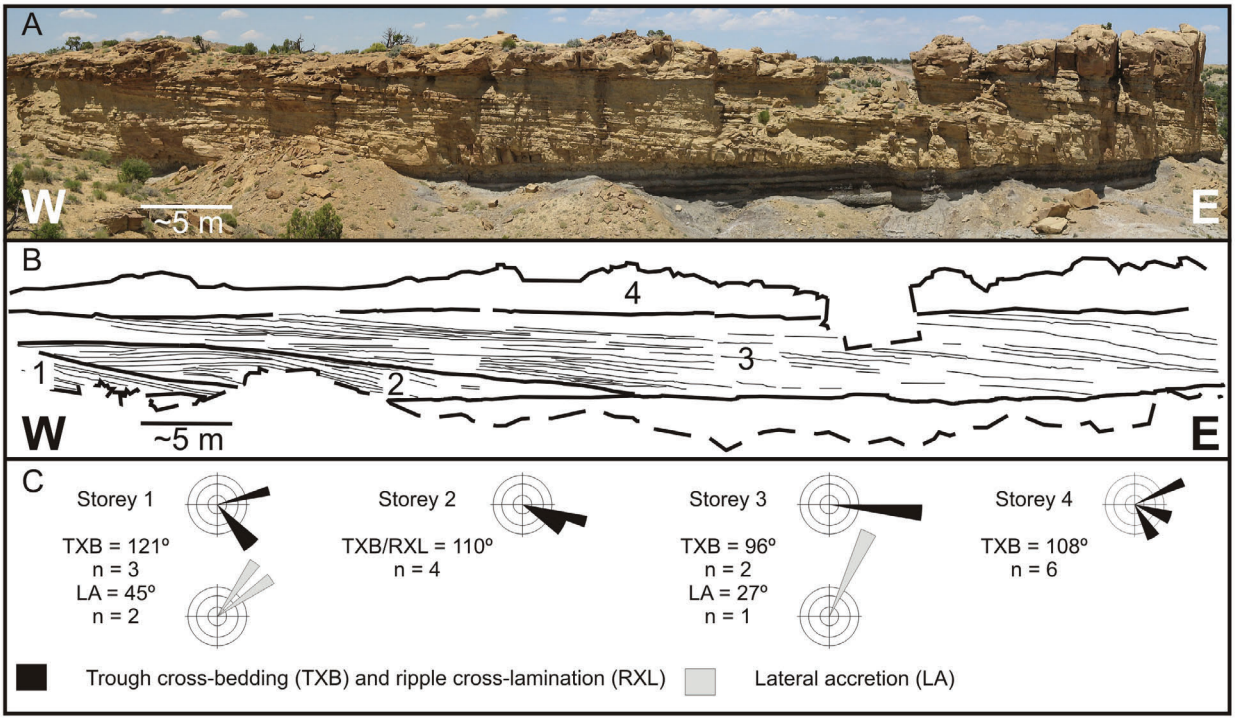

Figure 12. Interpretation of architectural features and paleocurrent measurements from a fluvio-estuarine channel body in the lower member of the Masuk Formation. A) West-east trending photo of channel body exposed ~44.5 m (146 ft) from the base of Section 4. B) Cross-strata and bounding surfaces traced within channel storeys. C) Rose diagrams from measurements of trough cross-bedding, ripple cross-lamination, and accretionary chanel storeys. Diagrams produced using EZ-ROSE (Baas, 2000).

upward into current ripple cross-laminated beds. The sandstones are erosionally-based and often accompanied by mud rip-up, clay ball clasts, and petrified wood debris. There is a diversity of architectural style expressed by Facies 5 deposits. The overall geometry of the sandstone bodies ranges from laterally extensive and sheet-like to large possibly lens-shaped units. Internal architecture is composed of stacked trough cross-bedding and large scale accretionary structures. Macroscale inclined strata are typical features of bar migration in fluvial systems, suggesting Facies 5 represents a series of thick sandstone channel fills (Miall, 1988; Bridge, 1993). The smaller discontinuous beds were formed by smaller isolated channels or overbank splays. Many of the sandstones contain trough cross-bedding with fine organic and paired mud drapes. Combined with a close association with Facies 4 IHS, which are often overlain by Facies 5 channel storeys (Figs. 11d, 12), this suggests some of these intervals are also affected by reversing currents. However, a unimodal paleocurrent direction for most of these units indicates only a weak tidal influence.

Facies 6: Intraformational Conglomerate

Facies 6 consists of intraformational conglormerate with pebble to boulder-sized clasts resting in a matrix of sand and silt. The outsized clasts are made of reworked fragments and blocks of mudrock resembling Facies 2 floodplain deposits. In most cases bedding is still intact within these clasts. As a result they are thought to have originated within the depositional environment (i.e., are intraformational).

Intervals of Facies 6 are found in most sections observed in this study, but are not particularly abundant or correlatable. Typically they form thin layers (< 1 m) interbedded with and along the basal portion of Facies 5 channel bodies. The origin of outsized clasts and ties to Facies 5 channel environments suggest that Facies 6 conglomerates formed as channel lags or bank collapse deposits. The latter event is indicated by a 10-m (33 ft) thick conglomerate interval in Section 7 containing many boulder-sized blocks of floodplain mudrock.

Fluvial Style

Shanley and McCabe (1991, 1994), Olsen and others (1995), and Catuneanu and others (2009) attribute amalgamation and sheet-like geometry of fluvial bodies to increased lateral migration of streams within a channel belt as a result of less available accommodation. This is evident in the multi-lateral channel belts throughout the Masuk Formation and the massive cliff of Tarantula Mesa Sandstone where it is particularly difficult to discern individual channel fill units. Overall, paleocurrent measurements for the entire Masuk Formation show an eastward mean of 101° (n = 162). Lateral accretion macroform elements are perpendicular to this mean (029°, n = 12), suggesting a high sinuosity planform geometry for the Masuk fluvial deposits. The mean estimate of bankfull flow depths calculated from the Masuk is 5.7 m (18.7 ft), with a mean range of individual channel belt width between 1387 – 2098 m (4551 – 6883 ft) (Corbett, 2009). However, the observed lateral extent of accretionary elements

across long exposures is significantly greater than this estimated width, suggesting a possible allogenic control on channel belt geometry and distribution. The fluvial bodies within the Masuk Formation are believed to have been deposited chiefly by high sinuosity upper estuary tidal channels to coastal plain streams.

Sequence Stratigraphic Interpretation

The results of this study place the Masuk Formation into a sequence stratigraphic framework for the first time with the goal of providing a stronger correlation to equivalent units across southern Utah. Terminology used to describe the sequence stratigraphy of the Masuk Formation follows standardized definitions provided by Catuneanu and others (2009). While a MFS may be more time significant than a subaerial unconformity (Catuneanu and others, 2009) a complete "genetic" stratigraphic sequence could not be identified and the latter surfaces are more extensive in these terrestrial settings. Therefore, criteria for identification of type III depositional sequences are used (*sensu* Van Wagoner and others, 1988; Van Wagoner and others, 1990; Christie-Blick, 1991; Catuneanu and others, 2009). This sequence definition uses subaerial unconformities as the major sequence boundaries (as opposed to other important stratigraphic surfaces, i.e., a MFS). Terminology relating to downstream controls still apply since identification of coastal deposits allow for relation to a paleo-shoreline. Recognition of tidal indicators in fluvial deposits was based on the methods detailed by Shanley and others (1992). Results from facies analysis and tracing of key surfaces between seven sections are summarized in Figure 13, and suggest that the Masuk Formation is a series of distal, coastal plain deposits spanning one long term (third order) sequence set. Widespread channel belts suggest allogenic controls on deposition, and mark several nested high-frequency sequences within an overall lower-frequency sequence set.

High-frequency Sequences

Several multi-lateral channel bodies within the Masuk are traceable over considerable distances (>2-4 km, 1.2-2.5 mi), suggesting an allogenic control on stacking patterns (Figs. 13 – 14). Consequently, erosional surfaces at the base of these channel bodies may correspond to higher frequency sequence boundaries (Fig. 13). In the lower member at least three intervals of fluvio-estuarine deposits are laterally extensive across the study area. Evidence from sedimentary structures and trace fossils suggest the streams recording the lower member were likely still under some tidal control during deposition (see Facies 4 description).

The middle and upper members consist of single to multi-storey channel belts dominated by Facies 5 and contain less tidal influence. Sparse mud drapes, Facies 4 inclined heterolithic stratification, and *Teredolites* borings (from a petrified log ~155 m, 500 ft from the base of Section 4) are still evident, but less prevalent. Two thick channel belts in the middle member appear to pinch out in nearby cliffs, though across large exposures along Tarantula Mesa they still crop out as widespread zones of fluvial deposition (Fig. 14). This suggests they may be correlatable along interfluves in areas not accessible in this study. The proportion of floodplain deposits (Facies 2) to channel sandstones increases in the middle member and there are a greater number of small isolated channels and splays (Fig. 13). The higher proportion of overbank facies and more isolated channels is a common feature of highstand fluvial deposits (Shanley and McCabe, 1991, 1994; Catuneanu and others, 2009). A thick multi-storey, fluvial, sheet-like sandstone body that forms the whole of the upper member is clearly traceable for great distances across Tarantula Mesa. Fluvial deposits are thought to become more extensive and amalgamated in the late highstand as the available accommodation is filled and relative base-level begins to fall (Olsen and others, 1995; Catuneanu and others, 2009). This may explain the change in channel belt geometry between the middle and upper members.

Widespread fluvial incision and migration within distinct channel belts throughout the succession support external forcing and changes to relative sea-level and argue against an entirely stochastic distribution. These interpretations are summarized in Figure 15, which presents an ideal model for these nested high-frequency sequences within the Masuk Formation. Amalgamated heterolithic channel fills (Facies 4) and sheet-like fluvial sandstones (Facies 5) overlie a widespread erosional surface created by lowstand fluvial incision. Sharp contacts between these deposits and floodplain mudrocks containing isolated channels likely mark the boundary between transgressive fluvio-estuarine and highstand coastal plain deposits. In most situations, lowstand deposits are not preserved and have been removed by subsequent fluvial amalgamation, suggesting a low accommodation setting. However, where underlying sheet-like sandstones are present, this systems tract may be represented (such as in the middle member, Fig. 13). In the lower member isolated highstand channels in these high-frequency sequences are uncommon or they are amalgamated with their upper sequence boundaries (Fig. 13). They become more prevalent in the middle member, further up-section in the longer third order sequence.

Lower-frequency Sequence Set

The lower-frequency sequence set within the Masuk Formation is bounded below by the uppermost (fourth) SB within the Muley Canyon Sandstone, just below the estuarine channel deposits that comprise the LST/TST (Plate 2, Fig. 15). The coal zone is interpreted to represent a zone of maximum flooding (MFZ) within the lower-frequency sequence set, when accommodation was greatest to accumulate and then preserve coal beds. (see "Muley Canyon Coal Zone" section below for discussion).

Overlying this flooding zone is a thick succession of fluvio-estuarine deposits, floodplain fines, and coastal plain meandering channel belts. These sediments comprise the highstand sequence set recording basin filling from a time of maximum flooding (MFZ) to the onset of relative base-level fall (Catuneanu and others, 2009).

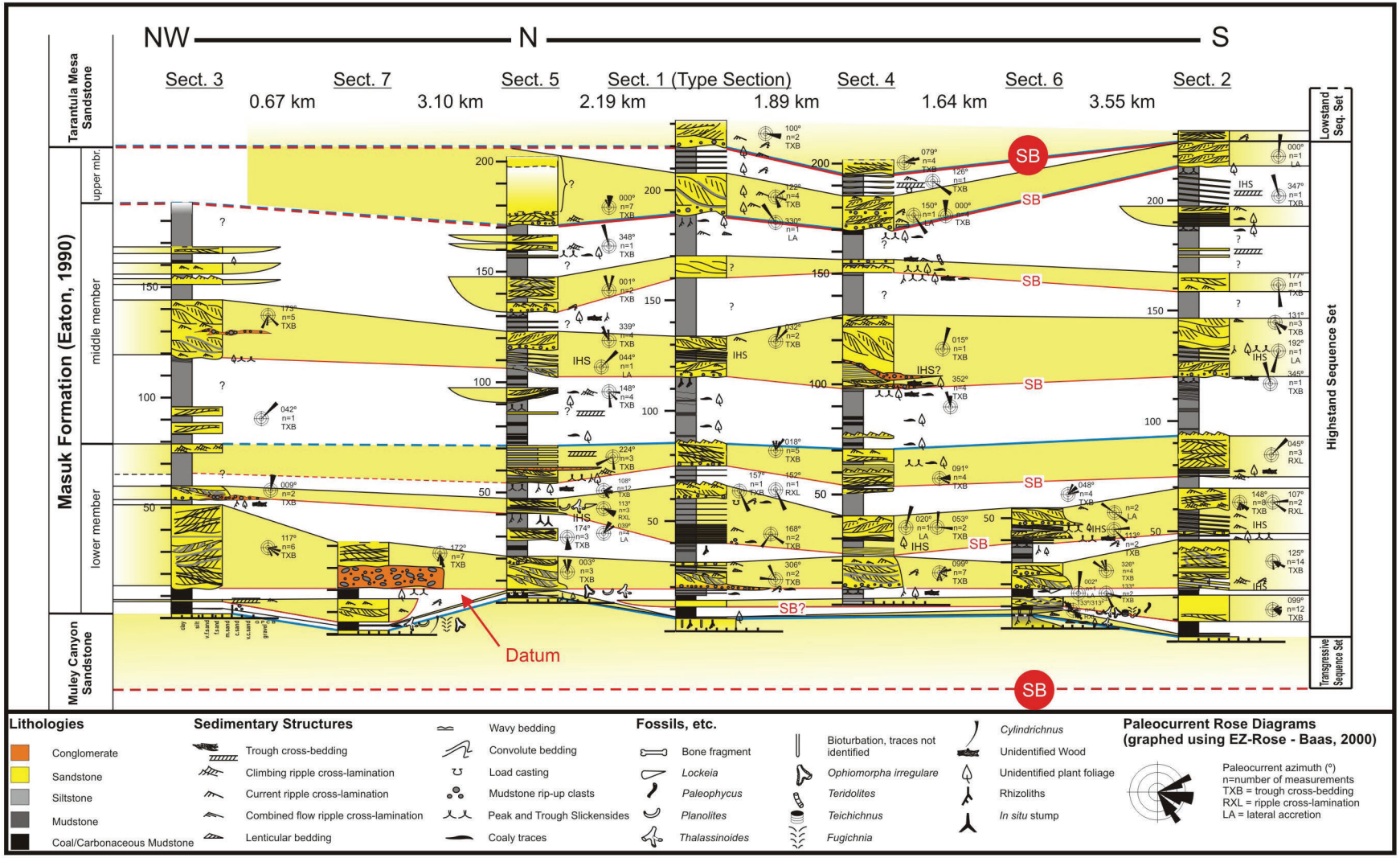

Figure 13. Correlation and sequence stratigraphic interpretation of measured sections used in this study (see Fig. 6 for location). Left side of diagram presents Eaton's (1990) Upper Cretaceous lithostratigraphic nomenclature. Right side of diagram is the sequence stratigraphic framework developed in this study. Shaded areas between section indicate correlation of sandstone bodies based on tracing across outcrops or from photomosaics. Extensive channel belts in the Masuk Formation overlie high-frequency sequence boundaries nested within a longer term, lower-frequency highstand sequence set. Blue lines mark formation and member contacts and red lines show sequence boundaries. Major lower-frequency sequence boundaries (SB) are marked by red circles while high-frequency sequence boundaries are indicated by small red lettering. Dashed lines are shown where contacts are approximate or unit is weathered. Rose diagrams produced using EZ-ROSE (Baas, 2000).

Figure 14. Annotated photograph of Blind Trail Butte showing labeled units and correlations along the eastward facing exposures along the northern edge of Tarantula Mesa. Dashed line marked by SB designates the upper lower-frequency sequence boundary between the Masuk Formation and Tarantula Mesa Sandstone. Smaller dashed lines show base of extensive channel belt sandstones and possible high-frequency sequence boundaries. Solid lines within the channel sandstones indicate accretionary surfaces.

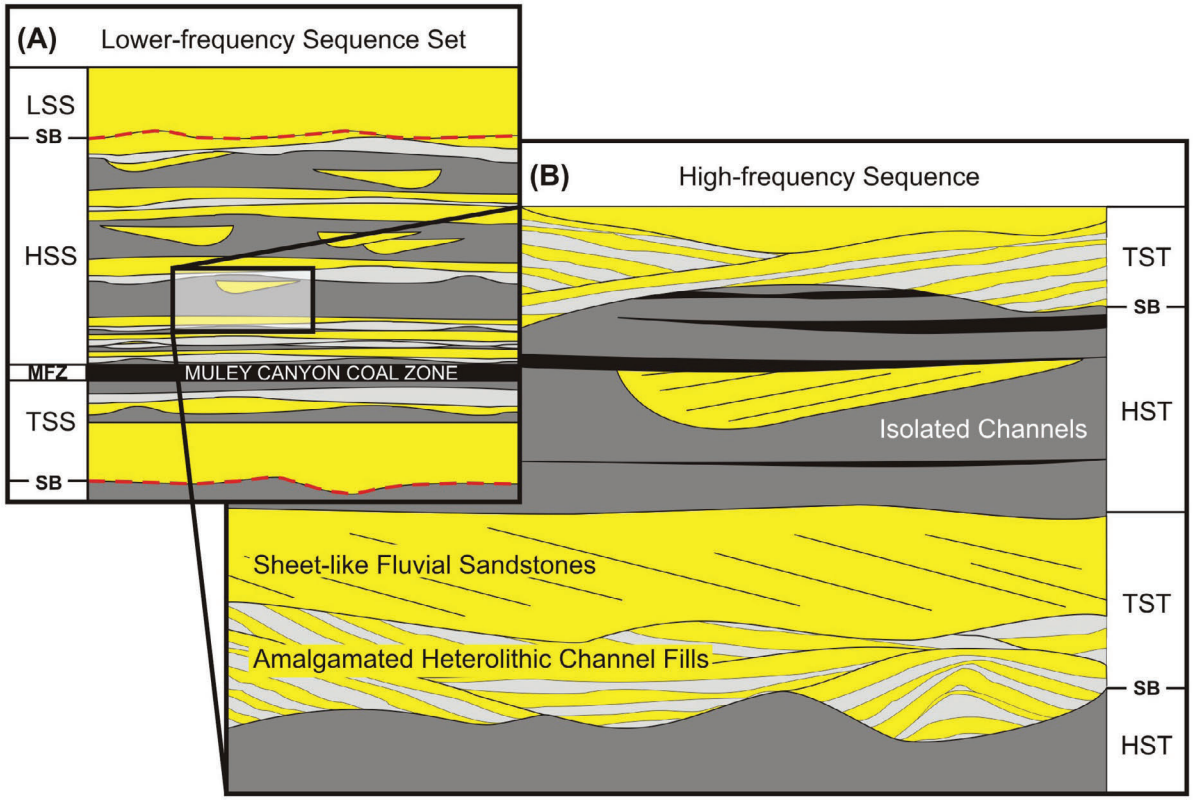

Figure 15. Schematic diagram showing high-frequency fluvial sequences within the context of the longer-term, lower-frequency sequence set. A) Low-frequency sequence set model for the upper strata of the Henry Mountains Syncline succession. The boundary between the transgressive sequence set (TSS) and highstand sequence set (HSS) is within the coal zone where the maximum flooding zone (MFZ) is identified. Fluvial stacking patterns within the HSS show an increase in floodplain mudrocks and greater preservation of isolated channels up-section. The HSS is truncated by thick fluvial deposits of the lowstand sequence set (LSS) overlying an upper sequence boundary (SB). B) Model for high-frequency fluvial sequences. Transgressive amalgamated tidally-influenced heterolithic channel fills (Facies 4) and sheet-like fluvial sandstones (Facies 5) overlie an erosional SB. Sharp contact with floodplain mudrocks marks the boundary with highstand deposits, which contain more isolated channel bodies. In the upper portions of the highstand, channels occasionally amalgamate with deposits from overlying sequences.

The contact of the Masuk Formation with the overlying Tarantula Mesa Sandstone is widespread and is recognizable as an erosional surface at the base of a large cliff of amalgamated fluvial sandstones (Figs. 13, 14). A dramatic decrease in the proportion of mudrock is obvious, even though only the very base of the Tarantula Mesa Sandstone was investigated in this study, and prior work describes an increase in grain size to coarse-grained sandstone with conglomerates 44.5-65.5 m (146.0-214.9 ft) farther up in the unit (Smith, 1983). There is also a shift in paleocurrent direction and a decrease in estimated stream depths across the contact (Fig. 13). Despite these features, the exact transition can be difficult to pinpoint and is often planar (as opposed to highly irregular) or is covered by talus. There are no obvious incised valley fills and the planar character of the basal Tarantula Mesa contact indicates deposition during low accommodation; a typical characteristic of lowstand fluvial successions (e.g. Olsen and others, 1995; Yoshida, 2000; Catuneanu and others, 2009). This surface, across which fluvial style appears to change from predominantly large and highly sinuous to smaller amalgamated streams, is a subaerial unconformity that defines the upper SB of the Masuk/upper Muley Canyon sequence set (Fig. 13).

MULEY CANYON COAL ZONE

Characteristic Units from Outcrop

The Muley Canyon Coal Zone at the base of the Masuk Formation is bounded below by a cliff-forming white sandstone unit at the top of the Muley Canyon Sandstone and above by the first major laterally extensive channel unit within the Masuk Formation (Plate 4). Key coal zone units followed along a 2.5 km (1.6 mi) N-S transect south of Blind Trail and correlated between eight measured sections over a ~12 km^2 (5 mi^2) area indicate these units are largely laterally extensive and correlatable over this distance, though exceptions are noted. Key units documented within the coal zone include coal beds, carbonaceous siltstone, intracoal sandstone channel bodies, and a coarsening upward unit that contains increasing bioturbation upwards. Intracoal sandstone channel bodies range from 30 cm (12 in) to 12 m (40 ft) in thickness. Though thickness changes laterally, most channel bodies can be traced laterally and are continuous over several km (Plate 4). However, at one location, south of section 2 (1st Gully S. of Blind Trail), a 12 m (40 ft) thick channel body pinches out completely to the south over a distance of less than 0.5 km (0.3 mi) (Plate 4). To the north, this channel body thins significantly. Therefore, in general, coal bed and carbonaceous siltstone packages above and below the intracoal sandstone channel bodies can be correlated and are continuous, though thickness changes, lateral changes between carbonaceous siltstone and coal, and minor coal bed splits are evident (Plate 4).

Examination of a laterally extensive coarsening upward unit along Sweetwater Creek (sections 8-10, Plate 4) reveals marine influence within the coal zone. The coarsening upward unit, which is found above the stratigraphically lowest coal bed, is characterized by carbonaceous siltstone at the base that passes upwards into bioturbated coarse siltstone and ultimately bioturbated sandstone containing current, wave, and wave-modified current ripples. In the eastern portion of the project area (sections 5, 6) this bed is 1-2 m (3.3-6.6 ft) thick and coarsens upward. The bioturbation index near the top of the unit reaches a maximum of 2-3 in some localities. Trace fossils include *Planolites*, *Thalassinoides*, *Lockeia*, *Ophiomorpha*, *Diplocraterion habichi*, *Teichichnus*, and *fugichnia*. This heavily bioturbated surface can be identified and correlated in measured sections containing good coal zone exposures (Plate 4). No other part of the Masuk Formation has the same number of ichnotaxa or relative trace density as does this bed.

Sequence Stratigraphic Interpretation from Outcrop

High-frequency Sequence

The facies analysis, trace fossil assemblage, and widespread continuity of the coarsening upward unit described above suggest that it records the greatest marine incursion or MFS (Plates 4 – 5). Deposits within the coal zone below the MFS, which include at least one coal bed, are interpreted to comprise the late TST, whereas, coal zone deposits above the MFS represent the HST (Plate 5). The underlying and overlying high-frequency SBs that accompany the MFS in the coal zone are, respectively, 1) the fourth or uppermost SB in the Muley Canyon Sandstone (base of estuarine channel deposits, unit E; Plates 4 – 5), and 2) the first or lowermost SB in the Masuk (at the base of the first regionally extensive sandstone channel belt, which defines the top of the coal zone in outcrop; Plates 4 – 5).

Lateral continuity of coal zone units suggests some degree of allogenic control on deposition within the coal zone itself, but individual sequences can not be defined. Evidence for autogenic controls on deposition in the form of laterally discontinuous intracoal sandstone channel bodies is also noted.

Lower-frequency Sequence Set

It follows that the coal zone also represents a zone of maximum flooding within a lower-frequency sequence set, bound below the intracoal zone MFS by the transgressive sequence set of the upper Muley Canyon Sandstone and above the MFS by the highstand sequence set of the Masuk Formation (Plate 5; Fig. 15). Conditions for coal preservation were optimal during late transgression to early highstand, a period of maximum accomodation when relative sea level was highest, both on the high-frequency sequence and lower-frequency sequence set level (Plate 5, Fig. 15).

Surface-Subsurface Correlation of Coal Zone

Lithologic, architectural, and sequence stratigraphic models developed from outcrop observations were successfully extended

into the subsurface using wireline log and limited lithologic log data. A S-N correlation of surface and subsurface data to the north of Blind Trail reveals a mudrock-rich coal zone with four intracoal sandstone channel bodies present (Plate 6). One of the intracoal channels or channel complexes is thick and isolated (<0.5 km, 0.3 mi in width), while the others are thinner and extend over ~1 – 2 km (0.6 – 1.2 mi) (Plate 6). The SB above the coal zone is readily identified at the base of a thick sandstone unit (Plate 6). The presence of a thin, laterally discontinuous coal within the thick sandstone unit above the main coal zone proper suggests the thick sandstone unit may contain more than one sequence (indicated with a dashed SB, Plate 6). Using the outcrop gamma ray profile of the Muley Canyon Sandstone at Blind Trail, the uppermost MFS (base of shoreface deposits, unit D) and SB (based of estuarine channel deposits, unit E) in the Muley Canyon Sandstone are recognized in one wireline logged borehole that extends through the formation (Plate 6), further supporting the sequence stratigraphic model developed from outcrop.

A W-E transect of wireline log data across Tarantula Mesa reveals at least five, possibly six, laterally extensive sandstone-dominated channel belts separated by mudrock-dominated successions (Plate 7), which is consistent with architectural interpretations of the Masuk Formation from outcrop (Fig. 14). When the W-E transect is tied to measured section #2, 11.9 km (7.40 mi) to the north, the same five to six sandstone-dominated channel belts can be correlated with the subsurface data. Extension of this architecture into the subsurface further supports the concept that the repetitive, erosionally-based vertical cycles of fluvial to estuarine channel and floodbasin deposits in the Masuk represent high-frequency sequences with sequence boundaries at the base of sandstone-dominated channel belts (Plate 7). Furthermore, all six sequence boundaries identified in outcrop can be identified in the subsurface data (Plate 7).

The coal zone thins markedly to the east across Tarantula Mesa (Plate 7), in the basinward direction. The presence of a thin, discontinuous coal in the east above the main coal zone documents a basinward progradational stacking pattern of sequences within the lower portion of the Masuk Formation. Progradation is consistent with the expected stacking pattern of a highstand sequence set, further supporting the interpretation that the Masuk Formation comprises a highstand sequence set.

Again in the W-E transect, the SB overlying the coal zone is placed at the base of a thick sandstone channel unit (Plate 7). The thick sandstone channel unit overlying the coal zone becomes more interbedded basinward to the east, where presumedly accomodation was greater (Plate 7). Hence, it is likely that, shoreward, towards the west, the unit is composed of amalgamated channel bodies that may record multiple condensed sequences. Basinward, towards the east, these sequences may become less condensed and more easily recognized by distinct changes in lithology. One possible such sequence boundary is marked with a dashed red line and question marks, just above the coal zone in Plate 7.

Successful correlation of key surfaces and packages from outcrop to the subsurface confirms their regional extent and supports the sequence stratigraphic significance of models developed from outcrop. Future investigation should focus on additional regional surface and subsurface correlation using data archived in the ArcGIS® database (Supplementary File 1), as such correlations will improve the ability to predict coal bed thickness and continuity and the location, thickness, and lateral extent of intracoal zone sandstone channel bodies. Both are crucial to coal resource evaluation and possible mine development.

SUMMARY AND CONCLUSIONS

The Muley Canyon Sandstone is interpreted to contain a basal deltaic mouthbar deposit (Facies 1, unit A) that is overlain by two packages of alternating offshore transition-shoreface (Facies 2 and 3, units B and D) and fluvial-estuarine deposits (Facies 4, 5 and 6, units C and E). Although some lateral and shoreward-basinward facies and thickness variations within these units are evident, their defining internal and bounding surface characteristics and stacking order are remarkably consistent over a large area (~100 km^2, 40 mi^2), suggesting an allogenic control on deposition.

Based on the recognition of key sequence stratigraphic surfaces of regional extent, we interpret the Muley Canyon Sandstone to contain four high-frequency sequences that are arranged into two lower-frequency sequence sets. The lower two high-frequency sequences, composed of deltaic mouthbar, offshore transition and shoreface deposits (Facies 1, 2, and 3, units A and B) both contain a falling stage systems tract, though the upper of the two sequences is interpreted to be a more distal expression of the lower. The lower two high-frequency sequences constitute a lower-frequency falling stage sequence set. The upper two sequences are composed of fluvial to tidally-influenced channels (unit C, SB at base), shoreface deposits (unit D, MFS at base), and estuarine channels to estuarine mouth deposits (unit E, SB at base), with units C and E comprising the LST to TST, and unit D the HST. The MFS is located within the coal zone overlying the Muley Canyon Sandstone. Channel-fill facies in the upper sequence represent a more distal system than those in the sequence below, suggesting longer-term transgression and a retrogradational stacking pattern. As such, we interpret the upper two high-frequency sequences to represent a lower-frequency transgressive sequence set. Clinoform sets observed just below the Muley Canyon Sandstone in the top of the Blue Gate Shale indicate a southeast (142°, n = 3) regional dip slope direction.

The Masuk Formation comprises a stack of fluvial to estuarine channel and floodbasin deposits, arranged in repetitive, erosionally-based vertical cycles. Widespread channel belts suggest allogenic controls on deposition, and mark several nested high-frequency sequences within an overall long-term, lower-frequency sequence set (Fig. 15). A facies analysis of the Masuk Formation reveals a succession recording deposits of transgressive

lagoons and coastal mires in the coal zone overlain by highstand fluvio-estuarine channel belts that form a highstand sequence set (Figs. 13, 14). Interpretation of architectural elements (Fig. 12) and paleocurrents from these highstand channels suggests they were deposited by high sinuosity meandering streams 5 – 7 m (15 – 23 ft) deep flowing east-northeast into the Cretaceous Western Interior Seaway within channel bodies much wider than empirically derived estimates of channel belt width (Corbett, 2009). The top of the Masuk Formation is truncated by lowstand amalgamated fluvial deposits of the Tarantula Mesa Sandstone (Fig. 13), and the boundary between these two units is interpreted as a lower-frequency sequence boundary.

Bound by the transgressive sequence set of the upper Muley Canyon Sandstone below and the highstand sequence set of the Masuk Formation above, the coal-bearing interval at the base of the Masuk Formation is interpreted to represent a zone of maximum flooding. Surface-subsurface correlations demonstrate packages of coal beds are fairly continuous over 10's of km (> 6 mi), suggesting a regional allogenic control on coal zone deposition. This work has resulted in an improved sequence stratigraphic understanding of the region that can be used to predict coal bed location and thickness in areas that lack subsurface data. More work is needed to correlate this succession to Campanian strata in the Book Cliffs region in order to test the regional extent of relative sea level variations on the eastern margin of the Cretaceous Interior Seaway during the Campanian.

ACKNOWLEDGMENTS

This work was supported by a Utah Geological Survey (UGS) grant to L. P. Birgenheier as part of the 2009 *Characterization of Utah's Hydrocarbon Reservoirs and Potential New Reserves* Program. Funding was also provided by the Mr. and Mrs. J.B. Coffman endowment in sedimentary geology at the University of Nebraska-Lincoln, Department of Geosciences. The authors greatly appreciate the help of D. E. Tabet, UGS, for preparing subsurface datasets, sharing his experience in key discussions, and editing. Many thanks to UGS, particularly to C. D. Morgan, for loaning a hand-held gamma ray spectrometer to carry out the project.

REFERENCES

Baas, J.H., 2000, EZ-ROSE; a computer program for equal-area circular histograms and statistical analysis of two-dimensional vectorial data: Computers & Geosciences, v. 26, p. 153-166.

Bann, K.L., Fielding, C.R., MacEachern, J.A., and Tye, S.C., 2004, Differentiation of estuarine and offshore marine deposits using integrated ichnology and sedimentology; Permian Pebbley Beach Formation, Sydney Basin, Australia, *in* McIlroy, D., ed., The application of ichnology to palaeoenvironmental and stratigraphic analysis: Geological Society of London Special Publication 228, p. 179-211.

Boyd, R., Dalrymple, R.W., and Zaitlin, B.A., 2006, Estuarine and incised-valley facies models, *in* Posamentier, H.W., and Walker, R.G., eds., Facies Models Revisited: Society for Sedimentary Geology (SEPM) Special Publication 84, p. 171-235.

Bridge, J.S., 1993, Description and interpretation of fluvial deposits: a critical perspective: Sedimentology, v. 40, p. 801-810.

Catuneanu, O., Bhattacharya, J.P., Blum, M.D., Dalrymple, R.W., Eriksson, P.G., Fielding, C.R., Fisher, W.L., Galloway, W.E., Gibling, M.R., Giles, K.A., Holbrook, J.M., Jordan, R., Kendall, C.G.S.C., Macurda, B., Martinsen, O.J., Miall, A.D., Neal, J.E., Nummedal, D., Pomar, L., Posamentier, H.W., Pratt, B.R., Sarg, J.F., Shanley, K.W., Steel, R.J., Strasser, A., Tucker, M.E., and Winker, C., 2009, Toward the standardization of sequence stratigraphy: Earth Science Reviews, v. 92, p. 1-33.

Christie-Blick, N., 1991, Onlap, offlap, and the origin of unconformity-bounded depositional sequences: Marine Geology, v. 97, p. 35-56.

Corbett, M.J., 2009, Sedimentology and Sequence Stratigraphy of the Lower Campanian Masuk Formation, Henry Mountains Syncline, Utah: University of Nebraska, Master's thesis, 60 p.

Dalrymple, R.W., Zaitlin, B.A., and Boyd, R., 1992, Estuarine facies models; conceptual basis and stratigraphic implications: Journal of Sedimentary Research, v. 62, p. 1130-1146.

Davies, R., Howell, J., Boyd, R., Flint, S., and Diessel, C., 2006, High-resolution sequence-stratigraphic correlation between shallow-marine and terrestrial strata: Examples from the Sunnyside Member of the Cretaceous Blackhawk Formation, Book Cliffs, eastern Utah: American Association of Petroleum Geologists Bulletin, v. 90, p. 1121-1140.

Eaton, J.G., 1990, Stratigraphic revision of Campanian (Upper Cretaceous) rocks in the Henry Basin, Utah: The Mountain Geologist, v. 27, p. 27-38.

—1991, Biostratigraphic framework for the Upper Cretaceous rocks of the Kaiparowits Plateau, southern Utah, *in* Nations, J.D., and Eaton, J.G., eds., Stratigraphy, depositional environments, and sedimentary tectonics of the western margin, Cretaceous Western Interior Seaway: Geological Society of America Special Paper, v. 260, p. 47-63.

Edwards, C.M., Howell, J.A., and Flint, S.S., 2005, Depositional and Stratigraphic Architecture of the Santonian Emery Sandstone of the Mancos Shale: Implications for Late Cretaceous Evolution of the Western Interior Foreland Basin of Central Utah, U.S.A: Journal of Sedimentary Research, v. 75, p. 280-299.

Fouch, T.D., Lawton, T.F., Nichols, D.J., Cashion, W.B., and Cobban, W.A., 1983, Patterns and timing of synorogenic sedimentation in Upper Cretaceous rocks of central and Northeast Utah, *in* Reynolds, M.W., and Dolley, E.D., eds., Mesozoic paleogeography of the West-Central U.S.: Society for Sedimentary Geology (SEPM) Rocky Mountain Paleogeography Symposium 2, p. 305-336.

Friedmann, J.D., and Huffman, C., 1998, Laccolith complexes of southeastern Utah: Time of emplacement and tectonic setting - Workshop Proccedings: United States Geological Survey Bulletin 2158.

Gradstein, F.M., Ogg, J.G., and Smith, A.G., 2004, A Geologic Time Scale 2004: Cambridge, U.K., Cambridge University Press.

Hintze, L.F., Willis, G.C., Laes, D.Y.M., Sprinkel, D.A., and Brown, K.D., 2000, Digital Geologic Map of Utah: Utah Geological Survey, Map 179DM.

Howell, J.A., and Flint, S.S., 2003, Siliclastics case study: The Book Cliffs, *in* Coe, A.L., ed., The Sedimentary Record of Sea-Level Change: Cambridge, UK, Cambridge University Press, p. 135-208.

Hunt, C.B., Averitt, P., and Miller, R.L., 1953, Geology and geography of the Henry Mountain region, Utah: United States Geological Survey Professional Paper 228, 234 p.

Kauffman, E.G., Sageman, B.B., Kirkland, J.I., Elder, W.P., Harries, P.J., and Villamil, T., 1993, Molluscan biostratigraphy of the Cretaceous Western Interior Basin, North America, Evolution of the Western Interior Basin: Geological Association of Canada Special Paper, v. 39, p. 397-434.

Law, B.E., 1979a, Coal deposits of the Emery Coal Zone, Henry Mountains Coal Field, Utah: United States Geological Survey Map MF-1082A.

—1979b, Surface Coal Sections in the Emery Coal Zone, Henry Mountains Coal Field, Utah: United States Geological Survey Map MF-1082B.

—1980, Tectonic and sedimentological controls of coal bed depositional patterns in Upper Cretaceous Emery Sandstone, Henry Mountains coal field, Utah, *in* Picard, M.D., ed., Henry Moutnain Symposium, Utah Geological Association Guidebook 8, p. 323-336.

Lawton, T.F., Pollock, S.L., and Robinson, R.A.J., 2003, Integrating sandstone petrology and nonmarine sequence stratigraphy - Application to the Late Cretaceous fluvial systems of southwestern Utah, U.S.A: Journal of Sedimentary Research, v. 73, p. 389-406.

MacEachern, J.A., Bann, K.L., Bhattacharya, J.P., and Howell, C.D., 2005, Ichnology of deltas; organism responses to the dynamic interplay of rivers, waves, storms, and tides, *in* Goisan, L., and Bhattacharya, J.P., eds., River Deltas - Concepts, Models, and Examples: Society for Sedimentary Geology (SEPM) Special Publication 83, p. 49-85.

MacEachern, J.A., Bann, K.L., Pemberton, S.G., and Gingras, M.K., 2007a, The ichnofacies paradigm - high-resolution paleoenvironmental interpretation of the rock record, *in* MacEachern, J.A., Bann, K.L., Gingras, M.K., and Pemberton, S.G., eds., Applied Ichnology: Society for Sedimentary Geology (SEPM) Short Course Notes 52, p. 27-64.

MacEachern, J.A., Pemberton, S.G., Bann, K.L., and Gingras, M.K., 2007b, Departures from the archetypical ichnofacies - effective recognition of physico-chemical stresses in the rock record, *in* MacEachern, J.A., Bann, K.L., Gingras, M.K., and Pemberton, S.G., eds., Applied Ichnology: Society for Sedimentary Geology (SEPM) Short Course Notes 52, p. 65-94.

McLaurin, B.T., and Steel, R.J., 2000, Fourth-order nonmarine to marine sequences, middle Castlegate Formation, Book Cliffs, Utah: Geology, v. 28, p. 359-362.

Miall, A.D., 1988, Reservoir heterogeneities in fluvial sandstones; lessons from outcrop studies: American Association of Petroleum Geologists (AAPG) Bulletin, v. 72, p. 682-697.

Morton, L.B., 1984, Geology of the Mount Ellen Quadrangle, Henry Mountains, Garfield County, Utah: Brigham Young University Geology Studies, v. 31, pt., 1, p. 67-95.

Nichols, D.J., 1997, Palynology and ages of some Upper Cretaceous formations in the Markagunt and northwestern Kaiparowits plateaus, southwestern Utah, *in* Maldonado, F., and Nealey, L.D., eds., Geologic Studies in the Basin and Range - Colorado Plateau Transition in Southeastern Nevada, Southwestern Utah, and Northwestern Arizona, 1995: United States Geological Survey Bulletin 2153, p. 79-105.

O'Byrne, C.J., and Flint, S., 1995, Sequence, parasequence, and intraparasequence architecture of the Grassy Member, Blackhawk Formation, Book Cliffs, Utah, U.S.A, *in* Van Wagoner, J.C., and Bertram, G.T., eds., Sequence Stratigraphy of Foreland Basin Deposits: Outcrop and Subsurface Examples from the Cretaceous of North America: American Association of Petroleum Geologists Memoir, v. 64, p. 225-255.

Obradovich, J.D., 1993, A Cretaceous time scale, Evolution of the Western Interior Basin, Geological Association of Canada Special Paper, v. 39, p. 379-398.

Ogg, J., and Lugowski, A., 2007, TS-Creator visualization of enhanced Geologic Time Scale 2004 database: http://www.stratigraphy.org and http://chronos.org.

Olariu, C., and Bhattacharya, J.P., 2006, Terminal distributary channels and delta front architecture of river-dominated delta systems: Journal of Sedimentary Research, v. 76, p. 212-233.

Olsen, T., Steel, R., Hogseth, K., Skar, T., and Roe, S.L., 1995, Sequential architecture in a fluvial succession; sequence stratigraphy in the Upper Cretaceous Mesaverde Group, Prince Canyon, Utah: Journal of Sedimentary Research, v. 65, p. 265-280.

Peterson, F., and Ryder, R.T., 1975, Cretaceous rocks in the Henry Mountains region, Utah, and their relation to neighboring regions: Field Symposium - Guidebook of the Four Corners Geological Society, 8, p. 167-189.

Peterson, F., Ryder, R.T., and Law, B.E., 1980, Stratigraphy, sedimentology, and regional relationships of the Cretaceous System in the Henry Mountains region, Utah, *in* Picard, M.D., ed., Henry Mountain Symposium: Utah Geological Association Publication 8, p. 151-170.

Plink-Bjorklund, P., 2005, Stacked fluvial and tide-dominated estuarine deposits in high-frequency (fourth-order) sequences of the Eocene Central Basin, Spitsbergen: Sedimentology, v. 52, p. 391-428.

Plint, A.G., and Nummedal, D., 2000, The falling stage systems tract; recognition and importance in sequence stratigraphic analysis, *in* Hunt, D., and Gawthorpe, R.L., eds., Sedimentary Responses to Forced Regressions: Geological Society of London Special Publication 172, p. 1-17.

Plummer, P.S., and Gostin, V.A., 1981, Shrinkage cracks; desiccation or synaeresis?: Journal of Sedimentary Research, v. 51, p. 1147-1156.

Posamentier, H.W., and Allen, G.P., 1999, Siliciclastic Sequence Stratigraphy - Concepts and Applications, SEPM Concepts in Sedimentology and Paleontology no. 7: Tulsa, OK, SEPM (Society for Sedimentary Geology), 204 p.

Posamentier, H.W., and Morris, W.R., 2000, Aspects of the stratal architecture of forced regressive deposits, *in* Hunt, D., and Gawthorpe, R.L., eds., Sedimentary Responses to Forced Regressions: Geological Society of London Special Publication 172, p. 19-46.

Retallack, G., 1990, Soils of the Past: London, Unwin Hynman Ltd., 520 p.

Roberts, E.M., Deino, A.L., and Chan, M.A., 2005, $^{40}Ar/^{39}Ar$ age of the Kaiparowits Formation, southern Utah, and correlation of contemporaneous Campanian strata and vertebrate faunas along the margin of the Western Interior Basin: Cretaceous Research, v. 26, p. 307-318.

Shanley, K.W., and McCabe, P.J., 1991, Predicting facies architecture through sequence stratigraphy - An example from the Kaiparowits Plateau, Utah: Geology, v. 19, p. 742-745.

—1994, Perspectives on the sequence stratigraphy of continental strata: American Association of Petroleum Geologists Bulletin, v. 78, p. 544-568.

Shanley, K.W., McCabe, P.J., and Hettinger, R.D., 1992, Tidal influence in Cretaceous fluvial strata from Utah, USA - a key to sequence stratigraphic interpretation: Sedimentology, v. 39, p. 905-930.

Smith, C., 1983, Geology, depositional environments, and coal resources of the Mt. Pennell 2 NW quadrangle, Garfield

County, Utah: Brigham Young University Geology Studies, v. 30, pt. 1, p. 145-169.

—2003, Interim Geologic Map of the Cave Flat (Mt. Pennell 2 NW) Quadrangle, Garfield County, Utah: Utah Geological Survey Open-File Report 406.

Tabet, D.E., 1999, Coal resources of the Henry Mountains Coalfield: Utah Geological Survey Open-File Report 362, 32 p.

—2000, Coal resources of the Henry Mountains coal field, Utah, *in* Kirschbaum, M.A., Roberts, L.N.R., and Biewick, L.R.H., eds., Geologic Assessment of Coal in the Colorado Plateau: Arizona, Colorado, New Mexico, and Utah: United States Geological Survey Professional Paper 1625-B, p. R1-R25.

Tabet, D.E., and Wakefield, S., 2006, Coal resource map of Utah: Utah Geological Survey, Map 226CM.

Thomas, R.G., Smith, D.G., Wood, J.M., Visser, J., Calverley-Range, E.A., and Koster, E.H., 1987, Inclined heterolithic stratification; terminology, description, interpretation and significance: Sedimentary Geology, v. 53, p. 123-179.

Van Wagoner, J.C., 1995, Sequence stratigraphy and marine to nonmarine facies architecture of foreland basin strata, Book Cliffs, Utah, U.S.A, *in* Van Wagoner, J.C., and Bertram, G.T., eds., Sequence Stratigraphy of Foreland Basin Deposits - Outcrop and Subsurface Examples from the Cretaceous of North America: American Association of Petroleum Geologists Memoir 64, p. 137-223.

Van Wagoner, J.C., Mitchum, R.M., Campion, K.M., and Rahmanian, V.D., 1990, Siliciclastic Sequence Stratigraphy in Well Logs, Cores and Outcrops, American Association of Petroleum Geologists, Methods in Exploration Series, v. 7, 55 p.

Van Wagoner, J.C., Posamentier, H.W., Mitchum, R.M., Vail, P.R., Sarg, J.F., Loutit, T.S., and Hardenbol, J., 1988, An overview of sequence stratigraphy and key definitions, *in* Wilgus, C.K., Hastings, B.S., Kendall, C.G.S.C., Posamentier, H.W., Ross, C.A., and Van Wagoner, J.C., eds., Sea Level Changes - An Integrated Approach, Society of Economic Paleontologists and Mineralogists (SEPM) Special Publication, v. 42, p. 39-45.

Whitlock, W.W., 1984, Geology of the Steele Butte Quadrangle, Garfield County, Utah: Brigham Young University Geology Studies, v. 31, pt. 1, p. 141-165.

Willis, A., 2000, Tectonic control of nested sequence architecture in the Sego Sandstone, Neslen Formation and upper Castlegate Sandstone (Upper Cretaceous), Sevier foreland basin, Utah, USA: Sedimentary Geology, v. 136, p. 277-317.

Yoshida, S., 2000, Sequence and facies architecture of the upper Blackhawk Formation and the lower Castlegate Sandstone (Upper Cretaceous), Book Cliffs, Utah, USA: Sedimentary Geology, v. 136, p. 239-276.

APPENDICES

Appendix A - Muley Canyon Sandstone and Masuk Formation Measured Sections #1-21

Explanation for Measured Sections 1-21

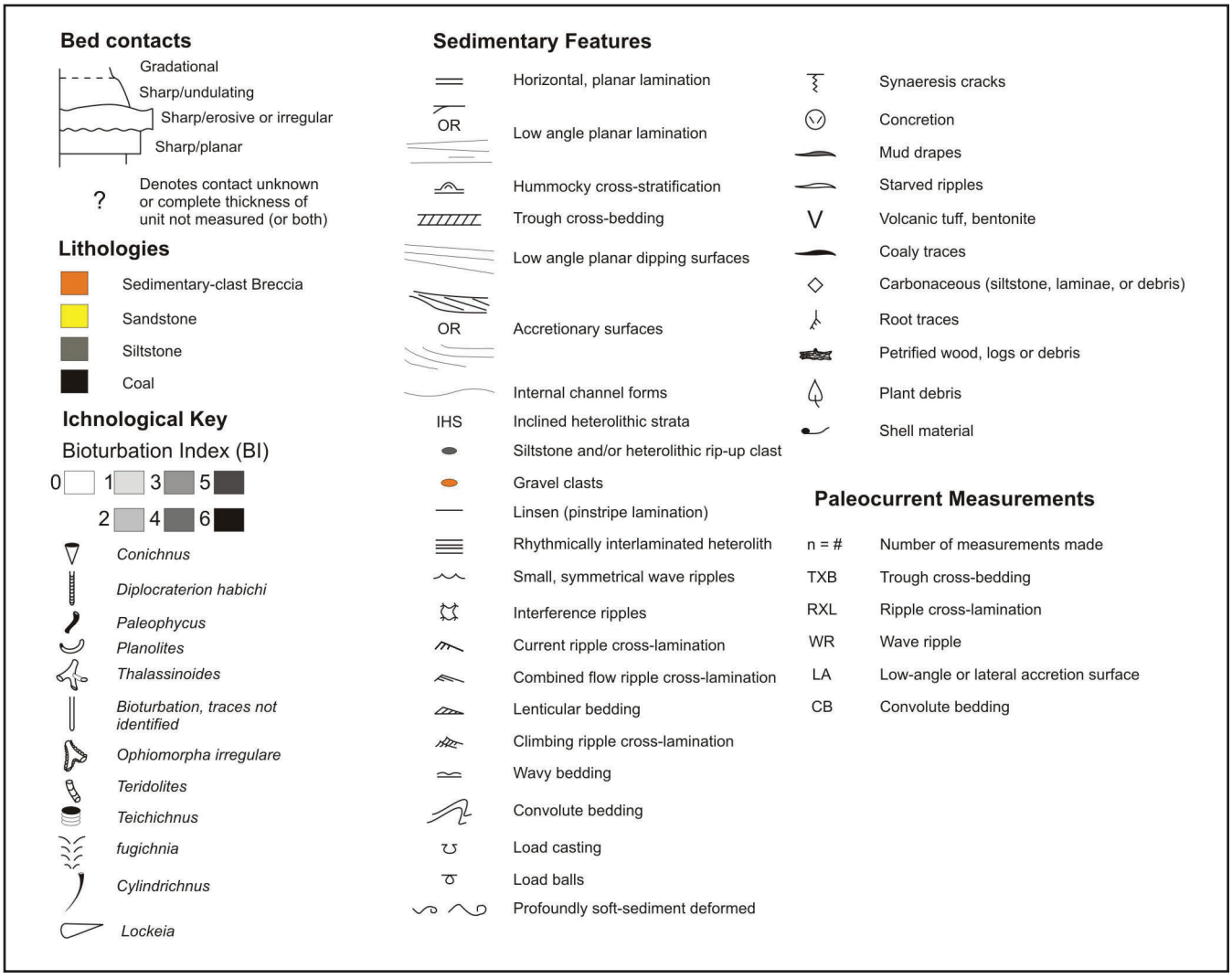

Section Name: Masuk Formation, Section 1, Type Section (Eaton, 1990)

Location (lat/long): N38°05.040' E111°00.410' **Total Thickness Measured:** 212.4m

Date Measured: 3/19-21/2008 **Measured By:** Matthew Corbett

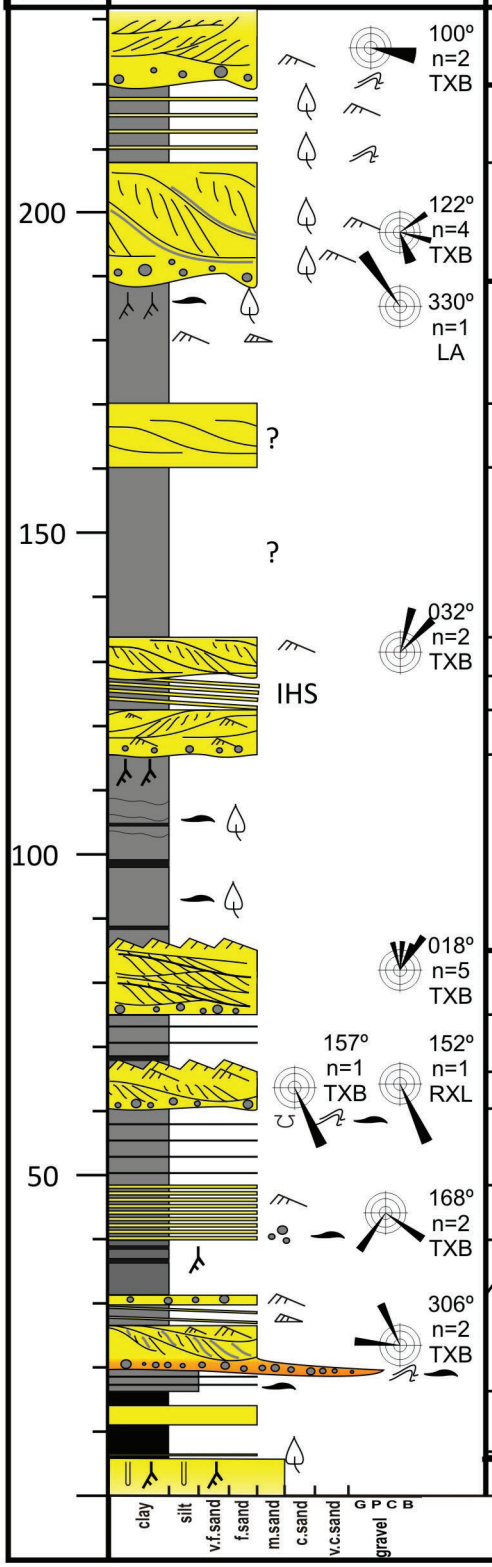

Facies	Depositional Environment	Description
5	Amalgamated Fluvial Sheet Sandstone	**Tarantula Mesa Sandstone** Fine Sandstone: amalgamated white to grey sandstones weathering pink and appears to coarsen upward in cliff, abundant trough x-beds, contact in lower slope and not cliff base
4	Multi-storey Fluvial Sheet Sandstones	**Upper Mbr, Masuk Fm** 200.4-212.4m, Interbedded Fine Sandstone and Mudstone: carbonaceous mud, abundant plant debris in mudstone and sandstone
5		180.9-200.4m, Fine Sandstone: sandstone with shale partings, abundant trough x-beds, large-scale lateral accretionary surfaces recognized across cliff face
2	Floodplain Deposits, Some Poorly Exposed Channels	**Middle Mbr, Masuk Fm** 126.4- 180.9m, Poorly Exposed Mudstone: few thin interbedded sandstones, large inaccessible portion of sandstone visible along cliff face; at top mudstone is grey/green and contains rhizoliths, coal fragments, and plant debris
5?		
2		
5	Tidally Influenced Multi-storey Channel Belt	108.1-126.4m, Fine Sandstone: trough x-bedded sandstones separated by heterolith and shale partings, some lateral accretion surfaces visible, base dominantly ripple x-laminated
4		
5		
2	Floodplain Deposits	78.4-108.1m, Mudstone: grey-grey/green w/ beds of carbonaceous and coaly mud; at top is a grey/green mudstone with rhizoliths (paleosol?)
5	Amalgamated Fluvial Sandstone	**Lower Mbr, Masuk Fm** 68.4-78.4m, Fine Sandstone: friable, abundant 0.5m thick trough x-beds, ripple topped by bimodal climbing ripples
2	Muti-storey Tidally Influenced Channels and Floodplain Deposits	59.8-68.4m, Mudstone: poorly exposed slope, carbonaceous mud and thin interbedded sandstone
5		53.86-59.8m, Fine Sandstone: trough x-bedded, ripple topped
3		41.86-53.86m, Interlaminated Fine Sandstone and Mudstone: 33.36-41.86m, Interbedded Fine Sandstone and Mudstone: trough x-bedded sands clay rip-up at base
4		
2		25.2-33.36m, Mudstone: interbedded w/ thin carbonaceous mud
5 & 6	Tidally Influenced Fluvial Sheet Sandstone	13.28-25.2m, Medium-fine Sandstone: pebble sized clay rip-up in coarse sand at base (intraformational conglomerate), paired mud drapes in trough x-beds, interbedded sand/silt at top 10.25-13.28m, Siltstone: grey, interbedded thin sandstone
1	Coastal Plain Mires and Single Storey Channels	0.65-10.25m, Coal: interbedded carbonaceous shale & thin sandstone
5		0.4-0.65m, Fine Sandstone: plant fossils
1		0-0.4m, Coal
		Muley Canyon Sandstone Medium Sandstone: bioturbated

Section Name: Masuk Section 2
Location (lat/long): N38°4'34.68" W111°0'17.64" **Total Thickness Measured:** 223.4m
Date Measured: 5/27-29/2008 **Measured By:** Matthew Corbett

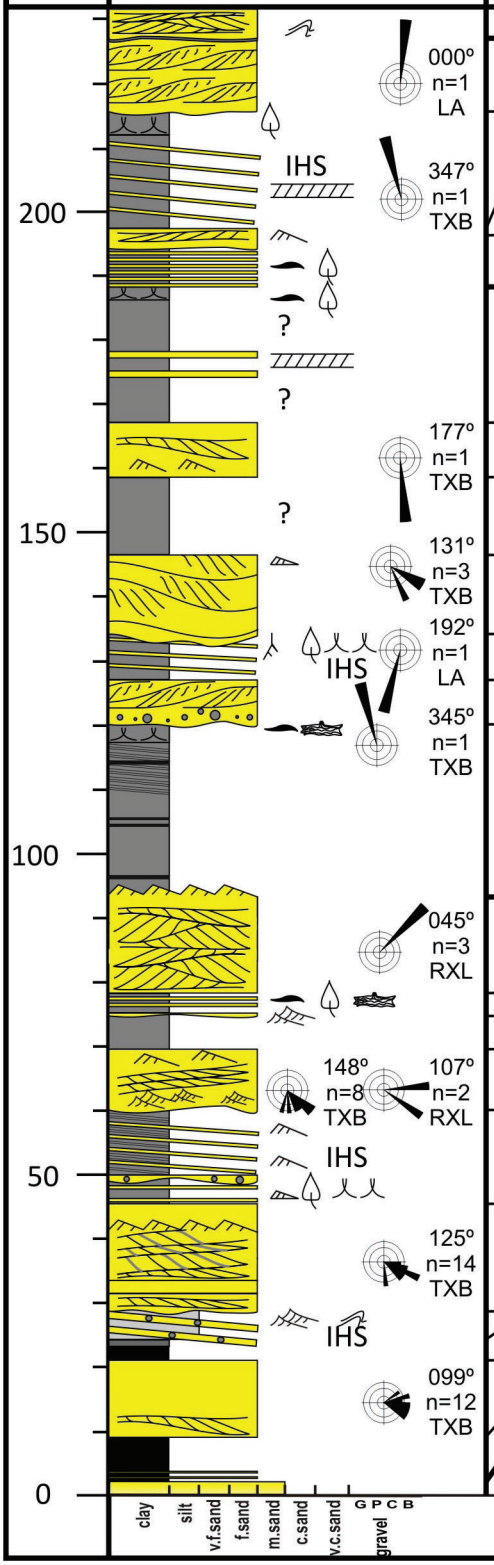

Facies	Depositional Environment	Description
5	Amalgamated Fluvial	**Tarantula Mesa Sandstone** Fine Sandstone: amalgamated trough x-bedded sandstones
5	Multi-storey Fluvial Sheet Sandstone	**Upper Mbr, Masuk Fm** 211.4-223.4m, Fine Sandstone: trough x-bedded sandstone bodies, separated in places by shale partings, lateral accretion surfaces visible
4	Single Storey Tidally Influenced Channels	193.9-211.4m, Sandstone Dominated Heterolith: top 3m has "peak and trough" slickensides, and plant debris
5		190.6-193.9m, Fine Sandstone: trough x-bedded and ripple x-laminated
4		184.8-190.6m, Interbedded Fine Sandstone and Mudstone: beds ~10cm thick
2	Single Storey Fluvial Sandstones and Floodplain Deposits	**Middle Mbr, Masuk Fm** 163.8-184.8m, Mudstone: mostly covered mud with a few thin sandstone beds; top 2m is dark grey, has "peak and trough" slickensides, and coal and plant fragments
5	Fluvial Channel	155.3-163.8m, Fine Sandstone: trough x-bedded, ripple x-laminated near base
2	Floodplain Deposits	143.3-155.3, Poorly Exposed Mudstone:
5	Tidally Influenced Multi-storey Channel Belt	130.3-143.3m, Fine Sandstone: abundant trough x-beds
4		123.8-130.3m, Interbedded Mudstone and Fine Sandstone: 0.5m at top has "peak and trough" slickensides, rhizoliths, and plant debris
5		116.5-123.8m, Fine Sandstone: trough x-bedded, some lateral accretion surfaces visible
2	Floodplain Deposits	90.5-116.5m, Mudstone: grey to grey/green, few beds of carbonaceous mudstone; top 2-3m has "peak and trough" slickensides and abundant plant and wood debris
5	Tidally Influenced Amalgamated Fluvial Sandstone	**Lower Mbr, Masuk Fm** 75.5-90.5m, Fine Sandstone: friable, alternately slope and cliff forming, abundant trough x-beds, bimodal ripple topped
4		71.8-75.5m, Interbedded Fine Sandstone and Mudstone: ripple x-lam. And ripple topped sandstone at base, unidirectional climbing ripples
2	Tidally Influenced Multi-storey Fluvial Sandstones and Floodplain Deposits	66.8-71.8m, Mud: poorly exposed, some sandy interbeds
5		56.8-66.8m, Fine Sandstone: climbing ripples and abundant trough x-bedding
4		45.8-56.8m, Interbedded Fine Sandstone and Mudstone: bedding 20-40cm thick, plane lamination in finer grained sed.
		42.6-45.8m, Interbedded Mudstone and Fine Sandstone: top 0.5m has "peak and trough" slickensides and abundant plant debris
5	Amalgamated Tidally Influenced Fluvial Sheet Sandstone	25.8-42.6m, Fine Sandstone: few shale partings, abundant trough x-beds (climbing?) And ripple x-lamination, some possible thin mud or organic drapes in trough and ripple x-bedding
4		21.8-25.8m, Interbedded Fine Sandstone and Mudstone: largely silty-fine, beds 40-60cm thick
1	Coastal Plain Mires and Single Storey Channels	18.7-21.8m, Coal: thin grey mudstone at top
5?		6.7-18.7m, Fine Sandstone: poorly exposed, contains trough x-bed with paired mud/organic drapes
1		0-6.7m, Coal: thin sandstone & carbonaceous mudstone at base
		Muley Canyon Sandstone Medium Sandstone: ripple x-laminated

Section Name: Masuk Section 3
Location (lat/long): N38°6'3.06" W111°1'18.16" **Total Thickness Measured:** ~165m
Date Measured: 6/30-31/2008 **Measured By:** Matthew Corbett

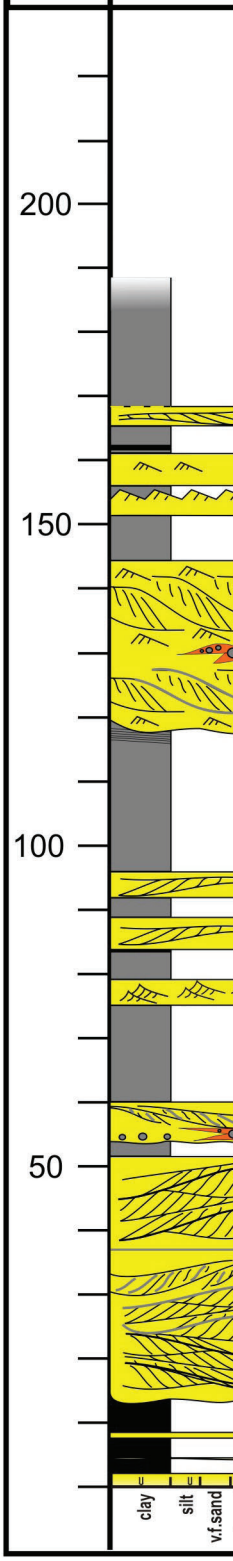

Facies	Depositional Environment	Description
2	Floodplain Deposits	**Middle Mbr, Masuk Fm** 165m+, Mudstone: rest of section inaccessible
2 & 5	Single Storey Sheet Sandstone and Floodplain Deposits	141.5-165m, Mudstone and Fine Sandstone Beds: thin sandstones within grey mudstones, trough x-bedded or ripple x-laminated
5 & 6	Multi-storey Fluvial Sheet Sandstones	114.5-141.5m, Fine Sandstone: trough x-bedded and ripple x-laminated, large scale lateral accretion surfaces or low angle bedding, shale partings between surfaces in lower portion, thin bed of pebble-cobble sized rip-up clasts in silt (intraformational conglomerate); a thicker mudstone interval separates the two sandstone bodies further to the south
2	Floodplain Deposits	93-114.5m, Mudstone: eroded and covered across open mesa
2 & 5	Single Storey Sheet Sandstone and Floodplain Deposits	**Lower Mbr, Masuk Fm** 57.5-93m, Mudstones and Thin Sandstones: since section is eroded and covered across open mesa, exact placement of the boundary is difficult, but is likely the top of the lowest sandstone; some thin trough x-bedded and ripple x-laminated sands; top 1.5m shows evidence of low angle bedding and plant debris
5		51-57.5m, Medium-fine Sandstone: trough x-bedded with mud drapes, bed of pebble-cobble sized clay rip up at base and in coarser lenses of sandstone (intraformational conglomerate)
2		49-51m, Mudstone: rhizoliths, plant debris and large woody fragments
5	Tidally Influenced Amalgamated Sheet Sandstones	10.5-49m, Fine Sandstone: mostly trough x-bedded with some possible mud drapes, shale/silt partings near top
1	Coastal Plain Mires and Single Storey Channels	6.1-10.5m, Carbonaceous Shale & Coal
5		5.2-6.1m, Fine Sandstone: trough x-bedded and ripple x-lam.
1		2.3-5.2m, Carbonaceous Shale
3?		2-2.3m, Fine Sandstone: bioturbated, possible clay rip-up
1		0-2m, Carbonaceous Shale
		Muley Canyon Sandstone Medium Sandstone: bioturbated

Section Name: Masuk Section 4

Location (lat/long): N38°4'58.10" W110°59'6.05" **Total Thickness Measured:** 193.07m

Date Measured: 6/1-6/2008 **Measured By:** Matthew Corbett

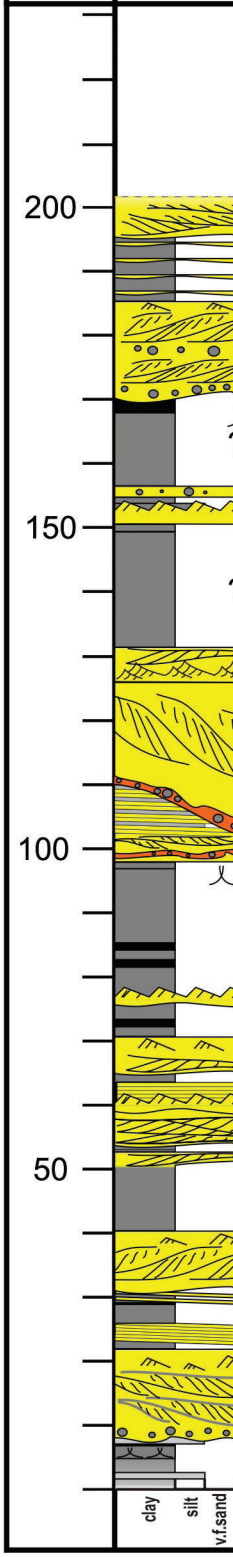

Facies	Depositional Environment	Description
5	Amalgamated Fluvial Sheet Sandstone	**Tarantula Mesa Sandstone** Fine Sandstone: abundant trough x-beds, contact near beginning of cliff
4	Multi-storey Fluvial Sheet Sandstones	**Upper Mbr, Masuk Fm** 183.37-193.07m, Interbedded Fine Sandstone and Mudstone: trough x-bedded sandstones and grey to carbonaceous mudstones, beds 20-40cm thick
5		167.47-183.37m, Fine Sandstone: trough x-bedded, large scale lateral accretionary structures, bone fragment found at base
2 & 5	Isolated Channels and Floodplain Deposits	**Middle Mbr, Masuk Fm** 129.52-167.47m, Poorly Exposed Mudstone: mostly covered by erosional debris, some thin sandstones and "peak and trough" slickensided mudstones with plant, woody, and coal fragments; one thin sandstone contains sandstone casts of burrows into what appears to be a hollow log mold (*Teredolites*)
5	Tidally Influenced (?) Multi-storey Channel Belt	108.52-129.52m, Fine Sandstone: trough x-bedded, cobble sized clay rip-up at base (intraformational conglomerate), some thin beds of climbing ripples near top, large scale lateral accretion surfaces, appears to incise into sandstones below
4		101.02-108.52m, Interbedded Fine Sandstone and Silt: beds alternating brown to grey, low angle bedding (inclined heterolithic strata?)
5		96.52-101.02m, Fine Sandstone: climbing trough x-beds, plant and coaly fragments and small beds of pebble sized clay rip-up clasts at base
2	Floodplain Deposits	69.42-96.52m, Mudstone: grey to grey-green mudstone with some thin sandstone and carbonaceous mudstone beds; top 1m is has "peak and trough" slickensides, plant debris, and woody/coaly fragments
5	Multi-storey (?) Fluvial Sheet Sandstones	**Lower Mbr, Masuk Fm** 63.42-69.42m, Fine Sandstone: trough x-bedded, ripple x-laminated at top
2		62.32-63.42m, Mudstone: slickensides, plant and coaly debris
3 & 5		58.72-62.32m, Fine Sandstone: interlaminated sandstone and mudstone, some thin carbonaceous beds
		52.22-58.72m, Fine Sandstone: friable sandstone, abundant trough x-bedding, thin ripple x-laminated at top
2 & 5	Tidally Influenced Multi-storey Fluvial Sandstone and Floodplain Deposits	51.52-52.22m, Mudstone: finely laminated
		39.22-51.52m, Mudstone-fine Sandstone: mudstone coarsening at top into trough x-bedded sand with large chert nodules
5		29.42-39.22m, Fine Sandstone: trough x-bedded with ripple x-lamination at top, large scale lateral accretion surfaces
4		27.92-29.42m, Interbedded Fine Sandstone and Mudstone: beds 5-20cm thick
3		20.92-27.92m, Fine Sandstone: some fine laminated sand and organic layers
5	Single Storey Sheet Sandstone and Floodplain Deposits	7.12-20.92m, Medium-fine Sandstone: abundant trough x-beds with ripple x-lamination at top, low angle bedding/lateral accretion with shale partings, abundant convolute/disturbed bedding
2		0-7.12m, Mud-siltstone: interbedded with 2m of "peak and trough" slickensides, abundant plant debris, and woody fragments

Section Name: Masuk Section 5
Location (lat/long): N38°5'24.00 W110°59'0.96" **Total Thickness Measured:** 171.51m
Date Measured: 6/7-8/2008 **Measured By:** Matthew Corbett

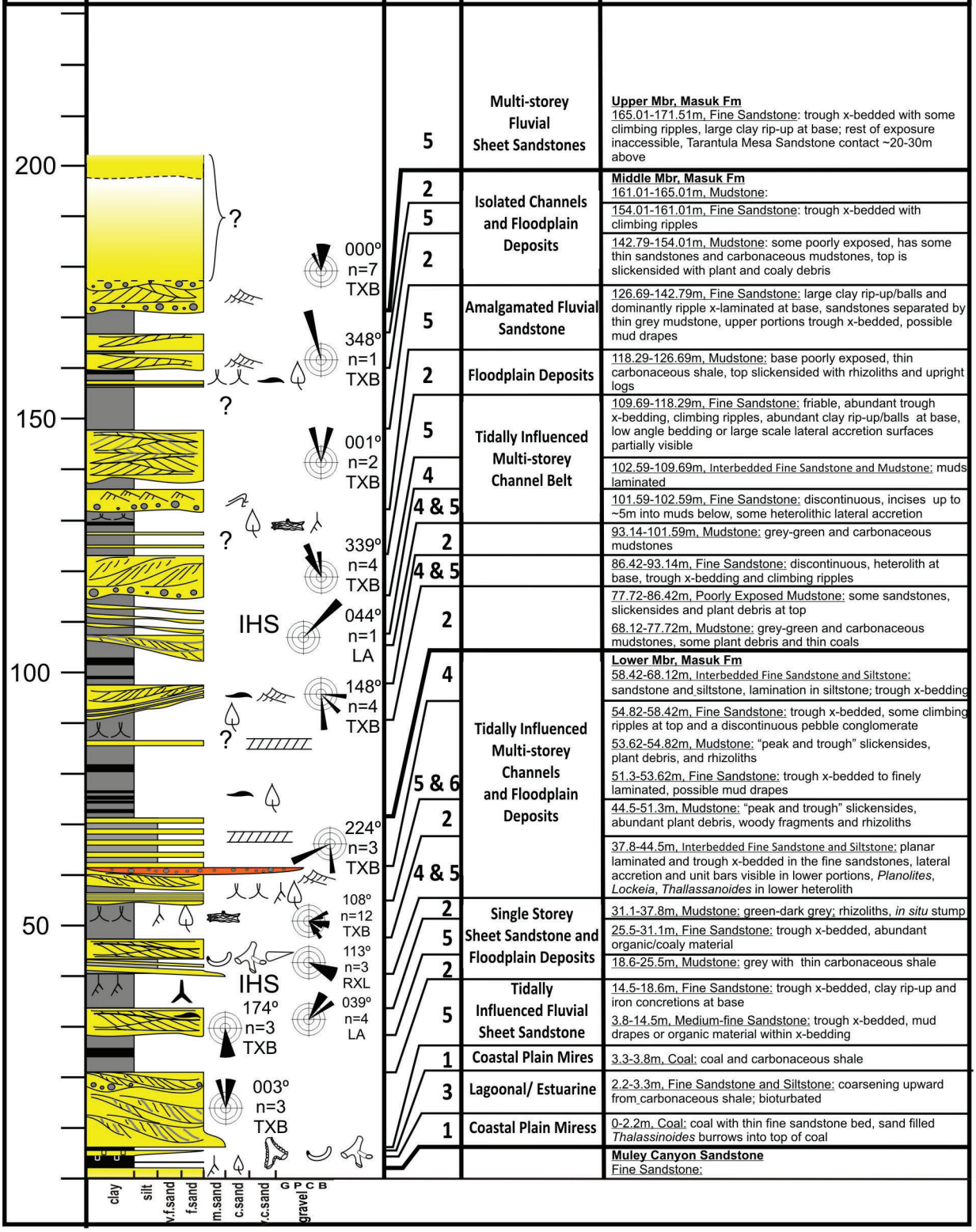

Section Name: Masuk Section 6
Location (lat/long): N38°5'3.84" W110°57'57.96" **Total Thickness Measured:** 47.7m
Date Measured: 6/12/2008 **Measured By:** Matthew Corbett

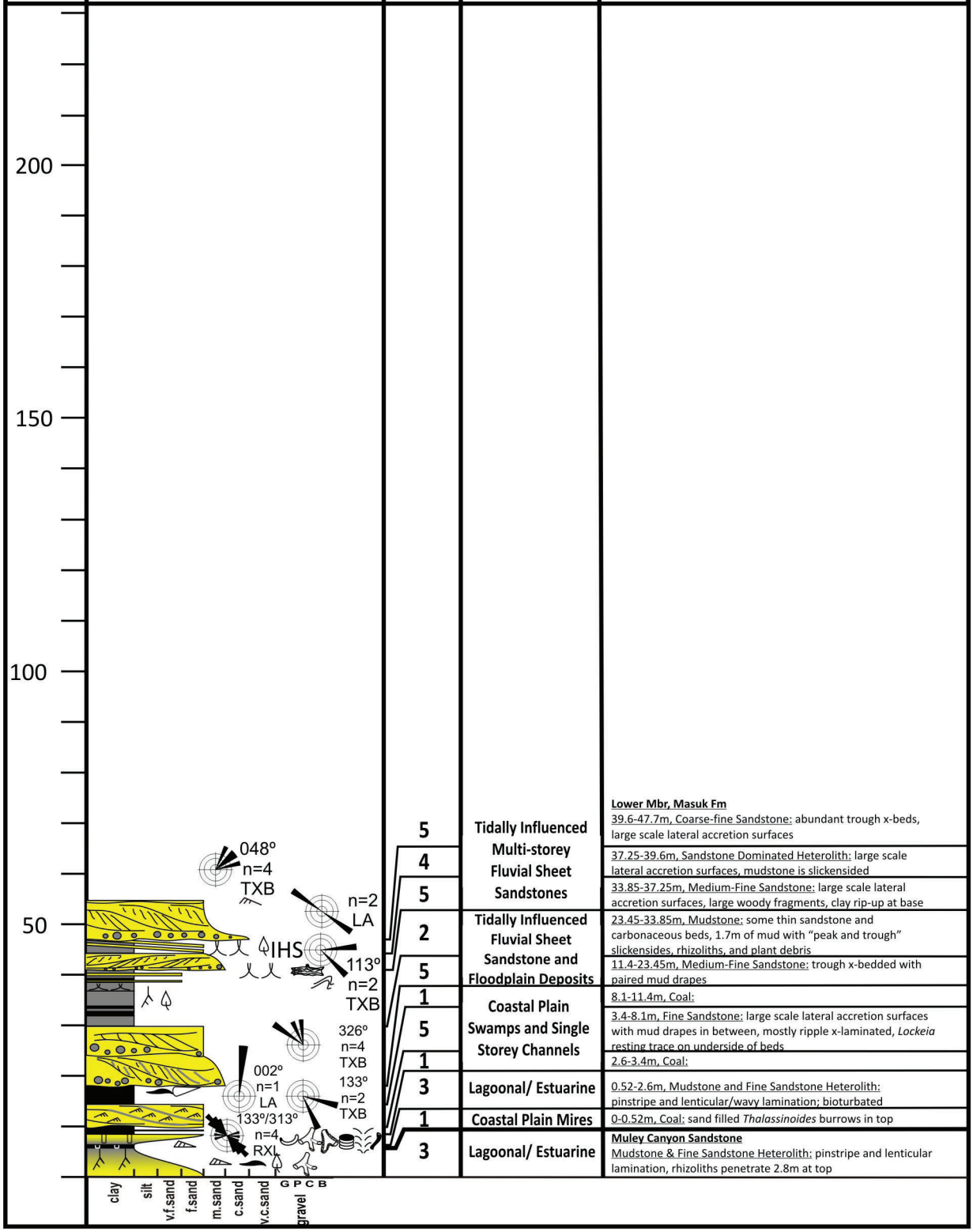

Section Name: Masuk Section 6
Location (lat/long): N38°5'3.84" W110°57'57.96" **Total Thickness Measured:** 47.7m
Date Measured: 6/12/2008 **Measured By:** Matthew Corbett

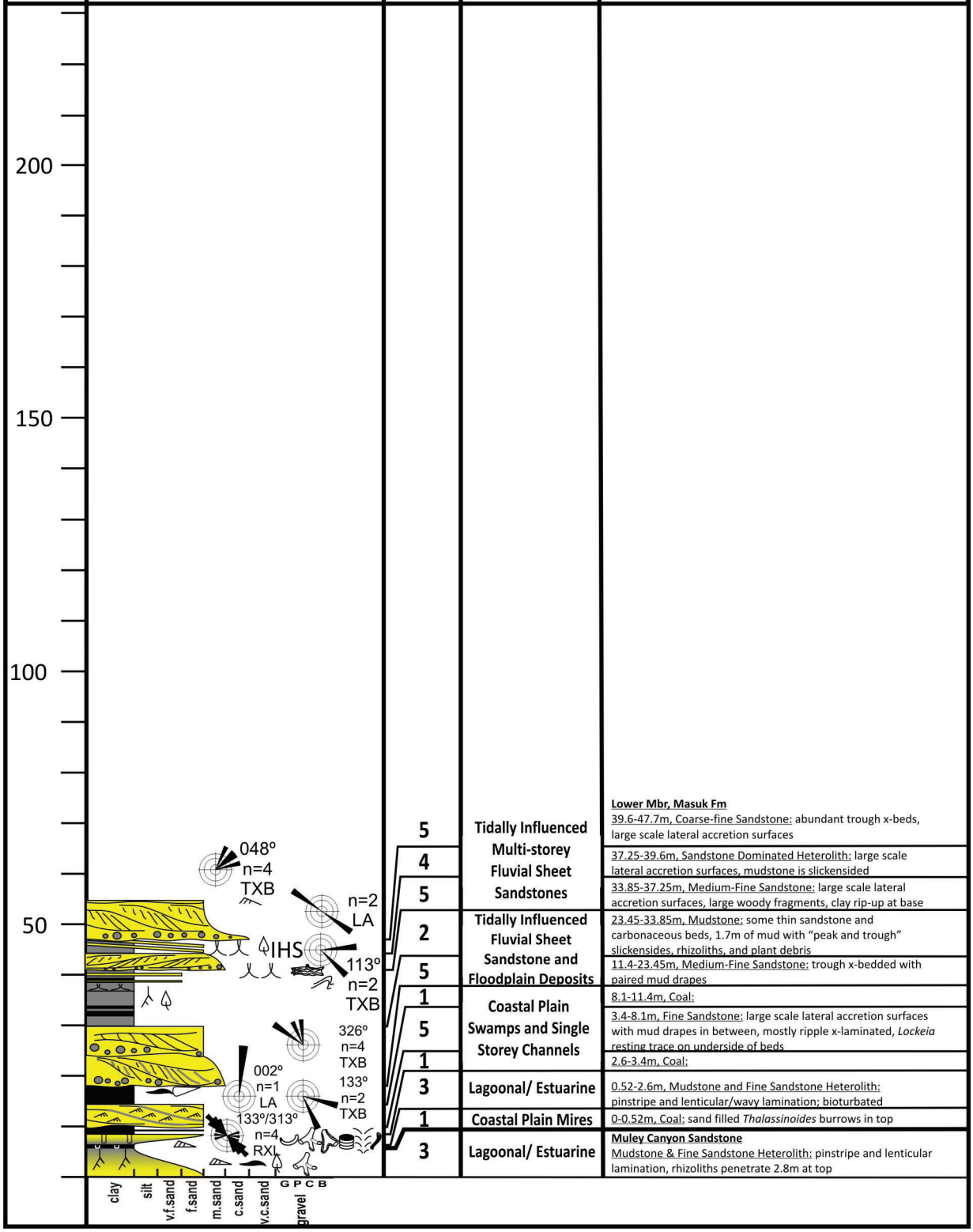

Section Name: Masuk Section 7

Location (lat/long): N38°5'42" W111°1'9.84" **Total Thickness Measured:** 39.1m

Date Measured: 6/12/2008 **Measured By:** Matthew Corbett

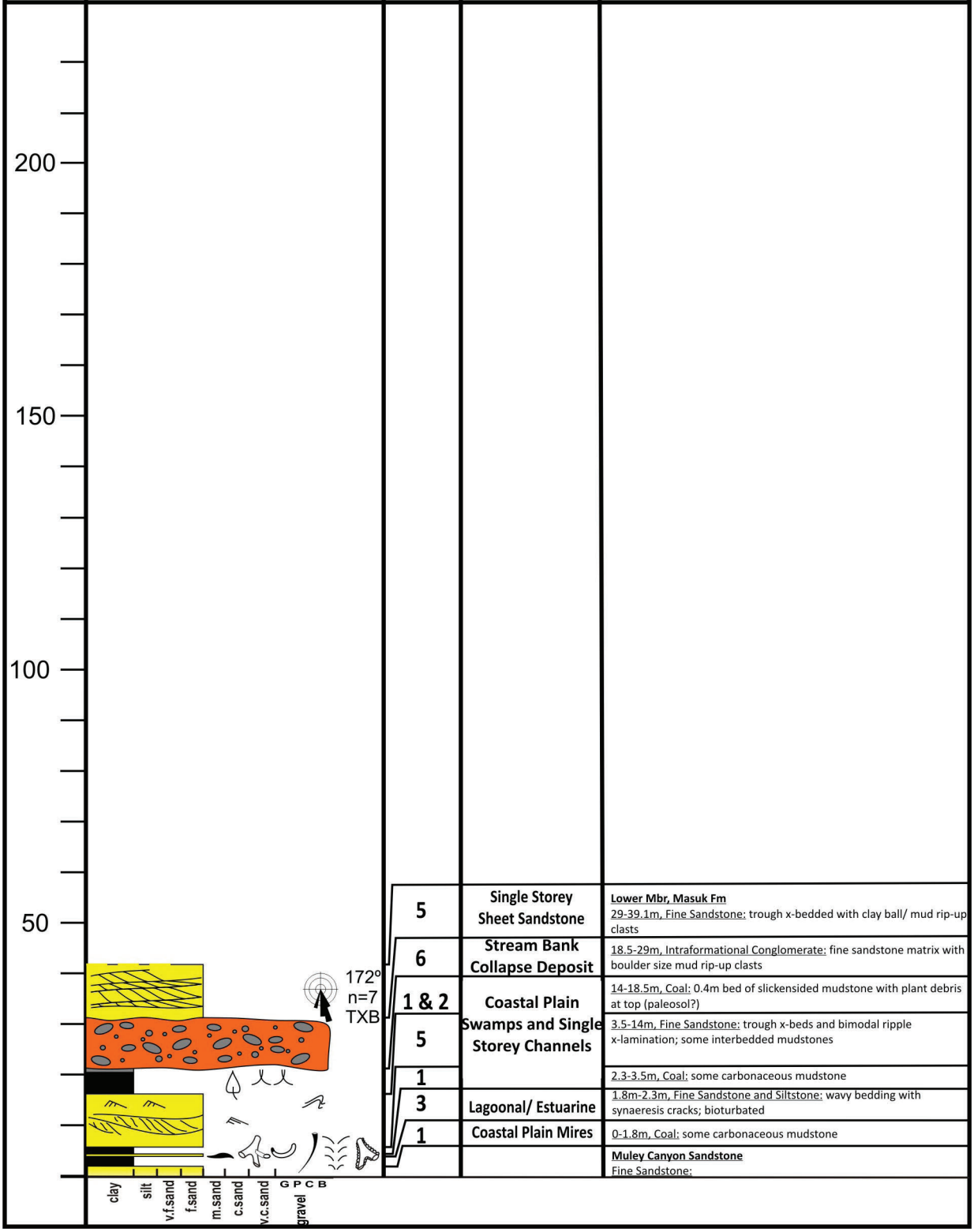

Facies	Depositional Environment	Description
5	Single Storey Sheet Sandstone	**Lower Mbr, Masuk Fm** 29-39.1m, Fine Sandstone: trough x-bedded with clay ball/ mud rip-up clasts
6	Stream Bank Collapse Deposit	18.5-29m, Intraformational Conglomerate: fine sandstone matrix with boulder size mud rip-up clasts
1 & 2	Coastal Plain Swamps and Single Storey Channels	14-18.5m, Coal: 0.4m bed of slickensided mudstone with plant debris at top (paleosol?)
5		3.5-14m, Fine Sandstone: trough x-beds and bimodal ripple x-lamination; some interbedded mudstones
1		2.3-3.5m, Coal: some carbonaceous mudstone
3	Lagoonal/ Estuarine	1.8m-2.3m, Fine Sandstone and Siltstone: wavy bedding with synaeresis cracks; bioturbated
1	Coastal Plain Mires	0-1.8m, Coal: some carbonaceous mudstone
		Muley Canyon Sandstone Fine Sandstone:

MULEY CANYON SANDSTONE AND MASUK FORMATION, LOWER MEMBER - North Sweetwater Creek SECTION 8

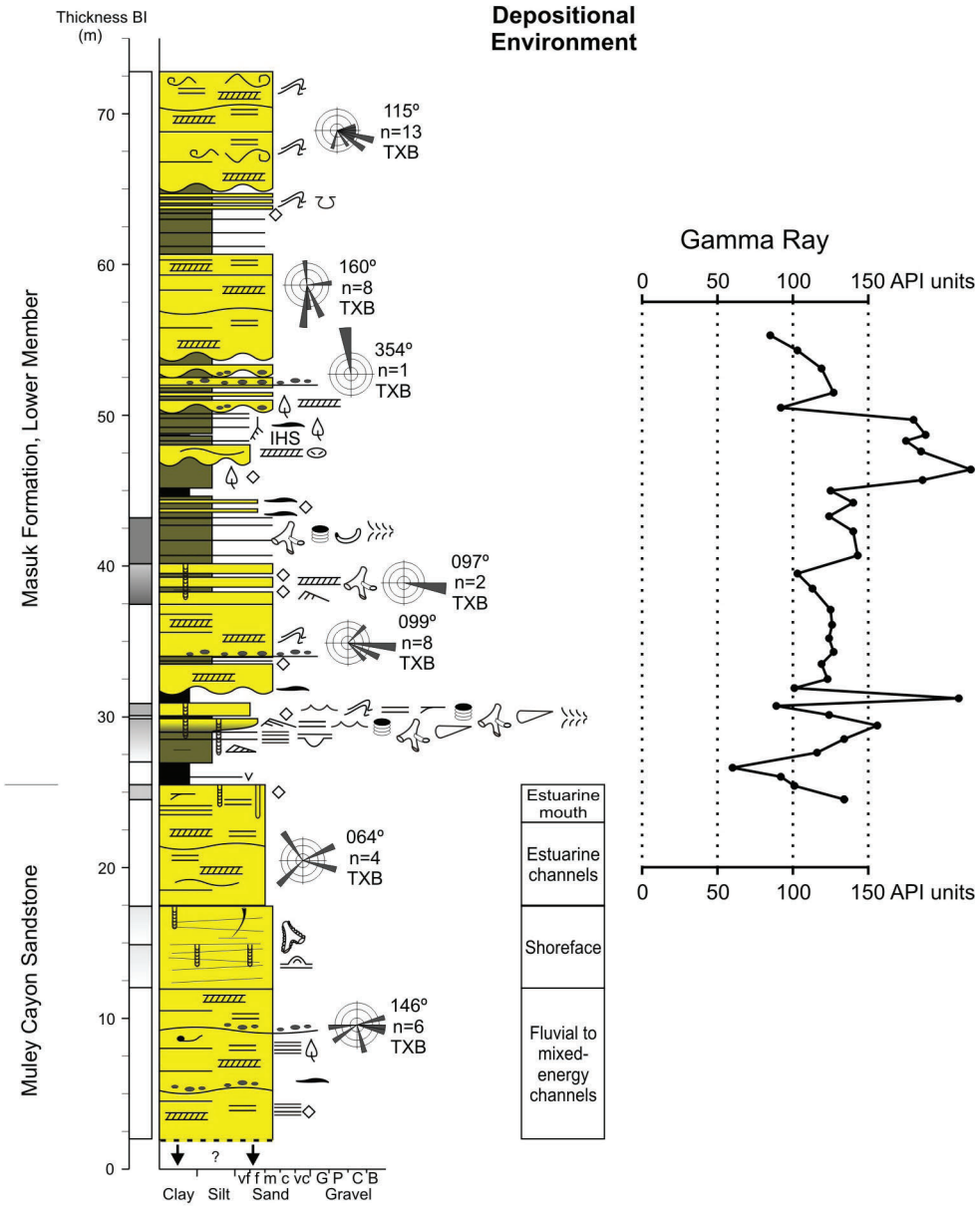

MULEY CANYON SANDSTONE AND MASUK FORMATION, LOWER MEMBER - Dripping Rock Seep SECTION 9

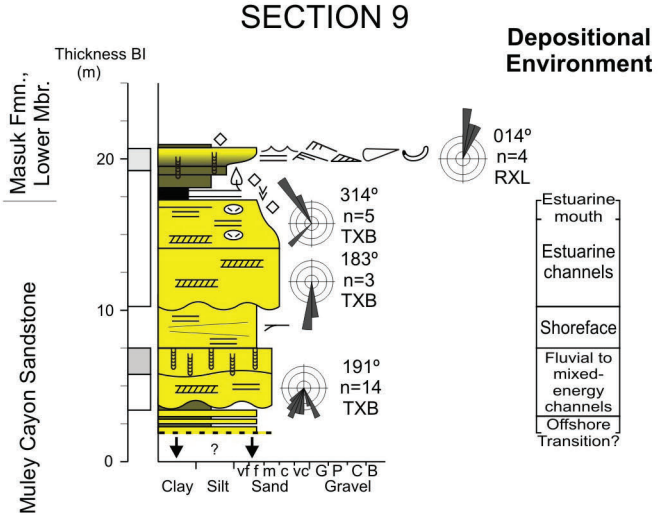

MULEY CANYON SANDSTONE AND MASUK FORMATION, LOWER MEMBER - Sweetwater Creek, Road Crossing SECTION 10

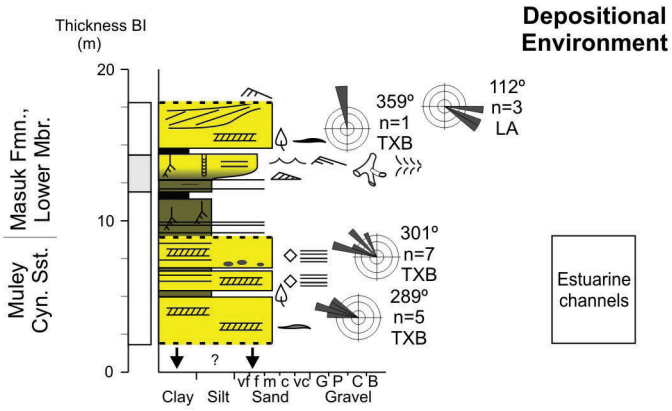

MULEY CANYON SANDSTONE AND MASUK FORMATION, LOWER MEMBER - 1.5 km South of Blind Trail SECTION 11

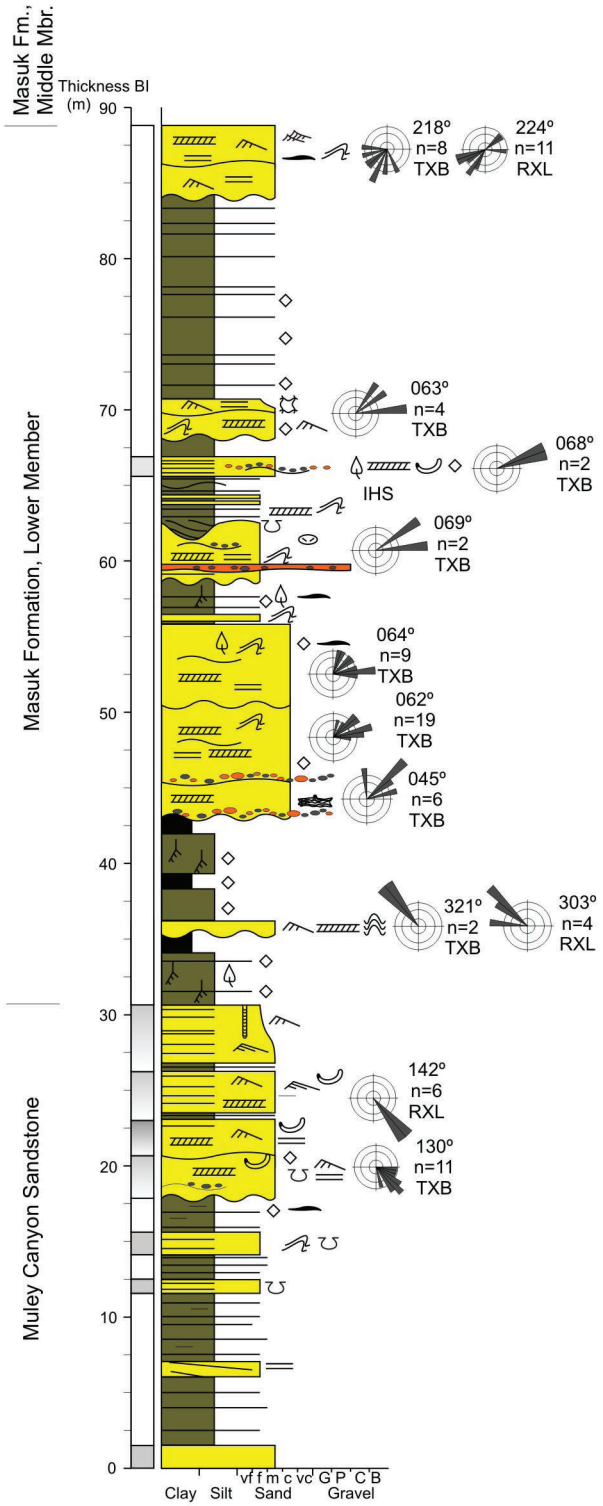

MULEY CANYON SANDSTONE AND
MASUK FORMATION, LOWER MEMBER -
2.5 km South of Blind Trail
SECTION 12

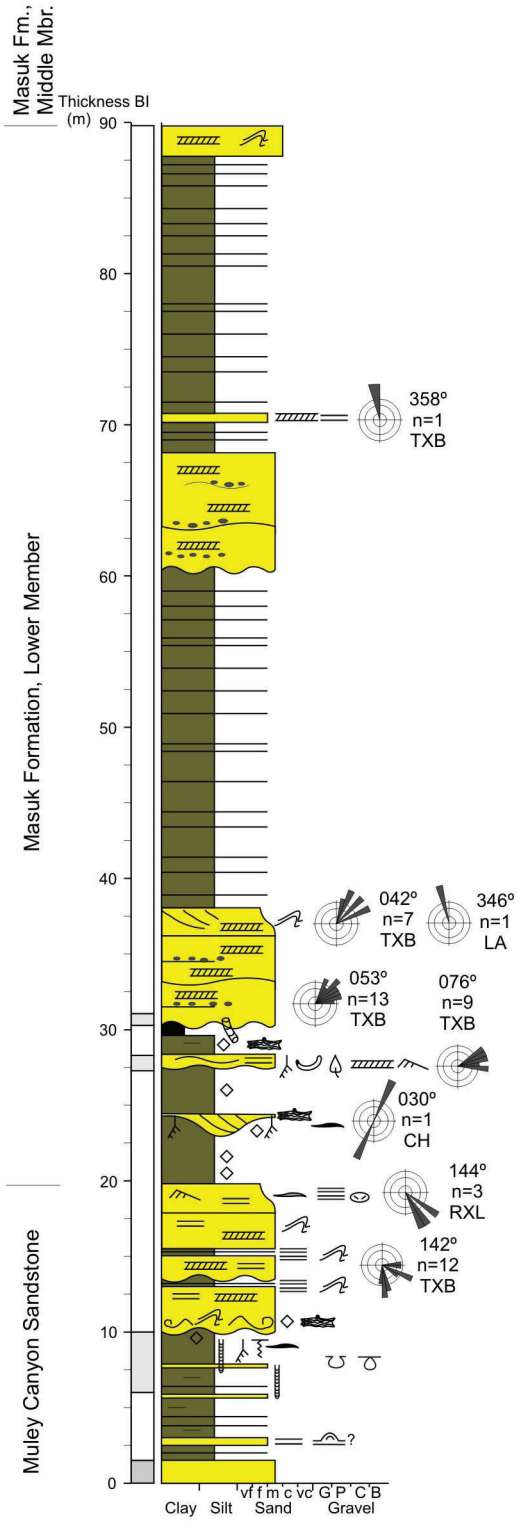

MULEY CANYON SANDSTONE - 1st Gullly North of Blind Trail SECTION 13

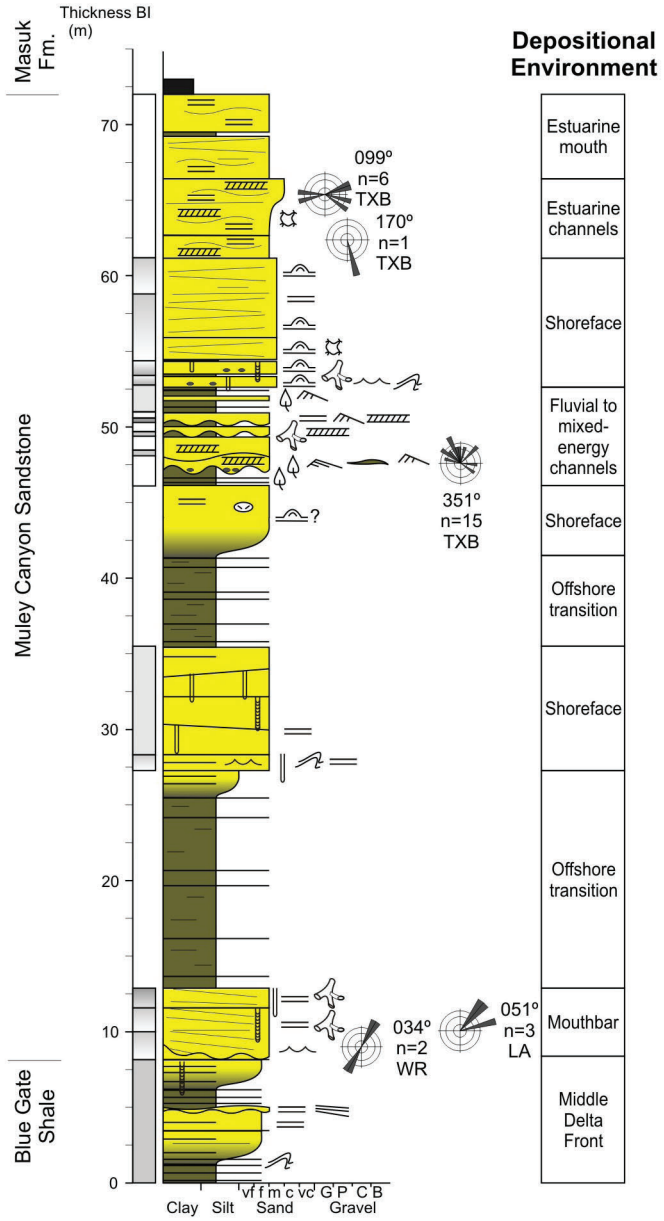

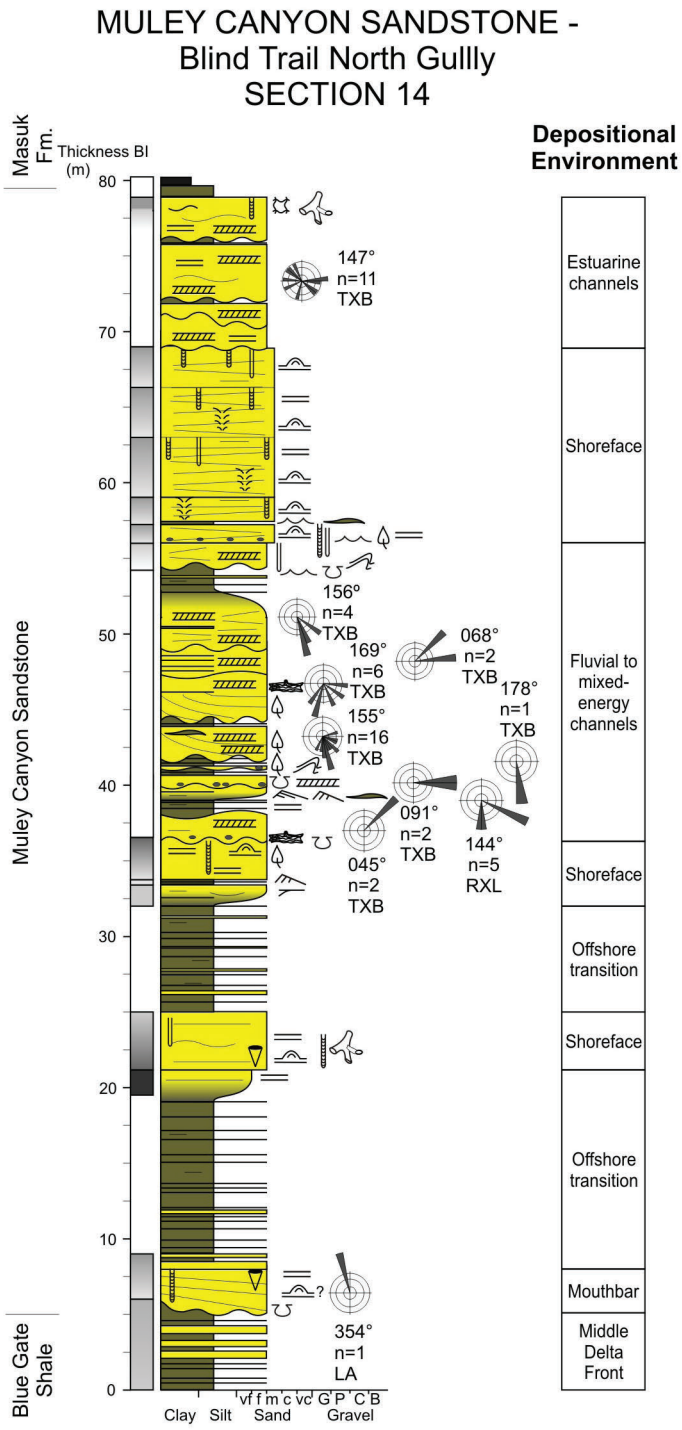
MULEY CANYON SANDSTONE -
Blind Trail North Gullly
SECTION 14
Masuk Fm.
Thickness BI (m)
Depositional Environment
Muley Canyon Sandstone
Blue Gate Shale
147° n=11 TXB
156° n=4 TXB
169° n=6 TXB
155° n=16 TXB
068° n=2 TXB
178° n=1 TXB
091° n=2 TXB
144° n=5 RXL
045° n=2 TXB
354° n=1 LA
Estuarine channels
Shoreface
Fluvial to mixed-energy channels
Shoreface
Offshore transition
Shoreface
Offshore transition
Mouthbar
Middle Delta Front
Clay Silt Sand Gravel

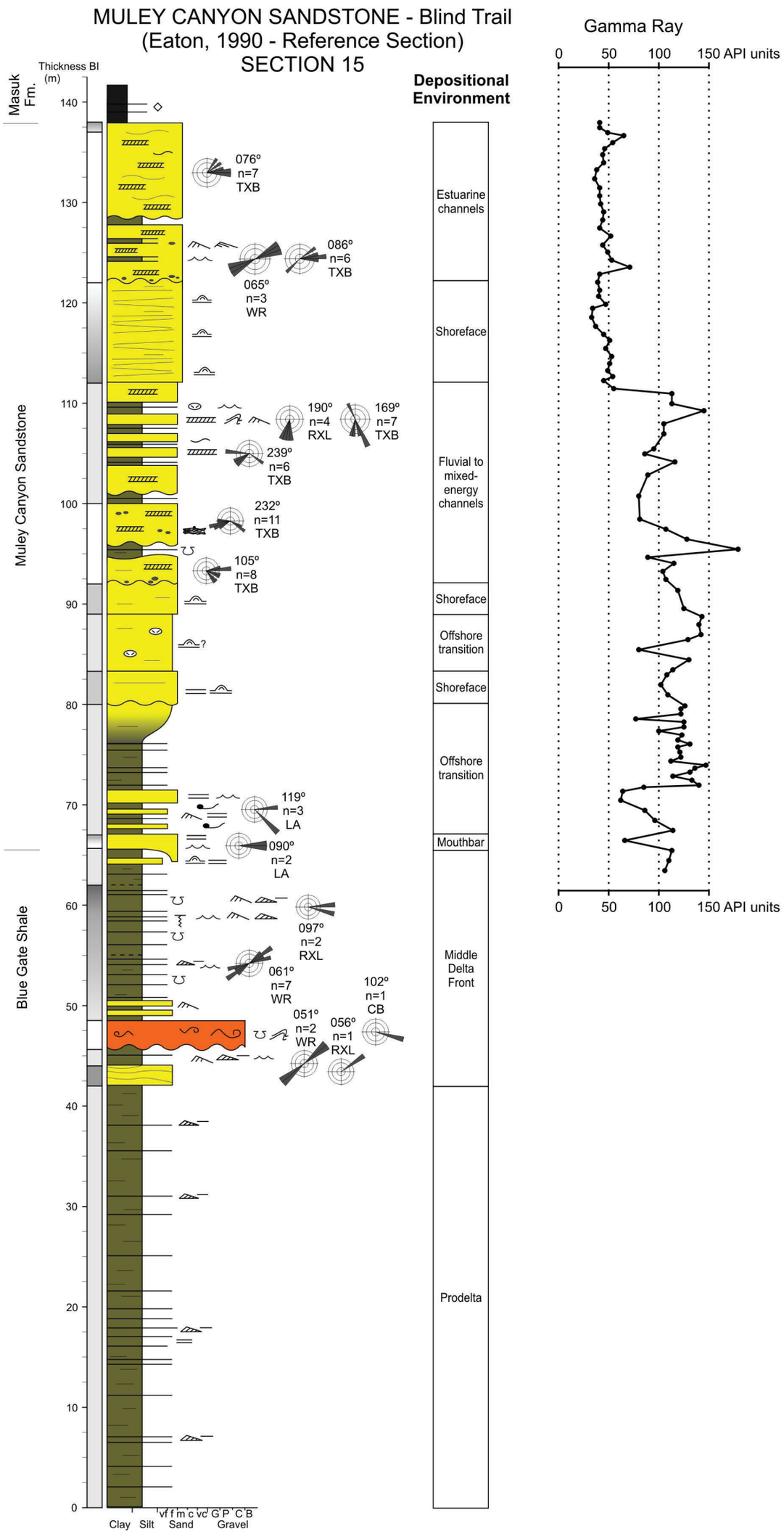
MULEY CANYON SANDSTONE - Blind Trail
(Eaton, 1990 - Reference Section)
SECTION 15
Thickness Bl (m)
Depositional Environment
Masuk Fm.
Muley Canyon Sandstone
Blue Gate Shale
076° n=7 TXB
086° n=6 TXB
065° n=3 WR
190° n=4 RXL
169° n=7 TXB
239° n=6 TXB
232° n=11 TXB
105° n=8 TXB
119° n=3 LA
090° n=2 LA
097° n=2 RXL
061° n=7 WR
102° n=1 CB
051° n=2 WR
056° n=1 RXL
Estuarine channels
Shoreface
Fluvial to mixed-energy channels
Shoreface
Offshore transition
Shoreface
Offshore transition
Mouthbar
Middle Delta Front
Prodelta
Clay Silt vf f m c vc Sand G P C B Gravel
Gamma Ray
0 50 100 150 API units
0 50 100 150 API units

MULEY CANYON SANDSTONE -
Blind Trail South Gullly
SECTION 16

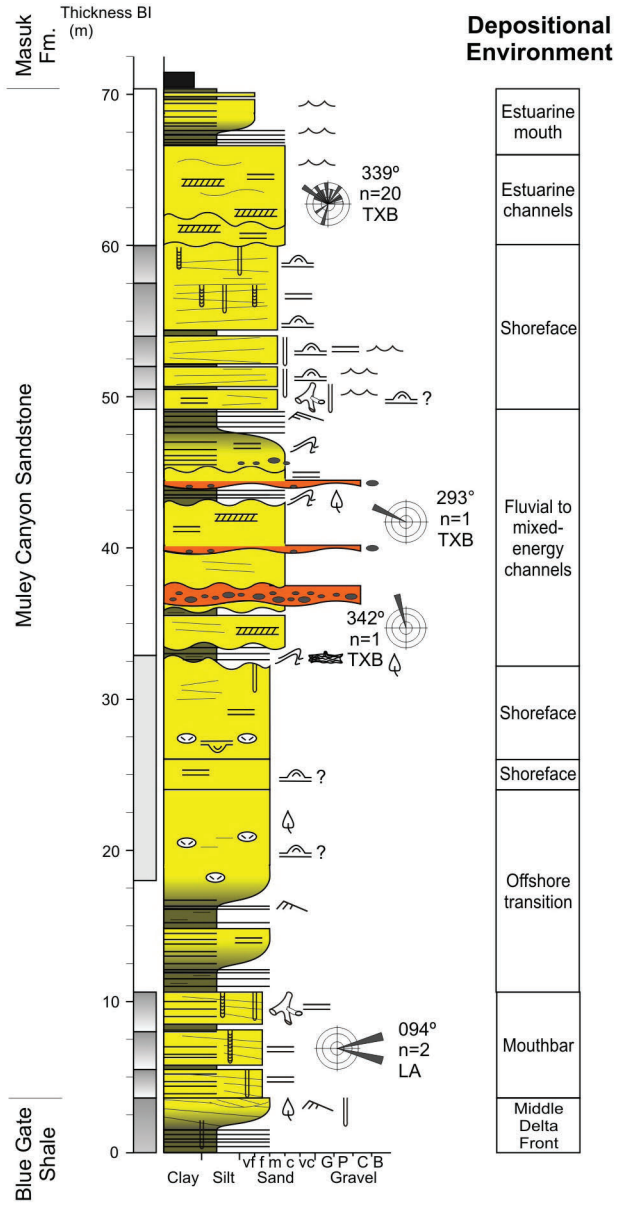

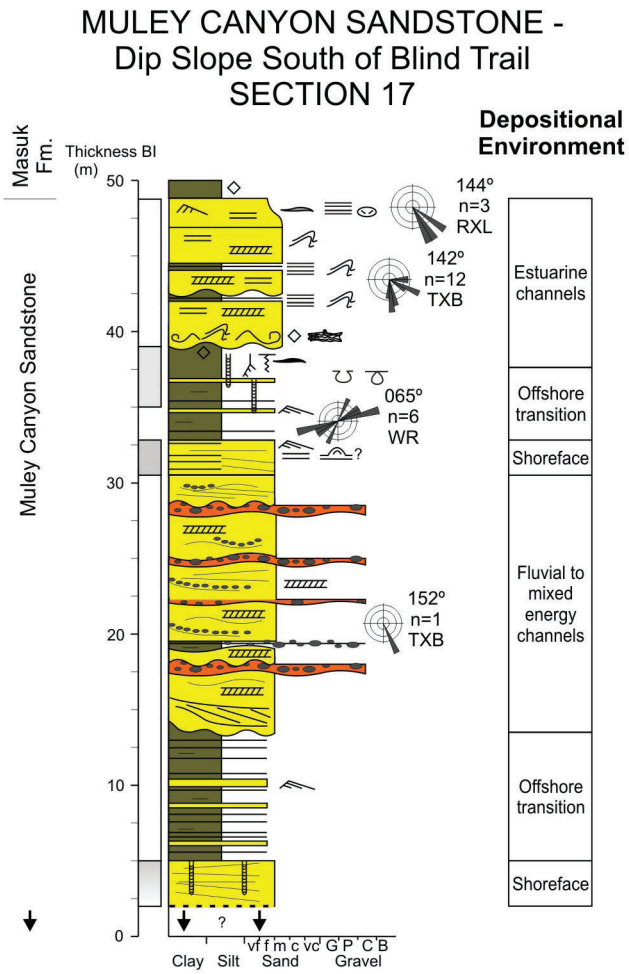
MULEY CANYON SANDSTONE -
Dip Slope South of Blind Trail
SECTION 17
Depositional Environment
Masuk Fm.
Muley Canyon Sandstone
Thickness BI (m)
50
40
30
20
10
0
144°
n=3
RXL
142°
n=12
TXB
065°
n=6
WR
152°
n=1
TXB
Estuarine channels
Offshore transition
Shoreface
Fluvial to mixed energy channels
Offshore transition
Shoreface
Clay
Silt
vf f m c vc
Sand
G P C B
Gravel

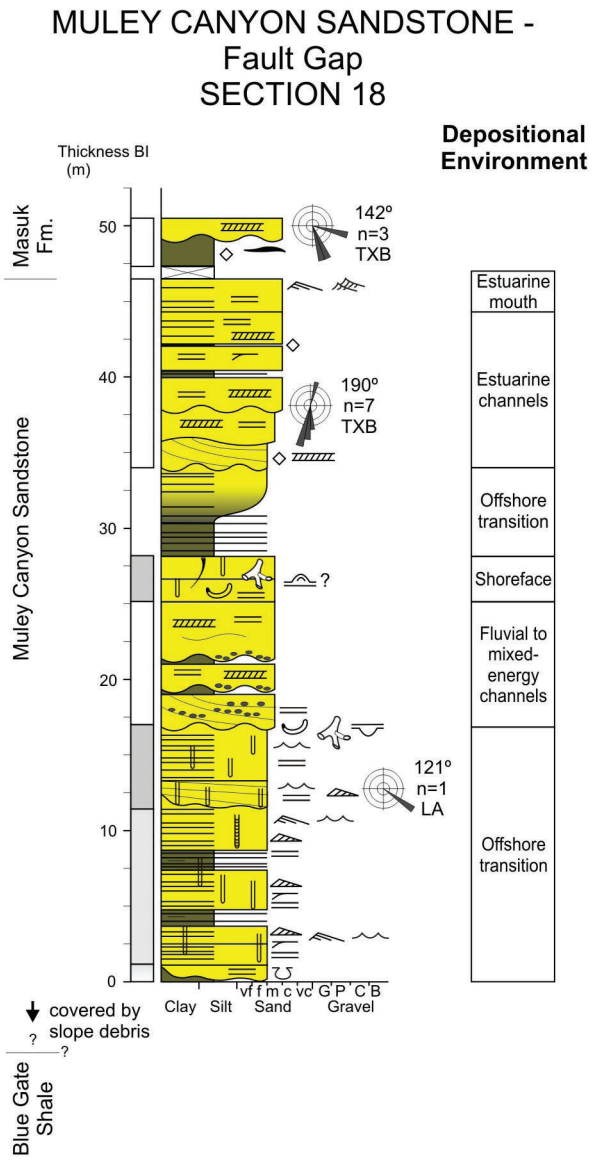
MULEY CANYON SANDSTONE -
Fault Gap
SECTION 18
Thickness Bl
(m)
Depositional
Environment
Masuk
Fm.
Muley Canyon Sandstone
Blue Gate
Shale
50
40
30
20
10
0
142°
n=3
TXB
190°
n=7
TXB
?
121°
n=1
LA
Estuarine
mouth
Estuarine
channels
Offshore
transition
Shoreface
Fluvial to
mixed-
energy
channels
Offshore
transition
covered by
slope debris
Clay
Silt
Sand
Gravel
vf f m c vc
G P C B

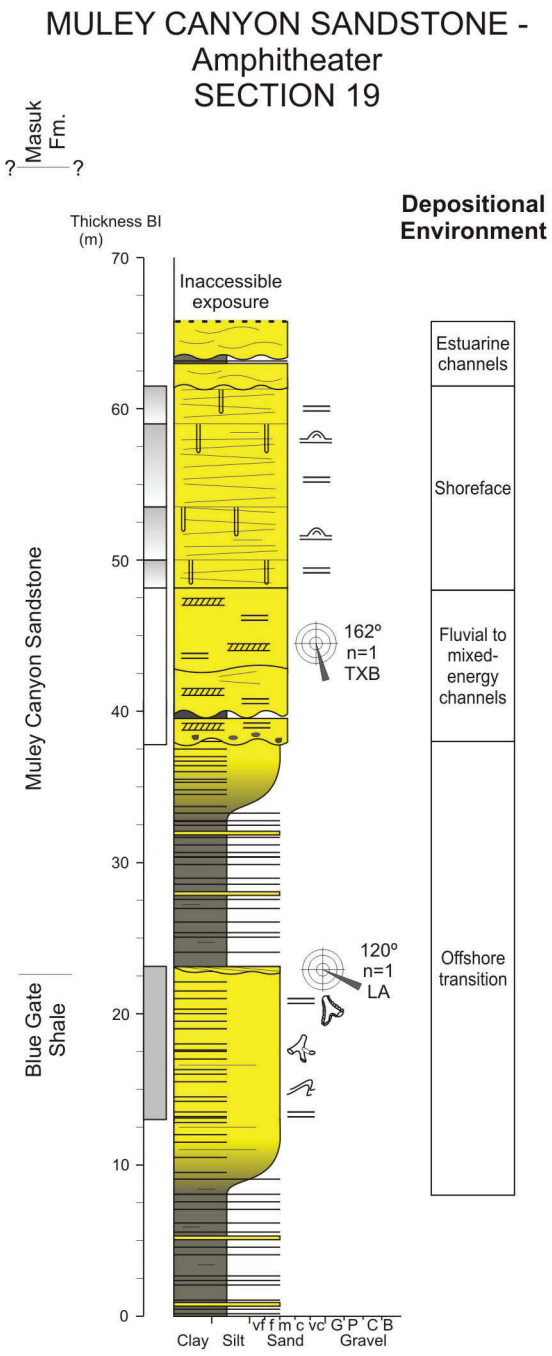
MULEY CANYON SANDSTONE -
Amphitheater
SECTION 19
Masuk Fm.
?
?
Thickness BI (m)
Depositional Environment
Inaccessible exposure
Estuarine channels
Shoreface
Fluvial to mixed-energy channels
Offshore transition
Muley Canyon Sandstone
Blue Gate Shale
162°
n=1
TXB
120°
n=1
LA
70
60
50
40
30
20
10
0
Clay
Silt
vf f m c vc
Sand
G P C B
Gravel

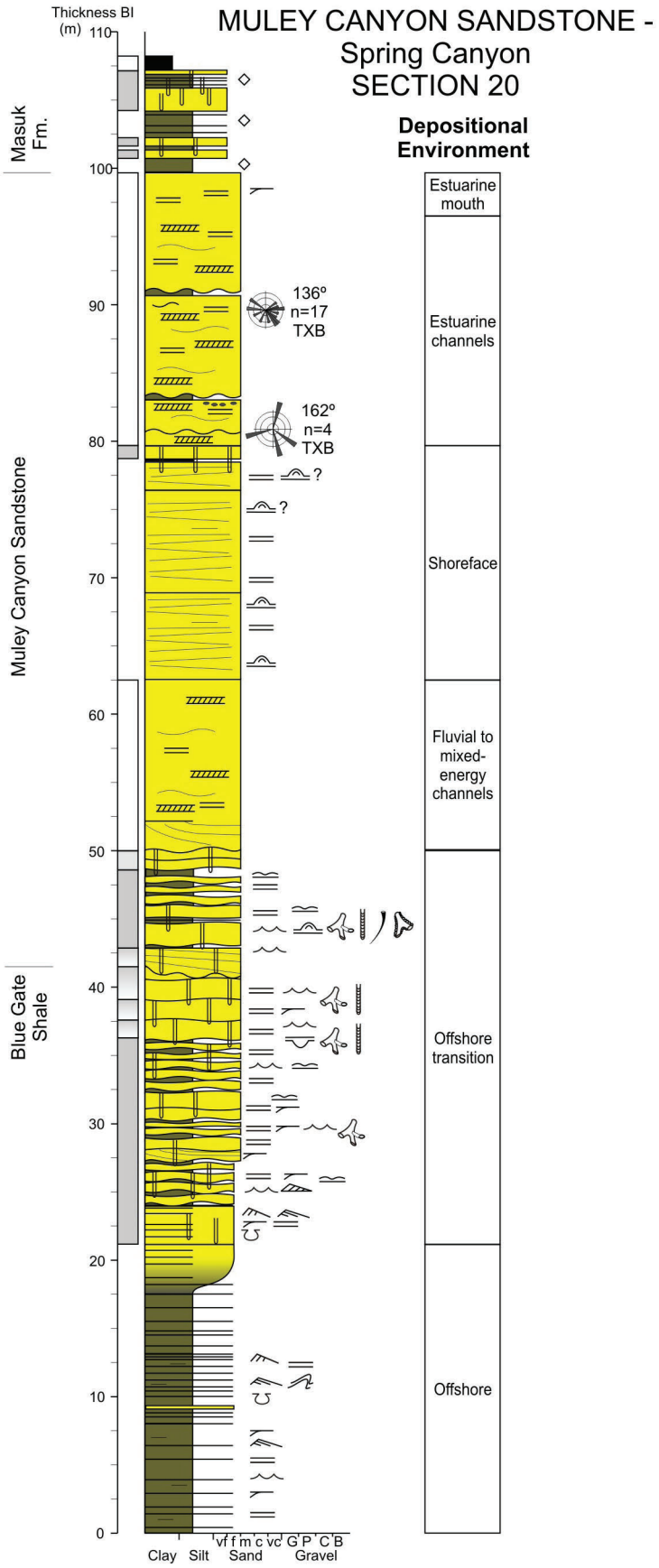
MULEY CANYON SANDSTONE -
Spring Canyon
SECTION 20
Thickness BI
(m)
110
100
90
80
70
60
50
40
30
20
10
0
Masuk Fm.
Muley Canyon Sandstone
Blue Gate Shale
136°
n=17
TXB
162°
n=4
TXB
?
?
Depositional Environment
Estuarine mouth
Estuarine channels
Shoreface
Fluvial to mixed-energy channels
Offshore transition
Offshore
Clay
Silt
vf f m c vc
Sand
G P C B
Gravel

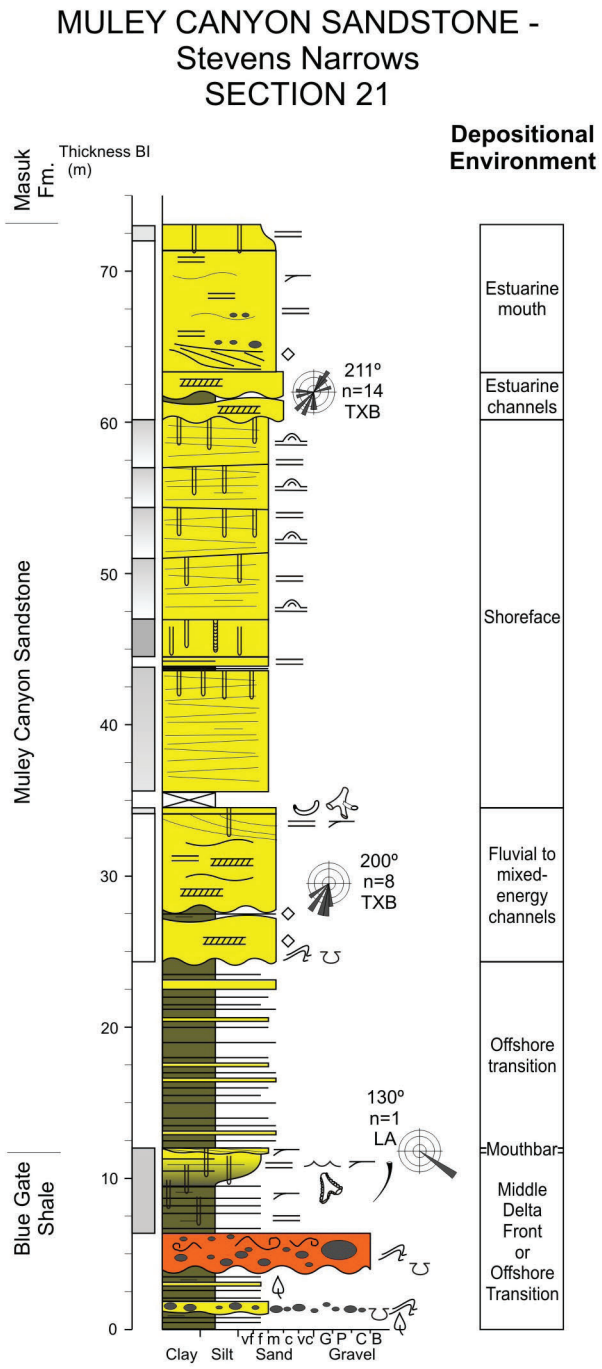
MULEY CANYON SANDSTONE -
Stevens Narrows
SECTION 21
Depositional Environment
Thickness Bl (m)
Masuk Fm.
Muley Canyon Sandstone
Blue Gate Shale
70
60
50
40
30
20
10
0
211°
n=14
TXB
200°
n=8
TXB
130°
n=1
LA
Estuarine mouth
Estuarine channels
Shoreface
Fluvial to mixed-energy channels
Offshore transition
Mouthbar
Middle Delta Front or Offshore Transition
Clay
Silt
vf f m c vc
Sand
G P C B
Gravel

Appendix B - ArcGIS® Database Summary and Instructions for Use

Installation

This study incorporates multiple sources of spatial data into a geographic information system or GIS framework. The software used to build this framework is commonly known as ArcGIS® Desktop version 9.2 service pack 6. There is one map document that contains and organizes all the spatial data layers. Each layer in the map document is accompanied with metadata that gives a basic description, purpose and source reference. This appendix provides an overview on installing the spatial data, gives descriptions of each layer presented in the map document, and elaborates on functionality of the map document.

The map document, spatial data, and supporting documents are all stored in a master GIS data folder named HenryMtnSynclineGIS_Final. This master GIS data folder contains a series of subfolders intended to organize the spatial data presented in the map document. The map document is named HenryMtnSynclineGIS_92.mxd and is stored at the top level of the master GIS data folder. Anyone who intends to explore the GIS data need only copy this master GIS data folder to a hard drive or network drive location, an installation of ArcGIS® 9.2 or later, and an installation of Acrobat® Reader. The map document uses a relative path to the spatial data, meaning drive letter designations are ignored and the map document will only look to the subfolders for a connection to the spatial data. Users should not change the names or preset structure of the subfolders inside the master GIS data folder as this will interrupt access to the spatial data through the map document.

Spatial Layer Descriptions

As discussed, the map document contains, organizes, and symbolizes the spatial data layers. All available spatial layers are listed in the map document on the left side when the map document is opened. All spatial data layers are stored in either a file–based geodatabase, ESRI® grid, or other common raster format. Each layer has an associated metadata file that may be accessed by right-clicking on a layer name, pointing to Data in the pop-up menu, and then clicking View Metadata. A floating window will appear with details that describe the layer.

ArcGIS® is required to view the metadata files. The table below describes each spatial data layer presented in the map document. The spatial data layer order in the table is the same order the spatial data layers are presented in the layer list of the map document.

Spatial Data Layer Name	Description	Source
Waypoints	Locations or waypoints collected using a hand held GPS unit in preparation for building correlation lines, measured sections, and photomosaic lines.	Waypoints collected by Lauren P. Birgenheier and Matthew J. Corbett for this study
Landmarks	This spatial data layer consists of point locations with corresponding feature names such as towns and natural landmarks.	Automated Geographic Reference Center, State of Utah – originally developed by the USGS.
Oil Wells	Digitized locations of wells drilled for oil and gas exploration in the region.	Utah Division of Oil, Gas and Mining online Data Research Center, Online Database Search
Coal Well Locations	Digitized locations of wells drilled for coal mining exploration and development in the region.	Utah Geological Survey Records, Dave Tabet, pers. comm.
Law, 1979, Surface Measured Section Locations	Digitized locations of surface measured sections shown on coal-section diagrams from Law, B.E., 1979 Map MF-1082A.	Law, B.E., 1979a, Coal deposits of the Emery Coal Zone, Henry Mountains Coal Field, Utah, USGS Map MF-1082A
Law, 1979, Surface Measured Section Correlation Lines	Correlation lines generated from digitized points taken from Law, 1979 Map MF-1082B.	Law, B.E., 1979b, Surface Coal Sections in the Emery Coal Zone, Henry Mountains Coal Field, Utah, USGS Map MF-1082B
ThisStudy_CorrelationLines	Locations of new surface and subsurface lines of correlation generated from this study.	This Study
ThisStudy_MeasuredSections	New detailed measured section locations generated from this study.	This Study
ThisStudy_PhotomosaicLines	Lines walked to produce photomosaics of cliff exposures for this study.	This Study
CoalSeams4ft_HenryMtnBasin	Approximate areas where coal seams are greater than or equal to 4 ft. within the study area.	Tabet and Wakefield (2006), Map 226DM, Utah Geological Survey - Automated Geographic Reference Center, State of Utah

Geology_lines	Subset of the original for this study. Contacts, faults, and other geologic features of the 1:500,000 scale Geology Map of Utah.Vectorized from scanned 1980 stable film separates of orginal linework and digitized from published maps, with minor modifications by compilers.	Hintze and others (2000), Utah Geological Survey – Digital Geologic Map of Utah
Geology_Cret	Subset of the original for this study. Cretaceous age contacts of the 1:500,000 scale Geology Map of Utah. Vectorized from scanned 1980 stable film separates of orginal linework and digitized from published maps, with minor modifications by compilers.	Geological Survey – Digital Geologic Map of Utah
plssSections	Public Land Survey System sections for the study area	Bureau of Land Management, U.S. Forest Service, Automated Geographic Reference Center
SGID_U024_StatewideStreets	Utah street centerline data for address location, cartography, routing	Automated Geographic Reference Center, State of Utah
SGID_U024_StreamsNHD	General purpose feature class of streams for cartographic purposes	U.S. Geological Survey in cooperation with U.S. Environmental Protection Agency, USDA Forest Service, and other Federal, State and local partners
CountyBoundaries	This dataset represents current county boundaries in SE Utah at 1:24,000 scale.	Automated Geographic Reference Center, State of Utah
StudyArea	Bounding rectangle delimiting the extent of this study.	Energy & Geoscience Institute–University of Utah
henrymtn_hs	Shaded relief raster derived from 5 meter Digital Elevation Model	Automated Geographic Reference Center, State of Utah
waynedrg24k.img	Mosaic of all 1:24,000 Digital Raster Graphics for the area of Wayne County, Utah that falls within the study area.	U.S. Geological Survey—Automated Geographic Reference Center, State of Utah
garfield24k.img	Mosaic of all 1:24,000 Digital Raster Graphics for the area of Garfield Country, Utah that falls within the study area.	U.S. Geological Survey—Automated Geographic Reference Center, State of Utah
Hunt Geologic Map.img	Geologic map of the Henry Mountain Region, Utah. This image has be georeferenced.	Hunt, C.B., Averitt, P., and Miller, R.L., 1953, Geology and geography of the Henry Mountain Region, Utah, U.S. Geological Survey Professional Paper 228, 234 p.
HenryMtn5mMosaic	5 meter Digital Elevation Model	Automated Geographic Reference Center, State of Utah

Six spatial data layers have a special functionality enabled through the map document known as hyperlinking. See the table below for layers with established hyperlinks. Hyperlinks allow additional data to be linked to features drawn in the map area of the map document. Hyperlinks are available in the map document by using the hyperlink tool, a small yellow lightning bolt icon found on the default toolbar. Clicking the hyperlink tool will show the user features that have available hyperlinks by changing the feature color to blue in the map area of the map document. Users may click any feature in the map area that shows a hyperlink with the hyperlink tool to see data that is specific to that feature. The related data is in the form of TIFF images or PDF® files for this report.

Spatial Data Layer Name	Description	Source
Oil Wells	WELLDATALINK	Folder containing well report in PDF® format and well logs in TIFF format
Landmarks	This spatial data layer consists of point locations with corresponding feature names such as towns and natural landmarks.	Folder containing well report and/or well logs in Tiff and PDF® format
Law, 1979, Surface Measured Section Correlation Lines	DATALINK	Folder containing correlation sections in TIFF format
ThisStudy_CorrelationLines	DATA_LINK	Direct hyperlink to correlation lines in PDF® format
ThisStudy_MeasuredSections	DATA_LINK	Direct hyperlink to measured sections in PDF® format
ThisStudy_PhotomosaicLines	DATA_LINK	Direct hyperlink to photomosaics in PDF® format

Appendix C - Henry Mountain Syncline Coal Well Data Table

WELL NAME	UGS POINT ID	USGS QUADRANGLE	COUNTY	UTM12X_83	UTM12Y_83	SOURCE	SURFACE ELEVATION (FT.)	TOTAL DEPTH (FT.)	HYPER-LINKED DATA?
DH H-101	MESW-C201	MOUNT ELLEN SW (7.5')	GARFIELD	505243	4212041	AMAX COAL COMPANY	5820	205	X
DH H-102	MESW-C202	MOUNT ELLEN SW (7.5')	GARFIELD	504914	4211097	AMAX COAL COMPANY	5800	302	X
DH H-103	MESW-C257	MOUNT ELLEN SW (7.5')	GARFIELD	505692	4209579	AMAX COAL COMPANY	5920	340	
DH H-104	MESW-C258	MOUNT ELLEN SW (7.5')	GARFIELD	505315	4212041	AMAX COAL COMPANY	5820	190	
DH H-105	MESW-C221	MOUNT ELLEN SW (7.5')	GARFIELD	501010	4215628	AMAX COAL COMPANY	5660	220	X
DH H-106	NSE-C47	NOTOM SE (7.5')	GARFIELD	498659	4216419	AMAX COAL COMPANY	5700	280	X
DH H-107	NSE-C38	NOTOM 4 SE(7.5')	GARFIELD	498391	4217113	AMAX COAL COMPANY	5760	220	X
DH H-108	NSE-C18	NOTOM 4 SE(7.5')	GARFIELD	498219	4218332	AMAX COAL COMPANY	5780	220	X
DH H-109	NNE-C36	NOTOM 4 NE (7.5')	GARFIELD	499125	4220922	AMAX COAL COMPANY	5680	155	X
DH H-110	NNE-C42	NOTOM 4 NE (7.5')	GARFIELD	499207	4220544	AMAX COAL COMPANY	5700	191	X
DH H-111	NNE-C47	NOTOM 4 NE (7.5')	GARFIELD	499489	4219976	AMAX COAL COMPANY	5660	192	X
DH H-112	NSE-C9	NOTOM SE (7.5')	GARFIELD	499308	4219375	AMAX COAL COMPANY	5640	180	X
DH H-113	NSE-C12	NOTOM SE (7.5')	GARFIELD	499971	4219278	AMAX COAL COMPANY	5640	170	X
DH H-114	NSE-C19	NOTOM 4 SE(7.5')	GARFIELD	498947	4218561	AMAX COAL COMPANY	5680	200	X
DH H-115	NSE-C15	NOTOM SE (7.5')	GARFIELD	499677	4218031	AMAX COAL COMPANY	5650	180	X
DH H-116	MESW-C74	MOUNT ELLEN SW (7.5')	GARFIELD	500773	4217161	AMAX COAL COMPANY	5680	200	X
DH H-201	NSE-C52	NOTOM 4 SE (7.5')	GARFIELD	499588	4216022	AMAX COAL COMPANY	5660	206	X
DH H-202	NSE-C54	NOTOM 4 SE (7.5')	GARFIELD	499856	4215597	AMAX COAL COMPANY	5700	240	X
DH H-203	MESW-C78	MOUNT ELLEN SW (7.5')	GARFIELD	500553	4216560	AMAX COAL COMPANY	5690	209	X
DH H-209	MPNW-C1	CAVE FLAT (7.5')	GARFIELD	509064	4197757	AMAX COAL COMPANY	5850	180	X
DH H-210	MPNW-C2	CAVE FLAT (7.5')	GARFIELD	508943	4197249	AMAX COAL COMPANY	5850	160	X
DH H-211	MPNW-C3	CAVE FLAT (7.5')	GARFIELD	508941	4195760	AMAX COAL COMPANY	5930	200	X
DH H-212	MPNW-C363	MOUNT PENNELL NW (7.5')	GARFIELD	508318	4196165	AMAX COAL COMPANY	5850	160	X
DH H-215	MPNW-C15	CAVE FLAT (7.5')	GARFIELD	509974	4197324	AMAX COAL COMPANY	5880	95	
DH H-216	NSE-C105	NOTOM 4 SE (7.5')	GARFIELD	499399	4216656	AMAX COAL COMPANY	5640	143	
DH H-217	NSE-C106	NOTOM 4 SE (7.5')	GARFIELD	498264	4218334	AMAX COAL COMPANY	5780	182	
DH H-218	NSE-C21	NOTOM 4 SE(7.5')	GARFIELD	498072	4218850	AMAX COAL COMPANY	5800	160	X
DH H-219	NNE-C41	NOTOM 4 NE (7.5')	GARFIELD	498587	4220571	AMAX COAL COMPANY	5740	120	X
DH H-220	MPNW-C336	MOUNT PENNELL NW (7.5')	GARFIELD	500993	4195563	AMAX COAL COMPANY	5530	220	X
DH H-221	MPNW-C337	MOUNT PENNELL NW (7.5')	GARFIELD	499987	4194287	AMAX COAL COMPANY	5480	185	X

WELL NAME	UGS POINT ID	USGS QUADRANGLE	COUNTY	UTM12X_83	UTM12Y_83	SOURCE	SURFACE ELEVATION (FT.)	TOTAL DEPTH (FT.)	HYPER-LINKED DATA?
DH H-222	MPNW-C338	MOUNT PENNELL NW (7.5')	GARFIELD	500255	4194643	AMAX COAL COMPANY	5480	220	X
DH H-223	MPNW-C339	MOUNT PENNELL NW (7.5')	GARFIELD	500026	4194252	AMAX COAL COMPANY	5480	154	
DH H-224	MPNW-C340	MOUNT PENNELL NW (7.5')	GARFIELD	501228	4196654	AMAX COAL COMPANY	5560	195	X
DH H-225	MPNW-C341	MOUNT PENNELL NW (7.5')	GARFIELD	501834	4197669	AMAX COAL COMPANY	5600	225	X
DH H-226	MPNW-C342	MOUNT PENNELL NW (7.5')	GARFIELD	503012	4195082	AMAX COAL COMPANY	5520	150	X
DH H-302	NSE-C8	NOTOM SE (7.5')	GARFIELD	498724	4219175	AMAX COAL COMPANY	5740	260	X
DH H-303	NSE-C44	NOTOM SE (7.5')	GARFIELD	499437	4216633	AMAX COAL COMPANY	5640	180	X
DH H-307	MPNW-C343	MOUNT PENNELL NW (7.5')	GARFIELD	509574	4197789	AMAX COAL COMPANY	5880	200	X
DH H-308	MPNW-C344	MOUNT PENNELL NW (7.5')	GARFIELD	509099	4196685	AMAX COAL COMPANY	5800	140	X
DH H-309	MPNW-C345	MOUNT PENNELL NW (7.5')	GARFIELD	508439	4196659	AMAX COAL COMPANY	5800	200	X
DH H-310	MPNW-C346	MOUNT PENNELL NW (7.5')	GARFIELD	510857	4197687	AMAX COAL COMPANY	5830	115	X
DH H-311	MPNW-C347	MOUNT PENNELL NW (7.5')	GARFIELD	510324	4197681	AMAX COAL COMPANY	5920	120	X
DH H-312	MPNW-C348	MOUNT PENNELL NW (7.5')	GARFIELD	509975	4197368	AMAX COAL COMPANY	5880	160	X
DH H-313	MPNW-C349	MOUNT PENNELL NW (7.5')	GARFIELD	510850	4197011	AMAX COAL COMPANY	5960	93	X
DH H-318	NSE-C53	NOTOM 4 SE (7.5')	GARFIELD	499905	4216531	AMAX COAL COMPANY	5640	200	X
DH H-319	NSE-C51	NOTOM 4 SE (7.5')	GARFIELD	498986	4215880	AMAX COAL COMPANY	5720	200	X
DH H-320	NSE-C109	NOTOM 4 SE (7.5')	GARFIELD	498275	4217695	AMAX COAL COMPANY	5780	180	X
DH H-321	NSE-C7	NOTOM SE (7.5')	GARFIELD	498342	4219394	AMAX COAL COMPANY	5780	220	X
DH H-322	NSE-C14	NOTOM SE (7.5')	GARFIELD	499899	4218625	AMAX COAL COMPANY	5680	220	X
DH H-323	MESW-C58	MOUNT ELLEN SW (7.5')	GARFIELD	500557	4218434	AMAX COAL COMPANY	5680	200	X
DH H-324	NSE-C20	NOTOM 4 SE(7.5')	GARFIELD	499242	4218373	AMAX COAL COMPANY	5650	200	X
DH H-325	NSE-C10	NOTOM SE (7.5')	GARFIELD	499602	4219073	AMAX COAL COMPANY	5640	160	X
DH H-326	MESW-C77	MOUNT ELLEN SW (7.5')	GARFIELD	500354	4216944	AMAX COAL COMPANY	5670	200	X
DH H-327	MPNW-C350	MOUNT PENNELL NW (7.5')	GARFIELD	500801	4194566	AMAX COAL COMPANY	5480	200	X
DH H-328	MPNW-C351	MOUNT PENNELL NW (7.5')	GARFIELD	500784	4194770	AMAX COAL COMPANY	5510	200	X
DH H-330	MPNW-C352	MOUNT PENNELL NW (7.5')	GARFIELD	501519	4196428	AMAX COAL COMPANY	5480	180	X
DH H-331	MPNW-C353	MOUNT PENNELL NW (7.5')	GARFIELD	501731	4196862	AMAX COAL COMPANY	5560	200	X
DH H-332	MPNW-C354	MOUNT PENNELL NW (7.5')	GARFIELD	501267	4196722	AMAX COAL COMPANY	5540	240	X
DH H-333	MPNW-C355	MOUNT PENNELL NW (7.5')	GARFIELD	500574	4196177	AMAX COAL COMPANY	5460	240	X
DH H-334	MPNW-C356	MOUNT PENNELL NW (7.5')	GARFIELD	500221	4196904	AMAX COAL COMPANY	5400	220	X
DH H-335	MPNW-C357	MOUNT PENNELL NW (7.5')	GARFIELD	500817	4197189	AMAX COAL COMPANY	5430	220	X
DH H-336	MPNW-C358	MOUNT PENNELL NW (7.5')	GARFIELD	500579	4197658	AMAX COAL COMPANY	5400	220	X

WELL NAME	UGS POINT ID	USGS QUADRANGLE	COUNTY	UTM12X_83	UTM12Y_83	SOURCE	SURFACE ELEVATION (FT.)	TOTAL DEPTH (FT.)	HYPER-LINKED DATA?
DH H-337	MPNW-C359	MOUNT PENNELL NW (7.5')	GARFIELD	500950	4198490	AMAX COAL COMPANY	5520	200	X
DH H-338	MPNW-C360	MOUNT PENNELL NW (7.5')	GARFIELD	502524	4197854	AMAX COAL COMPANY	5680	220	X
DH H-339	MPNW-C361	MOUNT PENNELL NW (7.5')	GARFIELD	500849	4196922	AMAX COAL COMPANY	5480	200	X
DH H-340	MPNW-C362	MOUNT PENNELL NW (7.5')	GARFIELD	500927	4196266	AMAX COAL COMPANY	5520	220	X
DH-204	NNE-C69	NOTOM NE (7.5')	GARFIELD	499576	4221562	AMAX COAL COMPANY	5697	160	
DH-205	MENW-C115	STEVENS MESA(7.5')(MT ELLEN)	GARFIELD	500132	4222081	AMAX COAL COMPANY	5622	95	
DH-206	MENW-C116	STEVENS MESA(7.5')(MT ELLEN)	GARFIELD	500257	4222629	AMAX COAL COMPANY	5632	110	
MS H-301	NNE-C46	NOTOM 4 NE (7.5')	GARFIELD	498398	4220030	AMAX COAL COMPANY	5780	180	X
W-1	MPNW-C62	MOUNT PENNELL NW (7.5')	GARFIELD	501188	4194930	BYU GEOL STUDIES V 30 PT 1	5500	207	
W-2	MPNW-C63	MOUNT PENNELL NW (7.5')	GARFIELD	501159	4196530	BYU GEOL STUDIES V 30 PT 1	5560	192	
W-3	MPNW-C64	MOUNT PENNELL NW (7.5')	GARFIELD	500931	4197170	BYU GEOL STUDIES V 30 PT 1	5470	189	
DH #6	WBNE-C65	BITTER CREEK DIVIDE (7.5')	GARFIELD	499057	4186730	CAYMAN CORP	5880	700	X
DH #7	WBNE-C66	BITTER CREEK DIVIDE (7.5')	GARFIELD	496505	4188140	CAYMAN CORP	5720	560	X
DH- #9	MPNW-C370	CAVE FLAT (7.5')	GARFIELD	503014	4195052	CAYMAN CORP	5525	246	X
DH-#2	MESW-C279	STEELE BUTTE (7.5')	GARFIELD	504060	4212028	CAYMAN CORP	5720	320	X
DH-#5	MPNW-C369	CAVE FLAT (7.5')	GARFIELD	510132	4197609	CAYMAN CORP	5910	440	X
DH-#3	MESW-C280	STEELE BUTTE (7.5')	GARFIELD	502745	4211694	CAYMAN CORP.	5720	240	X
DH HM-1	MENE-C1	MT ELLEN 3 NE (7.5')	WAYNE	512279	4232206	CONSOLIDATION COAL CO	5010	260	X
DH HM-10	MESW-C53	MOUNT ELLEN SW (7.5')	GARFIELD	503429	4217915	CONSOLIDATION COAL CO	5740	125	X
DH HM-11	MESW-C23	MOUNT ELLEN SW (7.5')	GARFIELD	501763	4217866	CONSOLIDATION COAL CO	5600	123	X
DH HM-12	MESW-C69	MOUNT ELLEN SW (7.5')	GARFIELD	506160	4218822	CONSOLIDATION COAL CO	5840	160	X
DH HM-13	MESW-C186	MOUNT ELLEN SW (7.5')	GARFIELD	504613	4213654	CONSOLIDATION COAL CO	5740	150	X
DH HM-14	MESW-C187	MOUNT ELLEN SW (7.5')	GARFIELD	505810	4213145	CONSOLIDATION COAL CO	5960	200	X
DH HM-15	MENW-C83	MT ELLEN 3 NW (7.5')	GARFIELD	508470	4221942	CONSOLIDATION COAL CO	5920	100	X
DH HM-16	MENW-C19	STEVENS MESA(7.5')(MT ELLEN)	WAYNE	508378	4223137	CONSOLIDATION COAL CO	5660	200	X
DH HM-17	MENW-C18	STEVENS MESA(7.5')(MT ELLEN)	WAYNE	509080	4223728	CONSOLIDATION COAL CO	5700	160	X
DH HM-18	MENW-C33	MT ELLEN 3 NW (7.5')	WAYNE	504122	4222906	CONSOLIDATION COAL CO	5740	140	X
DH HM-19	MESW-C174	MOUNT ELLEN SW (7.5')	GARFIELD	502545	4212898	CONSOLIDATION COAL CO	5740	120	X
DH HM-2	MENE-C2	MT ELLEN 3 NE (7.5')	WAYNE	513682	4232222	CONSOLIDATION COAL CO	5020	185	X
DH HM-20	MESW-C175	MOUNT ELLEN SW (7.5')	GARFIELD	502625	4213963	CONSOLIDATION COAL CO	5670	100	X
DH HM-21	MESW-C109	MOUNT ELLEN SW (7.5')	GARFIELD	504113	4215651	CONSOLIDATION COAL CO	5660	75	X
DH HM-22	MPNW-C297	MOUNT PENNELL NW (7.5')	GARFIELD	510749	4202601	CONSOLIDATION COAL CO	6120	100	X

WELL NAME	UGS POINT ID	USGS QUADRANGLE	COUNTY	UTM12X_83	UTM12Y_83	SOURCE	SURFACE ELEVATION (FT.)	TOTAL DEPTH (FT.)	HYPER-LINKED DATA?
DH HM-23	MPNW-C298	MOUNT PENNELL NW (7.5')	GARFIELD	510673	4202271	CONSOLIDATION COAL CO	6100	80	X
DH HM-24	MPNE-C20	MOUNT PENNELL NE (7.5')	GARFIELD	511445	4203574	CONSOLIDATION COAL CO	6160	110	X
DH HM-25	MPNW-C299	MOUNT PENNELL NW (7.5')	GARFIELD	509803	4200767	CONSOLIDATION COAL CO	6000	95	X
DH HM-26	MPNW-C300	MOUNT PENNELL NW (7.5')	GARFIELD	509993	4199005	CONSOLIDATION COAL CO	5880	95	X
DH HM-27	MPNW-C301	MOUNT PENNELL NW (7.5')	GARFIELD	509050	4199031	CONSOLIDATION COAL CO	5880	171	X
DH HM-28	MPNW-C302	MOUNT PENNELL NW (7.5')	GARFIELD	509633	4199634	CONSOLIDATION COAL CO	5960	120	X
DH HM-3	MENW-C4	MT ELLEN 3 NW (7.5')	WAYNE	510291	4232229	CONSOLIDATION COAL CO	5060	415	X
DH HM-4	MENW-C2	MT ELLEN 3 NW (7.5')	WAYNE	509146	4233251	CONSOLIDATION COAL CO	4920	250	X
DH HM-5	MENW-C3	MT ELLEN 3 NW (7.5')	WAYNE	508994	4232244	CONSOLIDATION COAL CO	4995	360	X
DH HM-6	MENW-C5	MT ELLEN 3 NW (7.5')	WAYNE	507361	4231977	CONSOLIDATION COAL CO	4900	330	X
DH HM-7	MENW-C1	MT ELLEN 3 NW (7.5')	WAYNE	503909	4232056	CONSOLIDATION COAL CO	4860	420	X
DH HM-8	MENW-C10	MT ELLEN 3 NW (7.5')	WAYNE	504220	4228809	CONSOLIDATION COAL CO	5180	400	X
DH HM-9	MESW-C48	MOUNT ELLEN SW (7.5')	GARFIELD	502893	4218838	CONSOLIDATION COAL CO	5680	190	X
DH-TARANTULA MESA #1	MPNW-C366	CAVE FLAT (7.5')	GARFIELD	502484	4204371	GULF MINERAL RESOURCES C	6430	1100	X
DH-TARANTULA MESA #3	MPNW-C367	CAVE FLAT (7.5')	GARFIELD	505119	4202930	GULF MINERAL RESOURCES C	6630	1160	X
DH-TARANTULA MESA #5C	MPNW-C368	CAVE FLAT (7.5')	GARFIELD	505295	4203041	GULF MINERAL RESOURCES C	6630	1047	X
DH-TARANTULA MESA #6	MESW-C278	STEELE BUTTE (7.5')	GARFIELD	501165	4211139	GULF MINERAL RESOURCES C	5920	620	X
DH-TRANTULA MESA #2	WBNE-C64	BITTER CREEK DIVIDE (7.5')	GARFIELD	499761	4188062	GULF MINERAL RESOURCES C	6330	1130	X
DH MH-3-MP	MPNW-C307	MOUNT PENNELL NW (7.5')	GARFIELD	502630	4201373	UGMS OFR 23	6425	1035	
DH 1 L-305	MESW-C66	MOUNT ELLEN SW (7.5')	GARFIELD	505194	4218234	USGS MF 1082 A LAW	5840	185	
DH 15 L-303	MESW-C79	MOUNT ELLEN SW (7.5')	GARFIELD	500169	4216677	USGS MF 1082 A LAW	5740	200	
DH 15-303	MESW-C259	MOUNT ELLEN SW (7.5')	GARFIELD	500104	4215776	USGS MF 1082 A LAW	5710	200	
DH 2 L-310	MESW-C110	MOUNT ELLEN SW (7.5')	GARFIELD	505253	4217164	USGS MF 1082 A LAW	5880	214	
DH 4 L-309	MESW-C106	MOUNT ELLEN SW (7.5')	GARFIELD	503660	4216188	USGS MF 1082 A LAW	5746	185	
DH 5 L-311	MESW-C111	MOUNT ELLEN SW (7.5')	GARFIELD	504831	4216642	USGS MF 1082 A LAW	5905	304	
DH 7 L-313	MESW-C113	MOUNT ELLEN SW (7.5')	GARFIELD	506237	4215981	USGS MF 1082 A LAW	6030	295	
DH 9-302	NSE-C107	NOTOM SE (7.5')	GARFIELD	498670	4216592	USGS MF 1082 A LAW	5705	170	
DH EMRIA 15 L-303	MESW-C79	MOUNT ELLEN SW (7.5')	GARFIELD	500169	4216677	USGS MF 1082 A LAW	5740	200	X
DH EMRIA 2 L-310	MESW-C110	MOUNT ELLEN SW (7.5')	GARFIELD	505253	4217164	USGS MF 1082 A LAW	5880	214	X
DH EMRIA 4 L-309	MESW-C106	MOUNT ELLEN SW (7.5')	GARFIELD	503660	4216188	USGS MF 1082 A LAW	5746	185	X
DH EMRIA 5 L-311	MESW-C111	MOUNT ELLEN SW (7.5')	GARFIELD	504831	4216642	USGS MF 1082 A LAW	5905	304	X
DH EMRIA 7 L-313	MESW-C113	MOUNT ELLEN SW (7.5')	GARFIELD	506237	4215981	USGS MF 1082 A LAW	6030	295	X

WELL NAME	UGS POINT ID	USGS QUADRANGLE	COUNTY	UTM12X_83	UTM12Y_83	SOURCE	SURFACE ELEVATION (FT.)	TOTAL DEPTH (FT.)	HYPER-LINKED DATA?
DH EMRIA 9 L-302	NSE-C107	NOTOM SE (7.5')	GARFIELD	498670	4216592	USGS MF 1082 A LAW	5705	170	X
DH I-305	MESW-C260	MOUNT ELLEN SW (7.5')	GARFIELD	505777	4218194	USGS MF 1082 A LAW	5890	185	
DH ME 13 L-308	MESW-C105	MOUNT ELLEN SW (7.5')	GARFIELD	503697	4216060	USGS MF 1082 A LAW	5745	220	X
DH ME 2 L-312	MESW-C112	MOUNT ELLEN SW (7.5')	GARFIELD	506634	4216421	USGS MF 1082 A LAW	6031	299	X
DH ME 3 L-316	MESW-C213	MOUNT ELLEN SW (7.5')	GARFIELD	505947	4209242	USGS MF 1082 A LAW	5916	313	X
DH ME 4 L-315	MESW-C212	MOUNT ELLEN SW (7.5')	GARFIELD	508652	4208146	USGS MF 1082 A LAW	6225	179	X
DH ME 5 L-317	MESW-C220	MOUNT ELLEN SW (7.5')	GARFIELD	510725	4206552	USGS MF 1082 A LAW	6760	235	X
DH MP 1 L-318	MPNW-C364	MOUNT PENNELL NW (7.5')	GARFIELD	509300	4204813	USGS MF 1082 A LAW	6870	1034	X
DH MP 3 L-321	MPNW-C365	MOUNT PENNELL NW (7.5')	GARFIELD	501952	4200677	USGS MF 1082 A LAW	6470	1110	
DH MP-5	NO INFO	MOUNT PENNELL NW (7.5')	GARFIELD	502235	4205958	USGS MF 1082 A LAW, L-314	6480	1077	X
DH-MP-2 (#319)	MPNW-C65	CAVE FLAT (7.5')	GARFIELD	506441	4203470	USGS MF 1082 AB LAW	6718	1099	X
DH 3 L-306	MESW-C54	MOUNT ELLEN SW (7.5')	GARFIELD	503647	4217780	USGS MF 1082 B LAW	5845	290	
DH EMRIA 3 L-306	MESW-C54	MOUNT ELLEN SW (7.5')	GARFIELD	503647	4217780	USGS MF 1082 B LAW	5845	290	X
DH ME 1 L-304	MESW-C277	MOUNT ELLEN SW (7.5')	GARFIELD	501862	4215426	USGS MF 1082 B LAW	5608	161	X
DH ME-12 L-307	MESW-C55	MOUNT ELLEN SW (7.5')	GARFIELD	504338	4217689	USGS MF 1082 B LAW	5845	320	X
DH WB 1 L-320	WBNE-C16	WAGON BOX MESA NE (7.5')	GARFIELD	498991	4202363	USGS MF 1082 B LAW	6262	1118	X
DH ME-6	MESE-C21	MOUNT ELLEN SE (7.5')	GARFIELD	510959	4208259	USGS OFG-77-41 0LAW	6475	300	
DH ME-10	MESW-C8	MOUNT ELLEN SW (7.5')	GARFIELD	508874	4219004	USGS OFR-77-41	6163	400	
DH ME-11	MESW-C199	MOUNT ELLEN SW (7.5')	GARFIELD	509730	4212763	USGS OFR-77-41 LAW	6743	600	
DH ME-7	MENE-C4	MT ELLEN 3 NE (7.5')	WAYNE	512352	4231767	USGS OFR-77-41 LAW	5034	300	
DH ME-8	MENE-C5	MT ELLEN 3 NE (7.5')	WAYNE	512540	4229431	USGS OFR-77-41 LAW	5232	380	
DH MP-4	MPSE-C20	MOUNT PENNELL SE (7.5')	GARFIELD	519945	4186447	USGS OFR-77-41 LAW	5200	300	
DH N-2	NSE-C60	NOTOM SE (7.5')	GARFIELD	498779	4214600	USGS OFR-77-41 LAW	5474	1000	
DH APPLE BRUSH FLAT	MESW-C1	MOUNT ELLEN SW (7.5')	GARFIELD	507867	4216971	WEBB RESOURCES INC 1971	6232	3200	
DH CAVE FLAT NO 24	MPNE-C9	MOUNT PENNELL NE (7.5')	GARFIELD	511704	4197273	WEBB RESOURCES INC 1971	5993	3000	

SUPPLEMENTARY FILES

Supplementary File 1. ArcGIS® document and associated files

These electronic files are located on the CD-ROM in a folder called HenryMtnSynclineGIS_Final. Instructions for use are included in Appendix B.

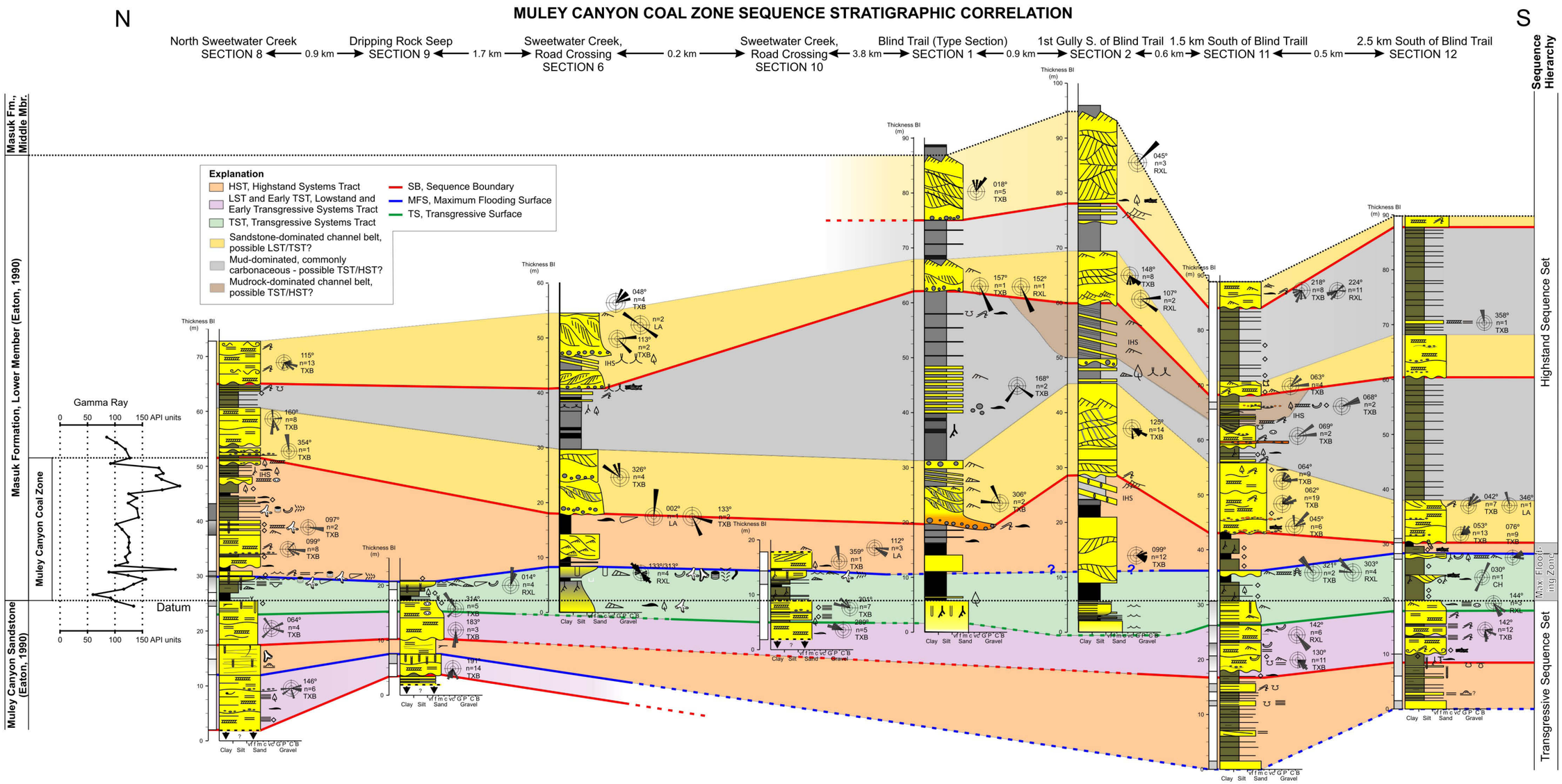

Plate 5. Surface sequence stratigraphic correlation the upper Muley Canyon Sandstone and lower Masuk Formation, with particular emphasis on the Muley Canyon coal zone. Location of measured sections used are highlighted in Figures 5 and 7. Outcrop gamma ray measurements of the coal zone are from section 8 at N. Sweetwater Creek. Explanation of measured section lithology and symbology shown in Appendix A, p. A-2.

MULEY CANYON COAL ZONE FACIES CORRELATION

N

S

North Sweetwater Creek SECTION 8 ← 0.9 km → Dripping Rock Seep SECTION 9 ← 1.7 km → Sweetwater Creek, Road Crossing SECTION 6 ← 0.2 km → Sweetwater Creek, Road Crossing SECTION 10 ← 3.8 km → Blind Trail (Type Section) SECTION 1 ← 0.9 km → 1st Gully S. of Blind Trail SECTION 2 ← 0.6 km → 1.5 km South of Blind Traill SECTION 11 ← 0.5 km → 2.5 km South of Blind Trail SECTION 12

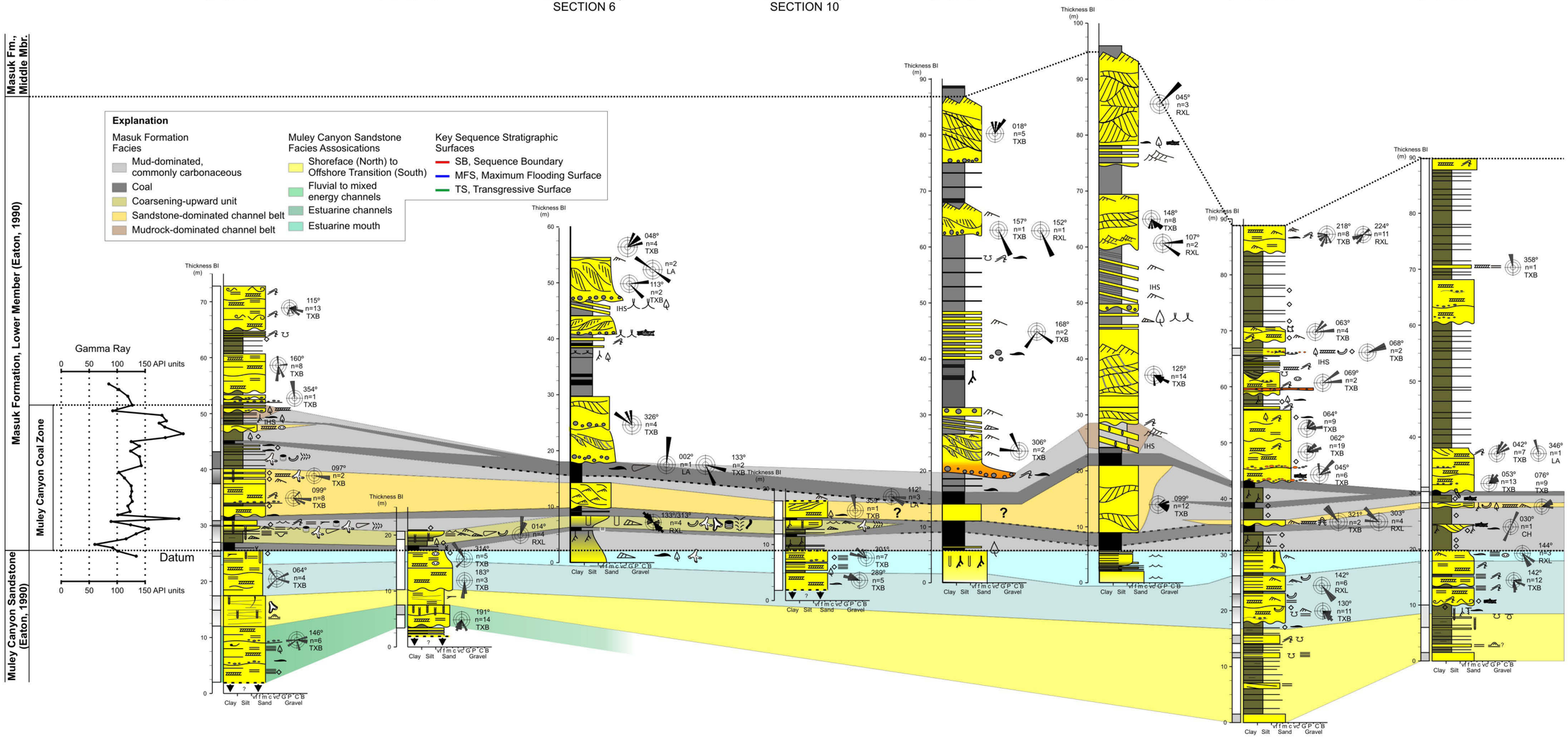

Plate 4. Surface correlation of units within the upper Muley Canyon Sandstone and lower Masuk Formation, with particular emphasis on the Muley Canyon coal zone. Location of measured sections used are highlighted in Figures 5 and 7. Outcrop gamma ray measurements of the coal zone are from section 8 at N. Sweetwater Creek. Explanation of measured section lithology and symbology shown in Appendix A, p. A-2.

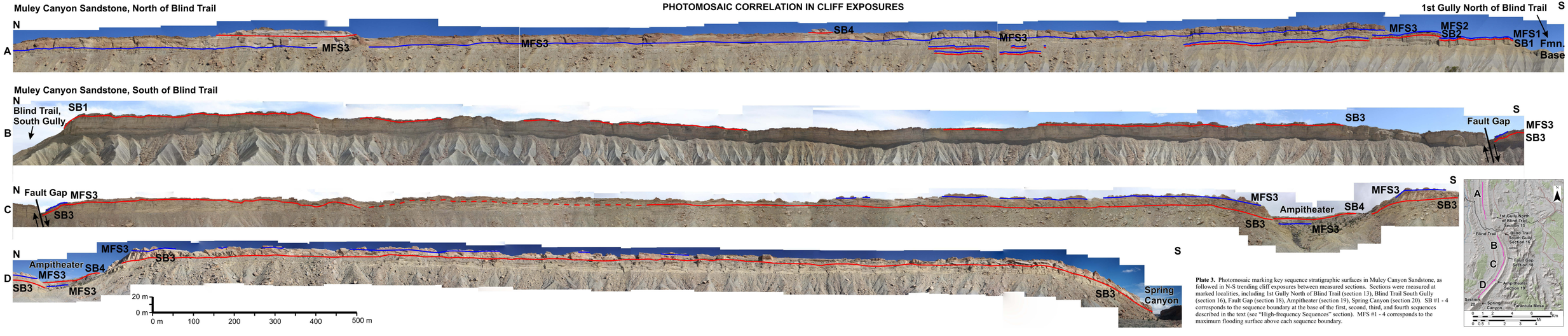

Plate 3. Photomosaic marking key sequence stratigraphic surfaces in Muley Canyon Sandstone, as followed in N-S trending cliff exposures between measured sections. Sections were measured at marked localities, including 1st Gully North of Blind Trail (section 13), Blind Trail South Gully (section 16), Fault Gap (section 18), Ampitheater (section 19), Spring Canyon (section 20). SB #1 - 4 corresponds to the sequence boundary at the base of the first, second, third, and fourth sequences described in the text (see "High-frequency Sequences" section). MFS #1 - 4 corresponds to the maximum flooding surface above each sequence boundary.

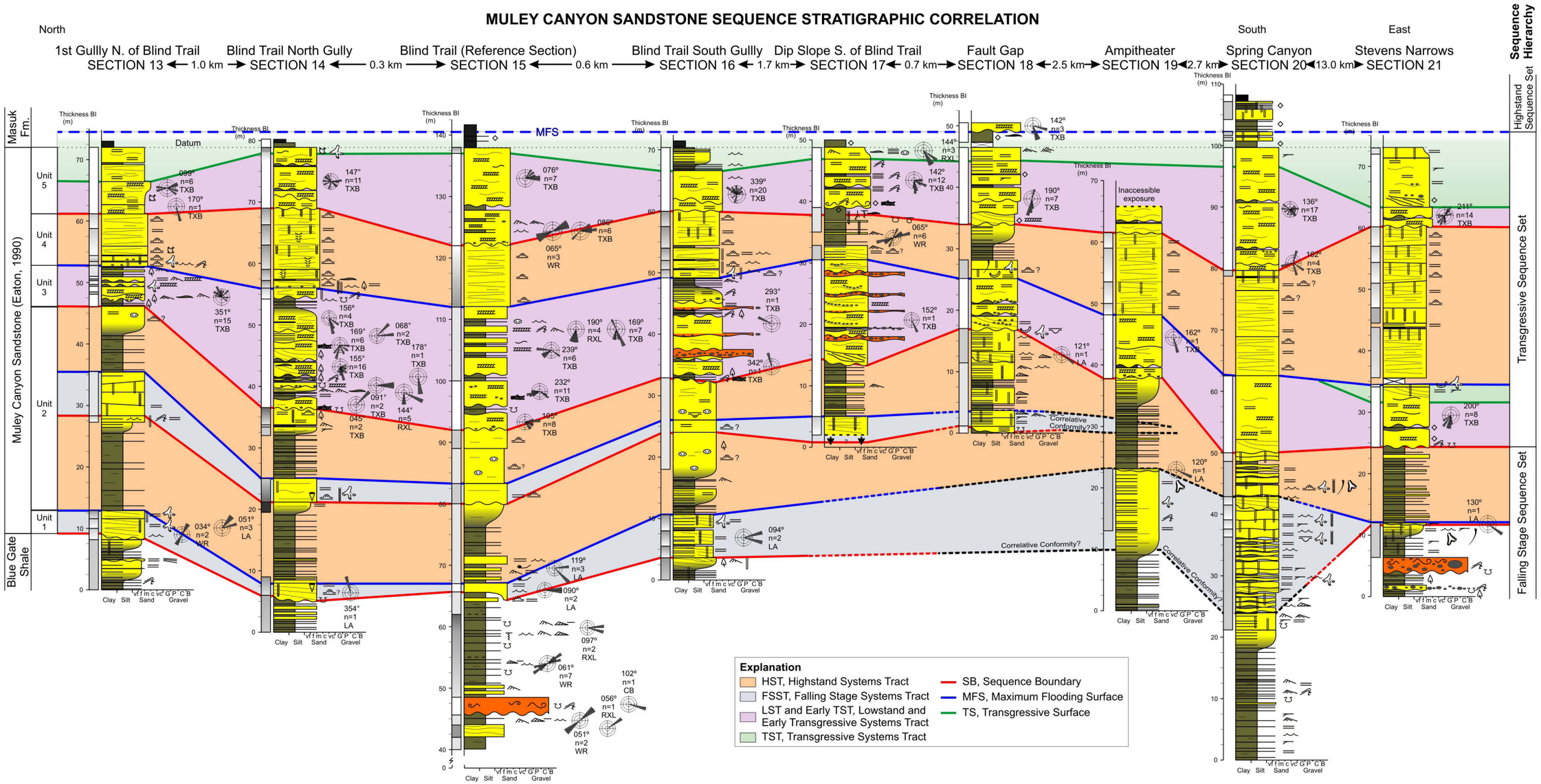

Plate 2. Sequence stratigraphic correlation of the Muley Canyon Sandstone, based on measured sections and following out units along cliff exposures. Location of measured sections are highlighted in Figures 5 and 6. Explanation of measured section lithology and symbology is shown in Appendix A, p. A-2.

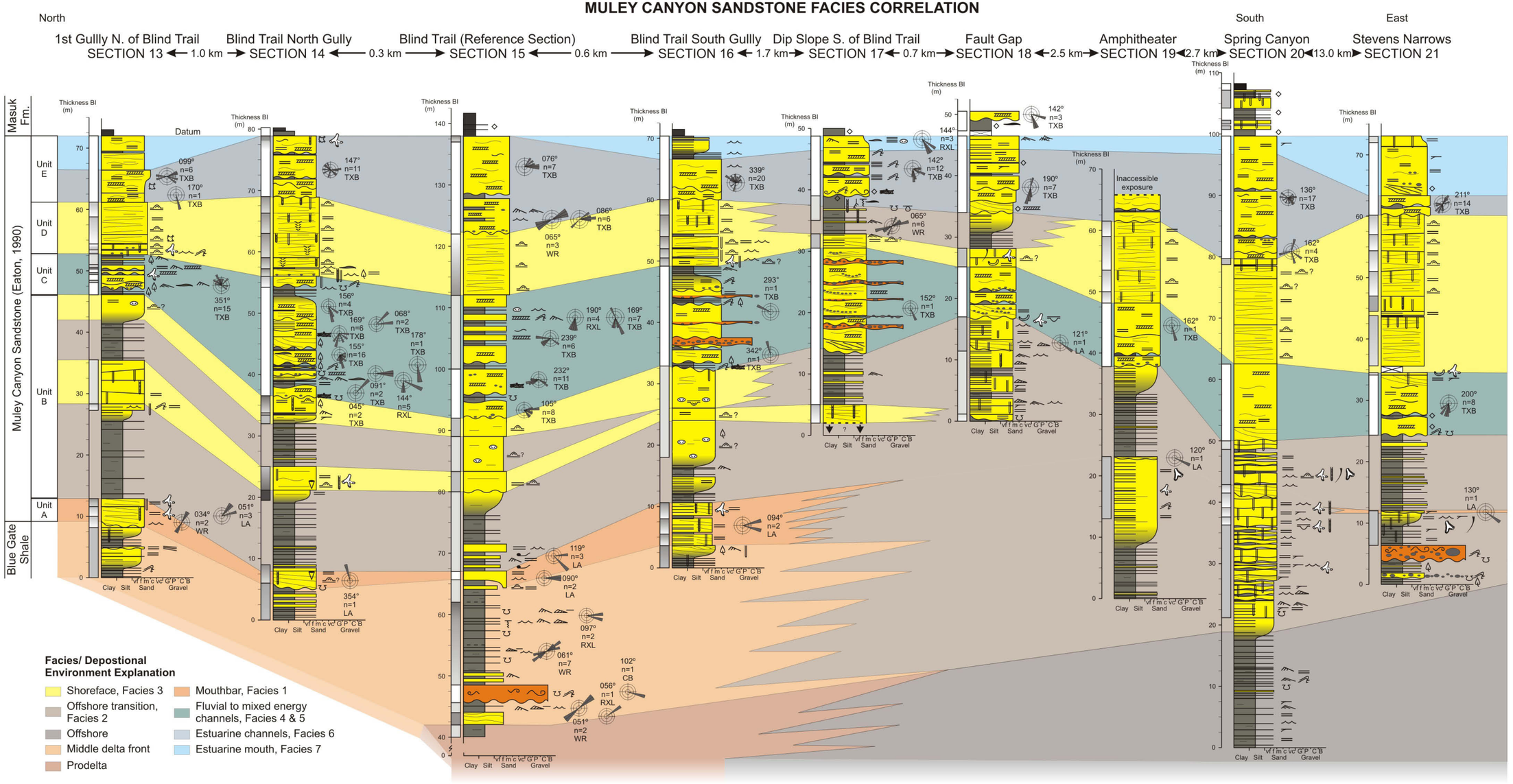

Plate 1. Correlation of interpreted facies and interpreted depositional environments within the Muley Canyon Sandstone, based on measured sections and following out units along cliff exposures. Location of measured sections are highlighted in Figures 5 and 6. Explanation of measured section lithology and symbology is shown in Appendix A, p. A-2.

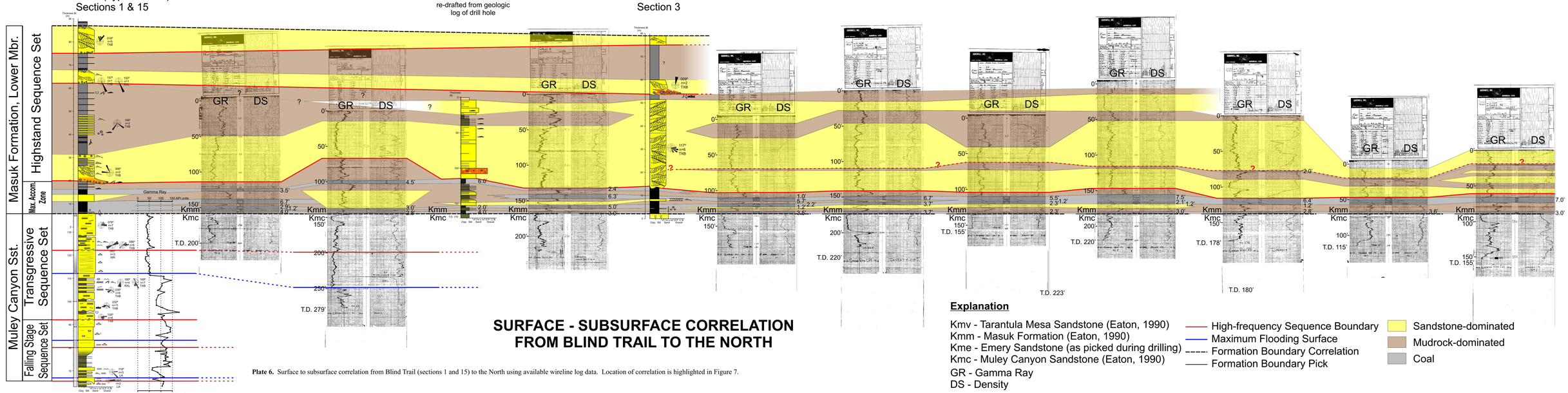

SURFACE - SUBSURFACE CORRELATION FROM BLIND TRAIL TO THE NORTH

Plate 6. Surface to subsurface correlation from Blind Trail (sections 1 and 15) to the North using available wireline log data. Location of correlation is highlighted in Figure 7.

Explanation

Kmv - Tarantula Mesa Sandstone (Eaton, 1990)
Kmm - Masuk Formation (Eaton, 1990)
Kme - Emery Sandstone (as picked during drilling)
Kmc - Muley Canyon Sandstone (Eaton, 1990)
GR - Gamma Ray
DS - Density

- High-frequency Sequence Boundary
- Maximum Flooding Surface
- Formation Boundary Correlation
- Formation Boundary Pick

- Sandstone-dominated
- Mudrock-dominated
- Coal

SURFACE - SUBSURFACE CORRELATION ACROSS TARANTULA MESA

North
Along Strike

West
Shoreward

East
Basinward

Section 2 ← 11.9 km → WB-1 ← 4.0 km → Tarantula-001 ← 2.9 km → Tarantula-003 ← 0.2 km → Tarantula Mesa 5C ← 1.3 km → MP-2 ← 3.2 km → MP-1 ← 2.3 km → ME-5

Stratigraphy
Seq. Strat. Interpretation

Tarantula Mesa Sst.

Masuk Formation
Highstand Sequence Set

Max. Flooding Zone

Muley Canyon Sst.
Transgressive Sequence Set

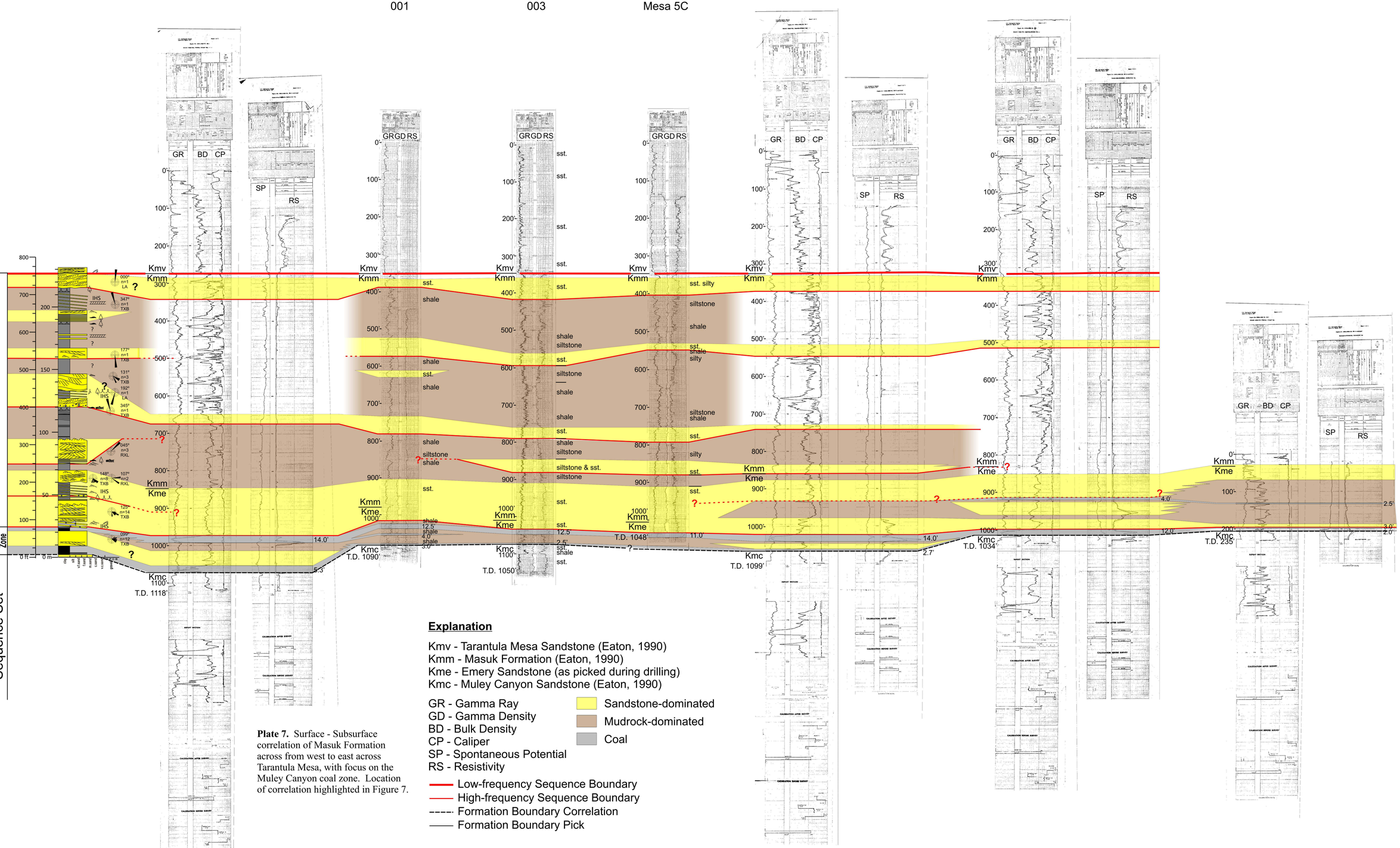

Explanation

Kmv - Tarantula Mesa Sandstone (Eaton, 1990)
Kmm - Masuk Formation (Eaton, 1990)
Kme - Emery Sandstone (as picked during drilling)
Kmc - Muley Canyon Sandstone (Eaton, 1990)

GR - Gamma Ray
GD - Gamma Density
BD - Bulk Density
CP - Caliper
SP - Spontaneous Potential
RS - Resistivity

Sandstone-dominated
Mudrock-dominated
Coal

Low-frequency Sequence Boundary
High-frequency Sequence Boundary
Formation Boundary Correlation
Formation Boundary Pick

Plate 7. Surface - Subsurface correlation of Masuk Formation across from west to east across Tarantula Mesa, with focus on the Muley Canyon coal zone. Location of correlation highlighted in Figure 7.